Role of IRF4 in the Regulation of Cellular Interferon Stimulated Genes and KSHV Lytic Gene Expression in Primary Effusion Lymphoma

by

Adriana Forero Rueda

Bachelor of Arts, Wesleyan College, 2004

Submitted to the Graduate Faculty of

School of Medicine in partial fulfillment

of the requirements for the degree of

Doctor of Philosophy

University of Pittsburgh

2013

UNIVERSITY OF PITTSBURGH

SCHOOL OF MEDICINE

This dissertation was presented

by

Adriana Forero Rueda

It was defended on

December 4th, 2013

and approved by

Lisa Borghesi, Ph.D.
Associate Professor, Department of Immunology

Carolyn B. Coyne, Ph.D.
Associate Professor, Department of Microbiology and Molecular Genetics

Neal A. DeLuca, Ph.D.
Professor, Department of Microbiology and Molecular Genetics

Saleem A. Khan, Ph.D.
Professor, Department of Microbiology and Molecular Genetics

Dissertation Advisor:
Saumendra N. Sarkar, Ph.D.
Assistant Professor, Department of Microbiology and Molecular Genetics

Role of IRF4 in the Regulation of Cellular Interferon Stimulated Genes and KSHV Lytic Gene Expression in Primary Effusion Lymphoma

Adriana Forero Rueda

University of Pittsburgh, 2013

The interferon regulatory factors (IRF) are a family of transcription factors that control intrinsic cellular responses to viral infections. The regulation of target gene expression by IRF proteins is mediated by binding to interferon-stimulated response elements (ISRE) DNA motifs located in the 5' regulatory region of Interferon-stimulated genes (ISGs). Interferon regulatory factor 4 (IRF4), a hematopoietic-specific transcription factor, is a potential dual regulator of ISRE-mediated gene expression although its transcriptional signature is still poorly understood. Primary effusion lymphoma (PEL), a rare B-cell malignancy is characterized by the expression of high level of cellular IRF4, a disrupted B-cell transcriptional program, and latent infection with Kaposi's sarcoma-associated herpesvirus (KSHV). The goal of this study is to elucidate the ability of IRF4 to alter the transcriptional expression of ISRE and ISRE-like sequence regulated genes in the absence of B-cell specific binding partners. Small-scale gene expression assays showed that IRF4 is capable of differentially regulating the expression of ISRE-responsive genes. The positive regulation of IRF4 target genes (ISG60 and Cig5) was shown to be in response to direct binding of IRF4 to chromatin regions corresponding to ISRE-motifs located at the 5' promoter regulator regions of ISG60 and Cig5. To understand the role of IRF4 beyond cellular gene expression, we tested KSHV-encoded latency associated genes that modulated IRF4-mediated gene expression. We identified the viral FLICE inhibitory protein (vFLIP) as an enhancer of IRF4-mediated ISG induction and showed that this function is dependent on the activation of NF-κB. Finally, we examined the role of IRF4 in the regulation of lytic gene expression. The replicator and transcription activator (RTA) protein, is a sequence specific transcription factor that regulates the expression of a subset of early genes through binding ISRE-like motifs on their promoters. Studies aimed at understanding the consequences of IRF4

expression in PEL cells showed that IRF4 acts as a negative regulator of lytic gene expression by inhibiting RTA expression and RTA-mediated gene transactivation. These data support a model in which IRF4 mediates an antiviral cellular response, inhibiting lytic replication of KSHV while contributing to the transformative effects of KSHV by promoting viral latency.

TABLE OF CONTENTS

LIST OF TABLES

LIST OF FIGURES

PREFACE

The completion of this study would not have been possible without the contribution and support of numerous individuals. I would like to thank my mentor, Dr. Saumen Sarkar, for his guidance, support, and patience through my development as an independent scientist. I would also like to acknowledge the members of the Sarkar lab, Rolando Cuevas, Dr. Arundhati Ghosh, Kevin McCormick, and Dr. Jianzhong Zhu for helpful discussions. I would specially like to acknowledge Jianzhong for his contribution to the work presented in Appendix B and C. I would also like to recognize the generous contributions and input of Dr. Yuan Chang and Dr. Patrick Moore and the members of their research team. I would like to specially thank Drs. Hyunjin Kwun and Tuna Toptan for helpful discussions and technical advice. I am very grateful for the guidance, collaboration, and generosity of Dr. James Pipas and the members of his laboratory, who were instrumental in the completion of the SV40 Large T antigen studies presented in Appendix A. Others who have contributed to the successful completion of the studies presented here are the members (past and present) of the Cancer Virology Program at the University of Pittsburgh Cancer Institute and our collaborators (past and present) at the UPCI who shared their expertise, equipment, and reagents used in the studies presented here – Drs. Frank Jenkins, Kathy Shair, Preet Chaudhary (UC Norris), Ole Gjoerup (Tufts), Christopher Bakkenist, and Stefan Duensing (U of Heidelberg), Pawel Kalinski, and Teresa Whiteside. I would also like to express my gratitude to my thesis committee members who took time to share their insight and expert

advice. Other reagents were kindly provided by Dr. Louis Staudt (NIH), Dr. David Lukac (Rutgers), Dr. Annette Duensing (U of Pittsburgh), and Katherine Fitzgerald (UMASS).

Finally, I would like to acknowledge the most crucial players in this wonderful journey. This would not have been possible without the guidance and support from my wonderful parents Daniel and Maria Elena, and my brothers, Santiago and Andres. Much gratitude is due to friends who provided me with unrelenting support and necessary distractions. I would like to recognize Caitlin Cameron for her unconditional love and support.

The work presented here is dedicated to the memory of Roberto Rueda Parra and Elsa Amorocho Serrano for teaching me that anything can be accomplished through love and commitment.

1.0 INTRODUCTION

1.1 INTERFERON SIGNALING

1.1.1 Viruses and Interferon

The innate immune responses to pathogen invasion are non-specific responses shared amongst several different cell types. This biphasic signaling cascade is summarized in Figure 1-1, and consists of an early phase characterized by the synthesis of type I interferons (IFNs) and a secondary phase or late response to secreted IFNs. The early phase of innate immune signaling is initiated by the recognition of virus-specific pathogen-associated molecular patterns (PAMPs) and is mediated by pattern-recognition receptors (PRRs). In humans, these include the nine membrane-spanning toll-like receptors (TLR), TLR1-9, the cytoplasmic retinoic-acid-inducible gene I (RIG-I)-like receptors (RLR), RIG-I and MDA5, various cytoplasmic and nuclear DNA sensors, and inflammasome activators. Engagement of TLRs initiates a signaling cascade mediated by either TIR-domain-containing adaptor protein-inducing IFNβ (TRIF) and the TRIF-related adaptor molecule (TRAM), or MyD88 and Toll/IL-1R (TIR) homology domain-associated protein (TIRAP). The activation of the RLRs engages the adaptor mitochondrial antiviral-signaling protein (MAVS). These adaptors stimulate the activation of signaling complexes like the Tumor Necrosis Factor (TNF) receptor associated factors -3 and -6 (TRAF3

and TRAF6), which further relay the signaling cascade by activating the kinases, TANK-binding kinase 1 (TBK1) and the inhibitor of kappa B (IκB) kinase complex. Kinase activity is essential for the activation of transcription factors such as the interferon regulatory factors (IRF) and nuclear factor kappa-light-chain-enhancer of activated B cells (NF-κB) required for the induction and secretion of type I IFNs, IFNβ and IFNα, as well as select pro-inflammatory cytokines and IFN stimulated genes (ISGs). [1]

Type I IFNs exert their pleiotropic antiviral effects by autocrine and paracrine activation of the type I IFN receptors, IFNAR1 and IFNAR2, located on the cellular membrane and are considered to be the late phase of viral recognition where the antiviral signals are amplified. Activation of IFNAR1/2 triggers the Janus kinase – signal transduction and activators of transcription (JAK-STAT) signaling pathway. Auto-phosphorylation of the receptor tyrosine kinases, Janus kinase 1 (JAK1) and TYK2, allows for the recruitment of the signal transduction and activators of transcription (STAT) proteins, STAT1 and STAT2, which, upon being phosphorylated, associate with the p48 subunit of the ISGF3 complex, IRF9, to form the active ISGF3 signal transduction complex. ISGF3 then translocates to the nucleus, binds to the interferon-stimulated response elements (ISRE) commonly located on the promoters of IFN-stimulated genes (ISGs), and induces mRNA transcription. Efficient innate immune signaling event is required for clearance of viral infections through antiviral responses that include the inhibition of cellular and viral gene translation, the inhibition of viral replication, and the promotion of viral nucleic acid recognition, and the death of the infected cell; moreover, these responses are paramount for the establishment of proper adaptive immune responses that further mediate viral clearance and provide long lasting immunity to subsequent infection. [2]

Increasing evidence suggests that innate immune responses are not only important for the recognition of foreign pathogens, but might also play an important role in cellular transformation, tumor progression, and tumor immune evasion [3]. A clear understanding of the mechanisms by which viruses counter innate immune responses and the function of antiviral genes would not only be beneficial for the development of new therapeutic antiviral strategies, but might also contribute to a better understanding of the role of innate immune signaling components in malignant transformation. This would ultimately allow us to exploit these signaling pathways for the development of novel immunotherapies for the treatment of cancer.

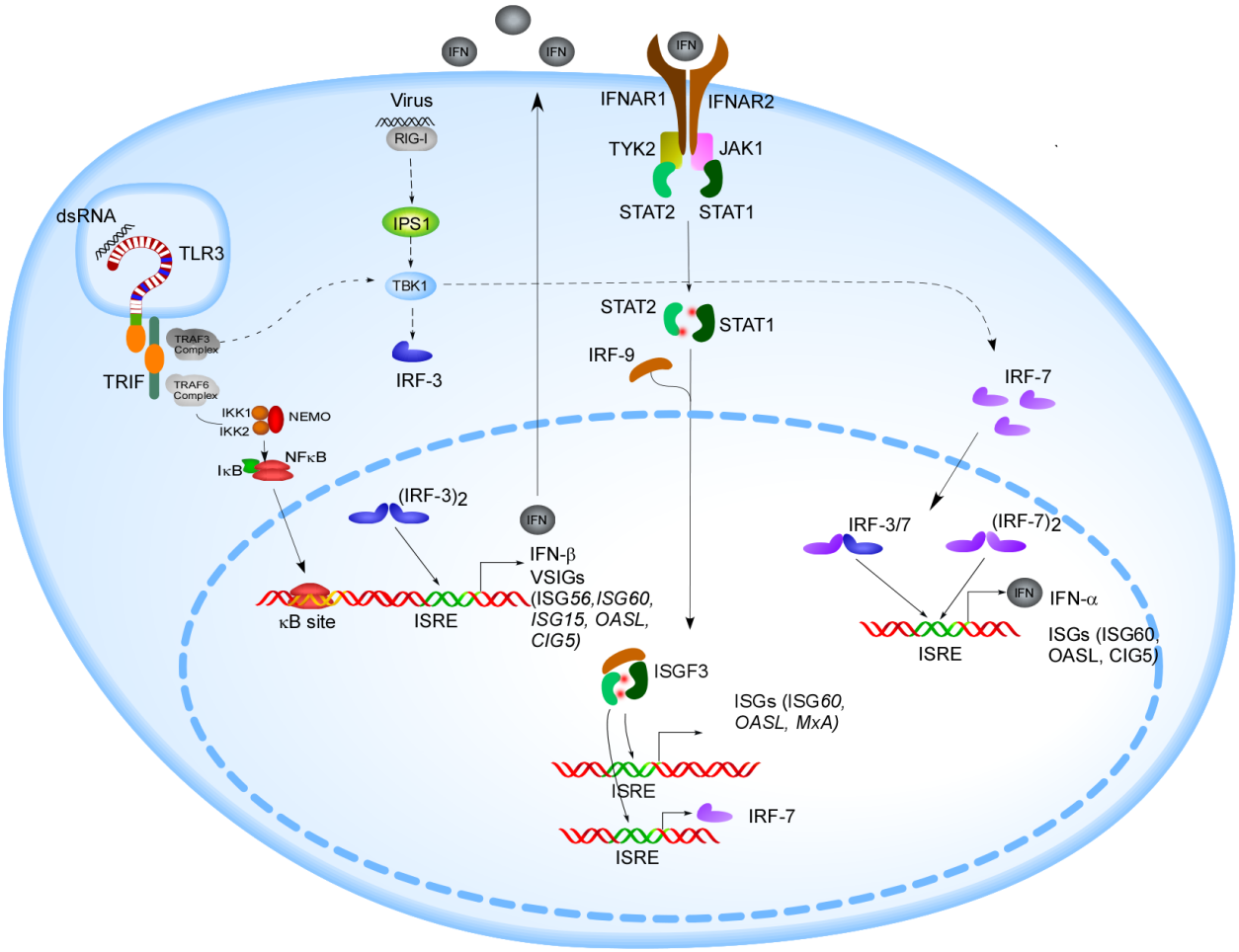

Figure 1-1. Interferon Production and Signaling Pathway.

Schematic representation of the biphasic interferon production and signaling pathway. The early phase of this pathway is characterized by the production of IFN and the induction of a subset of ISGs known as VSIGs. The late phase corresponds to the response to IFN stimulus and the further induction of VSIGs and interferon-responsive genes.

1.1.2 Interferon Regulatory Factors

The IFN regulatory factor (IRF) proteins are central mediators of the type I IFN secretion and signaling pathways, although their function extends to the regulation of development and

maturation of immune cells, amongst other biological processes [3]. To date, nine members of the IRF family of proteins, IRF1 through IRF9, have been identified in mammals. Although the specific expression and function of the IRF proteins varies between each member (Table 1), they all share common structural domains. In their amino (N)-terminus, they possess a highly conserved DNA-binding domain (DBD) containing a pentad of tryptophan residues required for binding to DNA. The carboxy (C)-terminus of IRF proteins are characterized by the presence of the IRF-association domain (IAD), which mediates protein interactions between IRF proteins or other transcription factors and an autoinhibitory element (AIE), which controls the activation of IRF proteins following conformational changes in response to serine/threonine phosphorylation.

The function of IRF proteins depends on their expression within the infected tissue, post-translational modifications, and localization to the nucleus. While the expression of a few IRF proteins is constitutive across tissue types (IRF3, IRF6, IRF9), the expression of IRF1, IRF2, IRF4, IRF5, IRF7, IRF8, and IRF9 proteins is differentially induced following infection, mitogenic stimuli, or DNA damage [4]. Following the induction of expression, these proteins are then localized to the cytoplasm where they exist as inactive monomers. Once IRFs have been phosphorylated at crucial C-terminal residues, IRF proteins form homo- and heterodimers with other transcription factors (IRFs, NFAT, PU.1, STAT1, STAT2, etc), and translocate to the nucleus. Following translocation, IRF dimers recognize and bind specific *cis*-elements located in promoter regulatory regions of target genes exerting distinct transcriptional regulatory functions either in cooperation or in competition with other factors. The IRF DBD recognition of the ISRE consensus sequence, 5'-GAAANNGAAA-3', is affected the transcriptional activity of IRFs are the nucleotides that flank this core element and the dimerization between IRFs and other transcription factors [5,6]. IRF expression, activation, and function help shape the intricate

cellular responses to pathogen infection, mitogenic stimuli, and stress. Thus, further investigation is required to better understand the molecular basis of IRF4 expression and activity and their role in maintaining cellular homeostasis.

Table 1. Human Interferon Regulatory Factor Expression and Function.

Interferon Regulatory Factor	Expression	Tissue Specificity	Function	Disease association
IRF-1	Inducible	Most tissue types	Promotes antiviral and antibacterial immune responses; tumor supressor	Susceptibility to viral infections and cancer
IRF-2	Constitutive and inducible by IFN	Most tissue types	Attenuates type I IFN responses; regulates lymphocyte differentiation	Dermatitis
IRF-3	Constitutive	Most tissue types	Promotes antiviral and antibacterial immune responses	Susceptibility to viral infections
IRF-4	Inducible by mitogenic stimuli	Lymphocytes and adipose tissues	Controls lymphocyte maturation and differentiation; regulates lipid handling; tumor suppressor; promotes oncogenesis	Lymphoproliferative diseases
IRF-5	Inducible	Most tissue types	Promotes antiviral and antibacterial immune responses; tumor suppressor	Susceptibility to viral infections; cellular transformation
IRF-6	Constitutive	Epithelial	Regulates epithelial development	Cleft palate; Van der Woude syndrome and popliteal pterygium syndrome
IRF-7	Inducible in most cell types; constitutive in pDCs	Most tissue types	Promotes antiviral and antibacterial immune responses; tumor supressor	Susceptibility to viral infections; cellular transformation
IRF-8	Constitutive and inducible	Lymphocytes	Controls lymphocyte maturation and differentiation an type I IFN secretion	Lymphoproliferative diseases
IRF-9	Constitutive and inducible by IFN	Most tissue types	Promotes antiviral and antibacterial immune responses; tumor supressor	Susceptibility to viral infections

1.1.2.1 Interferon Regulatory Factor 4

IRF4 (Uniprot: Q15306) is a 451 amino acid, multidomain protein, belonging to the IRF family of transcription factors. In the N-terminus, it has the characteristic helix turn helix DNA-binding domain (aa 20-137) containing the pentad of tryptophan residues (W27, W42, W54, W74, and W93), followed by a functional regulatory domain at the C-terminus composed of a proline-rich domain (PRO) (aa 150–237), the IAD domain (aa 245- 412), and an AIE (aa 412–450) domain that regulates IRF4 activation (Figure 1-2). Expression of IRF4 (also known as: MUM1, Pip, ICSAT, LSIRF) was initially thought to be restricted to B- and T-lymphocytes although recent evidence shows that IRF4 is also expressed in dendritic cells and macrophages [7] and adipose tissue [8,9]. Unlike other IRFs, which are involved in the secretion and response of type I IFN and type II IFN, the most characteristic function of IRF4 is the regulation of lymphocyte maturation.

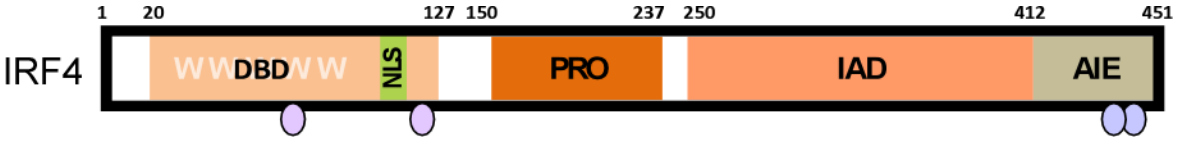

Figure 1-2. IRF4 Functional Domains.

Schematic representation of the IRF4 functional domains. IRF4 has an N-terminal DNA-binding domain (DBD) and nuclear localization signal (NLS). The C-terminus of the IRF4 protein is characterized by having a proline rich domain (PRO), an IRF association domain (IAD), and an autoinhibitory element (AIE). IRF4 is regulated by phosphorylation at serine (purple) and tyrosine (pink) residues.

Studies with mouse deficient in IRF4 and IRF8 *(Irf4,8-/-)* expression were shown to have a block in the transition from pre-B to resting B-cell development [10], suggesting that IRF4 plays an important role in early B-cell development. It has now been shown that IRF4 controls

the downregulation of the pre-BCR receptor through the suppression of surrogate light chain expression [11], the inhibition of pre-B cell proliferation [12], and Ig light chain transcription [7,13]. Studies using IRF4 deficient (*Irf4-/-)* mice showed normal early development of B- and T-lymphocytes, yet fail to develop a mature B-cell repertoire and eventually develop lymphoadenopathies. Furthermore, these mice do not form germinal centers upon antigen stimulation [14]. IRF4 expression has also been shown to be crucial for the control of PRDM-1 expression, which inactivates BCL-6 and PAX5 expression, marking the transition from resting B-cells to activated plasma cells [15].

The distinct transcriptional regulatory function of IRF4 is dictated by protein expression, the post-translational modifications that control its activation, and the interactions of IRF4 with partnering transcription factors. B-cell receptor engagement, CD40 cross-linking, and interleukin-4 (IL-4) stimulation [14,16,17] activate NF-κB and c-Myc and results in the induction of IRF4 transcription [16,18]. Post-transcriptional regulation of IRF4 also plays a crucial role in the functions of IRF4 expression. Direct binding of immunophilin FK506 binding protein 52 (FKBP52) results in the structural modification of IRF4 and prevention of IRF4/PU.1 dimer formation and DNA binding [19]. Furthermore, analysis of the IRF4 amino acid sequence predicts 21 amino acid residues that can be post-translationally modified by phosphorylation or covalent modifications, suggesting the importance of these regulatory modifications controlling IRF4 function. To date, four residues have been identified as being important for the phosphorylation of IRF4 and its transcriptional activation. One study identified ROCK2 as mediating the serine phosphorylation of IRF4 at residues 446 and 447 in T cells (Figure 1-2, purple circles) [20]. Other studies demonstrated that tyrosine phosphorylation at residues 61 and 124 (Figure 1-2, pink circles) was also essential for IRF4 transcriptional activity. Interestingly,

although c-Src was shown to stimulate IRF4 phosphorylation and transcriptional activation, the authors speculate that there are likely other kinases which are responsible for the direct phosphorylation of IRF4 at these tyrosine residues [21]. The potential ubiquitination and acetylation of IRF4 and its consequences in regulating protein stability and function still remain to be identified.

The differential role of IRF4 in transcription modulation stems from the interaction between IRF4 and other transcription factors. IRF4 possesses weak DNA binding activity, and thus, transcriptional regulation and DNA recognition is defined by the proteins that interact with IRF4 [22]. The better characterized binding partners of IRF4 are the Ets family of transcription factors, PU.1 and Spi-B, which can interact with the IAD of IRF4 forming ets/IRF4 dimers [13]. This allows IRF4 to bind DNA in a sequence specific manner by recognizing ets/IRF composite elements (EICE) on target gene promoters (5'-GGAANNGAAA-3'). Binding to EICE sequences found in the Igk and Igλ light chain enhancer in B cells and the ISG15 promoter leads to positive activation of transcription of these genes [13,23,24]. On the contrary, IRF4 has been shown to dimerize with IRF8 resulting in binding to ISRE elements, negatively regulating the activation of the ISG15 promoter [25]. Interestingly, expression of IRF4 resulted in weak activation of ISG15 promoter, suggesting a potential for positive ISG regulation by IRF4 [23]. These studies highlight the diverse functions of IRF4 in regulation of transcription and the importance of balanced IRF4 activity in maintaining homeostasis and the potential regulation of innate immune responses.

1.1.2.2 Association of IRF4 with Lymphoproliferative Disease

IRF4 expression and function has been associated with a variety of diseases. It has been shown that IRF4 is involved in the pathogenesis of autoimmune diseases (reviewed in [26]), negative regulation of diet-induced inflammation [8,9], and various lymphoproliferative diseases. While IRF4 expression has been found to negatively regulate the proliferation of BCL-6 associated malignancies [27,28], there is vast evidence that also implicates IRF4 as a mediator of oncogenesis [15,18,29-33]. In particular, IRF4 was first identified during the characterization of a chromosomal translocation commonly found in multiple myeloma (MM) cells, a plasmablastic malignancy. This translocation, (6;14)(p25;q32), apposes the IgH locus with the IRF4 gene resulting in IRF4 overexpression [31], thus enhancing transcription of c-Myc and deregulation of cell cycle regulatory proteins. The oncogenic potential of IRF4 in MM is further illustrated by a study showing that functional silencing of IRF4 leads decreased cell viability [18] and the transformation of Rat-1 cells by ectopic IRF4 expression [34].

Interestingly, high IRF4 expression has been described in various lymphoproliferative diseases associated with latent viral infections and is thought to be involved in the deregulation of cellular functions. Human T-lymphotropic virus 1 (HTLV-1) infected adult T-cell leukemia (ATL) [35,36], Epstein-Barr Virus (EBV) transformation of B cells [37-40], and primary effusion lymphoma (PEL) [29] are all associated with high levels of IRF4 protein expression. The HTLV-1-encoded oncogene, Tax-1, is a potent NF-κB activator [41] and has been shown to induce the expression of IRF4 in infected cells [35]. IRF4 expression has been correlated with resistance to antiviral therapy [42], immune evasion and cellular survival [39].

There have been various associations of IRF4 with malignancies associated to latent Epstein-Barr virus (EBV) infections. The viral encoded latency-membrane protein 1 (LMP-1), like Tax-1, activates NF-κB and induces the expression of IRF4 [37]. Furthermore, it was shown

that the EBV nuclear antigen 3C (EBNA3C) can bind and stabilize IRF4 to promote the proliferation of in vitro EBV-transformed lymphoblastoid cell lines (LCLs) from primary B cells [40]. IRF4 expression in EBV transformed cells is crucial for the inhibition of IRF5 anti-apoptotic functions and the regulation of microRNAs involved in the regulation of innate immune evasion and cellular proliferation [39], thus making IRF4 a contributor to the oncogenic potential of EBV.

Lastly, primary effusion lymphoma, a rare malignancy associated with KSHV infection, has been shown to correlate with high IRF4 expression. To date, neither the mechanisms of IRF4 induction or activation nor the consequences of IRF4 expression in regulating cellular survival and proliferation or antiviral immune responses have been examined. As previous studies have shown that interference of IRF4 expression is lethal to multiple myeloma cells, making IRF4 an "Achilles' heel" and potential therapeutic target [18], understanding the functions of IRF4 in PEL will help establish whether therapeutic strategies developed for the treatment of MM can be applied in the treatment of this rare malignancy.

1.2 VIRUSES AND CANCER

The notion of cancer as an infectious disease dates back to the 19th century. Studies in the early 1900s showed that a "filterable agent" isolated from chicken leukemia cells could recapitulate the disease in healthy chickens [43]. However, these studies were not followed up until 1911, when Peyton Rous convincingly demonstrated that solid tumors from hens were transmissible via inoculation with a filterable agent, Rous sarcoma virus (RSV) [44,45]. Later studies by Ludwig Gross, who identified murine leukemia virus (MLV) and mouse polyomavirus (MPyV),

provided support to the concept of virus-induced cancers [46,47]. Thus, the field of tumor virology was established.

Seminal studies led by Renato Dulbecco were instrumental in the establishment of quantitative methodology that would be applied to the exploration of the molecular principles of cellular transformation and solidified the use of tumor viruses as models for understanding cellular transformation. Work by Howard Temin and Harry Rubin led to the development of quantitative techniques for the study of RSV transformation that would revolutionize modern scientific research [48,49]. Rubin and Temin's assay would allow their colleagues, Dominique Stehelin, Harold Varmus, J. Michael Bishop, and Peter Vogt, to discover both viral [50,51] and cellular oncogenes [52]. In collaboration with Marguerite Vogt, the mechanisms of Mouse Polyoma (Py) virus cellular transformation were described [53-55]. Tumor viruses would then go on to be useful tools in the study of malignant transformation and would aid in the discoveries and development of new advances in molecular biology, such as the identification and isolation of reverse transcriptase (RT) by Howard Temin and David Baltimore [56,57].

1.2.1 Human Tumor Viruses

Today, it has been established that cancers arise due to both genetic and exogenous non-infectious causes. However, it is estimated that infectious agents cause one in five cancers [58]. While numerous oncogenic viruses have been described, only seven viruses have been associated with human proliferative diseases (Table 2). The first human tumor virus to be identified was Epstein-Barr virus (EBV), a ubiquitous gammaherpesvirus present in over 95% of the world's population. Using electron microscopy, M. Anthony Epstein, Bert Achong, and Yvonne Barr identified herpes-like viral particles in Burkitt's lymphoma tissues [59]. While the oncogenic

potential of EBV is “undermined” by the small percentage of EBV positive individuals that go on to develop tumors, in vitro experiments have shown that EBV could prolong the growth of normal lymphocytes [60] and is sufficient to transform primary B cells resulting in the establishment of lymphoblastoid cell lines (LCL) with enhanced proliferation capacity. Thus, EVB is considered an important contributing factor to tumorigenesis. To date, EBV has been strongly associated with a range of malignancies including: all cases of endemic Burkitt’s lymphoma, nasopharyngeal carcinomas, and EBV-associated lymphoproliferative diseases common to both AIDS-related and iatrogenic immunosuppression; and some cases of Burkitt’s lymphoma in non-endemic areas and Hodgkin’s disease [61].

One year later, in 1965, analysis of sera from leukemia patients allowed Baruch Blumberg to first identify the Australia (Au) antigen [62]. This antigen was also observed in patients with chronic or acute hepatitis and in 1968, the Au antigen was shown to be the surface antigen of the Hepatitis B virus (HBV), a hepadna virus [63]. Both the expression of viral proteins (HBx) that induce proinflammatory cytokines and the chronic inflammation induced in response to persistent virus infection, increase the incidence of hepatocellular carcinoma (HCC) in HBV infected individuals [64].

Fifteen years would pass after the discovery of HBV until another tumor virus would be discovered. At the time, the involvement of retroviruses in lymphocytic malignancies had been well established and new developments in tissue culture techniques were available. This facilitated the discovery and isolation of a retrovirus, human T-cell lymphotropic virus-1 (HTLV-1), from a patient with cutaneous T cell lymphoma [65]. Robert Gallo’s research group would go on to demonstrate that infection with HTLV-1 led to cellular transformation [66,67] and subsequent studies determined HTLV-1 to be the causative agent of adult T cell leukemia

(ATL) [68]. Viral encoded genes, Tax-1 and HBZ, have been linked to HTLV-1 transformation and pathogenesis, and their functions continue to be explored at present [69].

While the identification of these three oncogenic viruses relied on elegant virology, the discovery of the next four tumor viruses relied on the use of molecular biology and sequence analysis. Given that cervical cancer had been attributed to sexual behavior and that human papilloma viruses (HPV) were known to contribute to genital warts [70], Harald zur Hausen set out in 1983 to determine whether there was a relationship between HPV and cervical cancer [71,72]. By cross-hybridization of HPV DNA with DNA isolated from cervical carcinomas, zur Hausen identified the high-risk HPV types 16 and 18. Since then, there have been 15 high-risk HPV types identified. It has also been shown that although viral integration and increased expression of the E6 and E7 oncogenes are necessary to develop cervical neoplasias, additional genetic and environmental factors must contribute to the development of cervical carcinomas [73].

Nearing the end of the decade, Qui-Lim Choo would focus on trying to identify an infectious cause for transfusion-transmitted non-A, non-B hepatitis. Screening cDNA libraries from sera of chimpanzees infected with the non-A, non-B hepatitis agent from a diagnosed individual [74], the investigators were able to identify genome fragments from the Hepatitis C virus (HCV) [75]. HCV would then be established as a causative agent for hepatitis, liver cirrhosis, and hepatocellular carcinoma. Like HBV, HCV does not encode known viral oncogenes and thus, the associated liver damage and transformation potential of these viruses is due to the inflammatory responses and stress associated to chronic liver infection [76]. HCV remains an important pathogen and contributor to the cancer burden affecting 185 million individuals, with 20% of those infected at risk of developing HCC [77].

The final two viruses to be discovered and associated to malignant transformation were discovered by Drs. Yuan Chang and Patrick Moore. Focusing on malignancies associated to AIDS and age-related immunosupression, and utilizing cutting edge techniques, Drs. Chang and Moore identified Kaposi's sarcoma-associated herpes virus (KSHV) in 1994 and Merkel cell polyomavirus (MCV) in 2008. Epidemiologic evidence suggested that Kaposi's sarcoma (KS) occurring in AIDS patients was likely due to an infection given the fact that men who have sex with men (MSM) AIDS patients were 20 times more likely to develop KS than hemophiliac AIDS patients [78]. In collaboration with Ether Cesarman, Drs. Chang and Moore utilized representational difference analysis (RDA) to identify herpes-like sequences from KS lesions. This technique allowed the identification of herpesvirus-like sequences in KS tissues that were shown to share some similarity to other gammaherpesviruses. The lack of complete homology to EBV supported the classification of this virus as a novel member of the gammaherpesvirus subfamily [79].

Using a similar approach and newly developed computational techniques [80], Huichen Feng, from the Chang-Moore laboratory, would go on to discover MCV in Merkel cell carcinomas (MCC) in 2008. Applying digital transcriptome substraction (DTS), Feng was able to computationally subtract annotated sequence data and identify sequences of non-human origins from MCC derived cDNA libraries. Subsequent analysis of viral databases revealed the presence of viral sequences belonging to a novel member of the polyoma viruses [81]. The complete viral genome was then sequenced and further experimentation confirmed the role of MCV in MCC tumorigenesis [82].

It must be noted that oncogenic viruses are diverse in their genome classifications (Table 2) and the means by which they promote cellular proliferation and transformation are varied.

Thus, current work is focused in understanding the molecular functions of viral encoded proteins and the role of host responses in malignant transformation. Additionally, other viruses are continuously proposed as potential tumor viruses, although for many, their role in cancer remains controversial.

Table 2. Human Tumor Viruses.

Virus	Genome	Year Described	Disease Association	References
Epstein-Barr virus (EBV)	dsDNA herpesvirus	1964	Burkitt's lymphoma, nasopharyngeal carcinoma, various lymphomas	[59]
Hepatitis B virus (HBV)	ssDNA and dsDNA hepadnavirus	1965	Hepatocellular carcinoma	[62]
Human T-cell lymphotropic virus-1 (HTLV-1)	(+) ssRNA retrovirus	1980	Adult T cell leukemia	[65]
High-risk human papilloma virus (HPV)	dsDNA papillomavirus	1983	Cervical cancer; penile carcinoma; anal carcinoma; head and neck squamous cell carcinoma	[71,72]
Hepatitis C virus (HCV)	(+) ssRNA flavivirus	1989	Hepatocellular carcinoma and lymphoma	[75,83]
Kaposi's sarcoma-associated herpesvirus (KSHV or HHV-8)	dsDNA herpesvirus	1994	Kaposi's sarcoma, primary effusion lymphoma, Multicentric Castleman's disease	[79]
Merkel Cell Polyomavirus (MCV)	dsDNA polyomavirus	2008	Merkel cell carcinoma	[84]

1.3 KAPOSI SARCOMA-ASSOCIATED HERPESVIRUS

1.3.1 KSHV Seroprevalence and Pathogenesis

The seroprevalence of KSHV is rare (<10% in North America, Europe, and Asia) compared to the other more ubiquitous human herpesviruses. However, three at risk populations have been identified. KSHV seroprevalence is higher amongst individuals in the Mediterranean (20-30%) and MSM (8-40% in North America and Europe) [85-87]. The highest incidence of infection is observed in Sub-Saharan Africa where the rates of infection exceed 60% of the population. To date, KSHV infection has been associated with three individual malignancies most commonly affecting immunocompromised and elderly individuals [88]. KS is an endothelial malignancy first described by the Hungarian physician, Moritz Kaposi. KS has four different subtypes: Classic KS, occurring in Mediterranean men; African endemic KS, the more aggressive form of KS found in Sub-Saharan Africa; AIDS-KS, which follows AIDS related immunosupression; and iatrogenic KS, which follows iatrogenic immunosupression of transplant recipients. KS is characterized by the presence of proliferating spindle cells capable of forming irregular vascular channels. KS is infected with KSHV [79].

KSHV infection has also been associated with malignancies of B cell origin. Fifty percent of multicentric Castleman's disease (MCD) cases are positive for KSHV infection [89,90]. MCD is a B cell malignancy localized to the mantle zone of lymph nodes and the spleen that is comprised of both KSHV negative and KSHV positive cells. MCD cells infected with KSHV are exclusively IgMλ plasmablasts and are polyclonal in nature, suggesting that multiple rounds of infection occur in these transformed cells.

A third KSHV-related malignancy, primary effusion lymphoma (PEL), has been described. The defining criterion for PEL diagnosis is the detection of KSHV infection [91,92]. While PEL cells can be co-infected with EBV, development of PEL in the absence of KSHV infection has not been described. Thus, KSHV infection seems to be a prerequisite for the development of this malignancy [93].

The study of KSHV infection and pathogenesis has been limited by the lack of animal models. In vivo studies have relied on the use of surrogate rhadinovirus, mouse herpesvirus 68 (MHV68) [94] and Rhesus rhadinovirus (RRV) [95] infectious models and several transgenic mouse models. The study of the KSHV lifecycle is further limited by the lack of in vitro models of KSHV infection and the difficulty establishing and maintaining latently infected KS cell lines. Thus, the use of readily established PEL cell lines has been instrumental for understanding KSHV biology. PEL cells contain 50-150 episomal copies of KSHV. Expression on viral genes is limited in these cells. The understanding of viral reactivation has mostly relied on these cells [96].

1.3.2 Primary Effusion Lymphoma

PEL is a rare KSHV-associated B cell neoplasm occurring primarily in the pleural, peritoneal, and pericardial cavities [97]. While development of PEL occurs primarily in AIDS patients, it has also been observed in immunocompromised transplant patients [88]. Diagnosis of PEL relies on morphologic, immunophenotypic, and genetic criteria. PEL cells are generally enlarged with round irregular nuclei and prominent nucleoli [98]. PELs show hypermutations in Ig loci, suggesting that they may originate from post-germinal center B-cells. They have the appearance of immunoblastic or plasmablastic cells, which they share expression of immunophenotypic

marker CD138 and IRF4 [29,30]. Conversely, PEL cells do not express other common B-cell markers [30,99]. Unlike other lymphomas, no common genetic abnormalities like *myc* translocations or mutations of the *bcl-2* or *ras* oncogenes have been described for PEL [93].

PEL is a rare disease accounting for about 3% of AIDS-related lymphomas. Advances in the treatment of AIDS and AIDS progression with highly active antiretroviral therapy (HAART) have resulted in decreased incidences of PEL [96]. Current chemotherapeutic approaches include cyclophosphamide, doxorubicin, vincristine, and prednisone (CHOP) and modified CHOP-like therapies [100] and have remained ineffective. Median survival rates range from 2 to 6 months [100,101]. Since KSHV is found to be latent in PEL cells with little to no viral DNA replication, treatment with herpes antiviral drugs has proven ineffective. A better understanding of KSHV pathogenesis is still necessary to develop efficient antiviral strategies for the treatment of KSHV infections and KSHV related malignancies.

1.4 MOLECULAR BIOLOGY OF KSHV

Kaposi's sarcoma associated herpesvirus (KSHV) is a large double-stranded DNA virus belonging to the gammaherpesvirus subfamily and Rhadinovirus genera. The 145 kilobase pairs genome consists of a long unique region flanked by 20-35 Kb terminal repeat (TR) sequences [102]. The genome is maintained as a close circular episome in infected cells and it is linearized during replication and virion packaging where it is enclosed in an icosahedral capsid [103].

The KSHV genome has over 80 genes encoding for structural and DNA-replication proteins conserved amongst the herpesviruses. Interestingly, KHSV also has a unique set of genes with homology to human genes that is unusual for the herpes viruses. This "molecular

piracy" allows KSHV to deregulate biological processes including cell cycle regulation, cellular growth and proliferation, angiogenesis, inhibition of cellular death, and innate immune evasion [104]. KSHV genes are named after the corresponding genes found in Herpesvirus saimiri, a related rhadinovirus (ORF4-ORF75). Genes unique to KSHV are given a K prefix, with open-reading frames K1-K15 having being identified [105].

Expression of viral genes is strictly regulated between the KSHV life cycle phases. Distinctive of the herpesviruses, during lytic infection, viral genomes are replicated and virions are assembled with genes being expressed in a temporal cascade (Immediate Early, Early, and Late). KSHV can also establish latency in the infected cell. During this phase, viral replication is stalled and gene expression is limited to a few genes required for immune evasion and maintenance of the viral genomes. Balanced regulation between the latent and lytic replication phases is crucial for efficient viral spread and persistence, thereby contributing to viral pathogenesis and cellular transformation.

1.4.1 Latency

KSHV infection results in the establishment of latency in the infected cell. Viral latency is characterized by limited viral gene transcription and protein synthesis. The expressed transcripts during latency or lytic replication have been categorized into three classes based on the expression in uninduced or TPA stimulated (lytically induced) PEL cells. Genes expressed in unstimulated cells were classified as class I genes, transcripts expressed in uninduced cells that were stimulated by TPA treatment were classified as class II genes, and those expressed only after induction were classified as class III genes [106]. Unfortunately, PEL cells in culture experience some degree of spontaneous reactivation, making it difficult to clearly define latent

genes. Thus, there are continued efforts in understanding the temporal expression of KSHV genes [107].

While the identity of truly latent genes still remains to be established, a few genes have been strongly associated with this phase of the lifecycle. These genes have been termed latency-associated genes and are encoded by open reading frames K12 (Kaposin), K13 (v-FLIP), ORF72 (v-Cyclin), ORF73 (LANA), and K10.5 (LANA2). Proteins synthesized from these transcripts are important for the episomal maintenance of viral genomes (LANA), cellular proliferation (v-FLIP, vCyclin), and inhibition of apoptosis (LANA, LANA2, v-FLIP, K12). [108] A few of these latency-associated genes have also been shown to be involved in the regulation innate immune responses [109]. Below, the specific functions of these proteins in the regulation of the IFN and ISG expression are discussed.

1.4.1.1 Latency-Associated Nuclear Antigen (LANA)

LANA is a 222-234 kDa nuclear protein encoded by ORF73 and it is a latent protein expressed in all forms of KSHV-associated malignancies. LANA is a multifunctional protein, interacting with both viral and cellular proteins and deregulating several cellular pathways, making it a major KSHV oncoprotein [110]. LANA contributes to cellular proliferation and transformation through interaction with the p53 and pRB tumor suppressor pathways, and the regulation of growth signaling pathways. Furthermore, LANA plays an important role in the persistence of KSHV genomes and maintenance of latency. Expression of LANA is required for the replication of viral DNA during latency and the tethering of viral genomes to host chromosomes important for the segregation of episomal viral DNA in the dividing cells. Inhibition of the lytic switch is also an important feature of LANA in the maintenance of latency (Reviewed in [110]).

LANA is also an inhibitor of host antiviral responses. LANA inhibits the transcription of IFNβ by competing with IRF-3 binding to the PRDI/III domains in the IFNβ promoter [111]. Further inhibition of innate immune signaling was observed by ChIP-Seq analysis of LANA binding to host chromosomes in BCBL-1 cells. This study demonstrated that LANA interferes with p53 and TNF-α signaling pathways as well as inhibiting IFNγ induced STAT1 gene transactivation [112].

1.4.1.2 LANA2 or viral IFN Regulatory Factor 3

The viral IFN-regulatory factors are a set of cellular IRF homologues uniquely expressed by the rhadinoviruses KSHV and RRV [113]. KSHV encodes four viral homologues of IRF (v-IRF1, v-IRF2, v-IRF3, and v-IRF4) encoded by the region encompassing ORFs K9-11 (Figure 1-3) and their expression is mostly restricted to lytic reactivation. The interferon inhibitory functions of these genes have been extensively studied and their functions have been elegantly summarized by Baresova et al. [114].

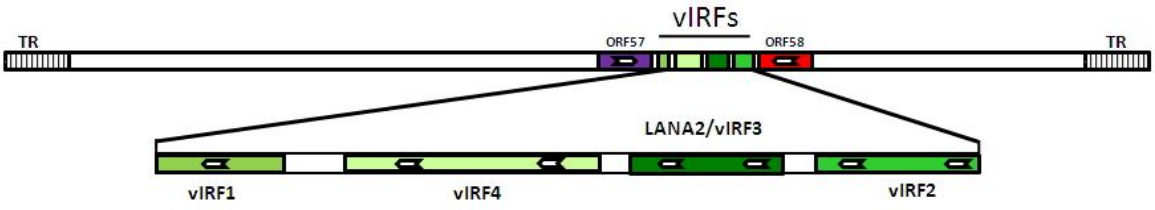

Figure 1-3. KSHV Homologues of Cellular IRF Proteins.

Arrangement of vIRF genes on the KSHV genome. KSHV encodes four homologues of cellular IRF proteins: vIRF1 (K9), vIRF4 (K10), LANA2/vIRF3 (K10.5), and vIRF2 (K11). The vIRF locus is clustered between ORF57 (purple) and ORF58 (red). Terminal repeats are represented by striped boxes.

LANA2 (vIRF3) is encoded by ORFK10.5 and it shares homology to IRF4 [115]. LANA2 is a particularly interesting member of this family of proteins given its restricted expression in infected cells. Its expression has been detected in PEL and MCD, but not in KS, suggesting that LANA2 is expressed in a lymphocyte specific manner [116]. LANA2 is a potential oncogene that modulates PEL cellular survival and proliferation through direct interaction with other host proteins. LANA2 inhibits p53 and Protein Kinase R (PKR) mediated apoptosis [116,117], and sequesters 14-3-3, which functions to inactivate FoxO proteins involved in cell growth and proliferation [118]. LANA2 contributes to cellular proliferation by enhancing c-Myc mediated gene induction [119]. Immunoprecipitation assays show that LANA2 and c-Myc directly interact and have been found to form a complex with the promoter of c-Myc target genes. Furthermore, LANA2 binds Myc Modulator-1 (MM1), disrupting its ability to bind and inhibit c-Myc activity. This association led to an increase in the activation of target genes. Ultimately, the most seminal study linking LANA2 to PEL oncogenesis showed that silencing of LANA2 expression by siRNA, led to cellular death by activation of caspase-3 and caspase-7 [120].

Studies on the pro-viral function of LANA2 have focused on the modulation of transcriptional activity of IRF3, IRF5, and IRF7 [115,120-123]. LANA2 has been shown to inhibit IRF5-mediated signaling by interacting with IRF5 and therefore inhibiting the DNA binding of IRF5 to interferon stimulated responsive elements (ISRE) on target gene promoters [123]. The regulatory function of LANA2 on IRF3 and IRF7 mediated gene induction has remained controversial with some studies suggesting that LANA2 expression can enhance IRF3/IRF7 mediated promoter activation [121]. However, other studies suggest that LANA2 expression inhibits IRF3/IRF7 mediated transcription [115,122]. Although it remains unclear

what the role of LANA2 is in innate immune modulation, these studies have established that LANA2 can directly bind IRF proteins affecting their transcriptional activity.

1.4.1.3 Viral FLICE Inhibitory Protein

The viral FLICE inhibitory protein (vFLIP) expressed during latent infection with KSHV is encoded by the ORF71 (K13) [124]. vFLIP shares structural homology with FLICE, also known as caspase-8, and it contains two homologous copies of the death effector domain (DED) [125,126]. In host cells, the DED is required for the recruitment of FLICE to receptors, like Tumor Necrosis Factor Receptor 1, containing death domains (DD) initiating receptor-mediated cell-death. vFLIP inhibits FLICE mediated cell death by binding to the DED and preventing its interaction with death domains in receptors. This led to an initial speculation that vFLIP could inhibit death receptor mediated cell death [126], although later studies demonstrated that vFLIP regulates cell survival and proliferation by acting as a potent activator of the NF-κB signaling pathway [127-136].

Briefly, vFLIP activates NF-κB by interacting with the IκB Kinase (IKK) complex [127,137,138]. These proteins phosphorylate IκB proteins and target them for degradation by the proteosome [137]. Thus, the active NF-κB subunits are released and translocated into the nucleus where it becomes functionally active. NF-κB activation results in gross changes in the transcriptional profile of vFLIP expressing cells. Gene set data analysis (GSEA) from transcriptome analysis studies in BCBL-1 (PEL cells) and HUVEC (endothelial cells) cell lines expressing vFLIP, demonstrated that the Toll, IL-1R and inflammatory pathways were affected by vFLIP. Interestingly, these studies also showed that that gene expression is differentially

affected in different cell lineages [139]. Besides the strong induction of proinflammatory cytokines induced by vFLIP, its expression also results in the enhanced induction of STAT1 dependent gene expression in endothelial cells, which is required for the characteristic spindle cell formation observed in KS lesions. Using a reverse genetic approach, Alkharsah et al. were able to show that infection of endothelial cells with ΔFLIP KSHV results in the diminished phosphorylation of both STAT1 and STAT2 and a decrease in ISG expression compared to WT infected cells. [140] These observations supported earlier observations that ectopic expression of vFLIP enhances IFNβ activation by stimulating NF-κB binding to the PRDII domain of the IFNβ promoter enhancer [141]. While these latency-associated associated proteins have been shown to regulate interferon and inflammatory responses, the consequences of gene expression regulation and the contribution of the specifically targeted genes in controlling or promoting viral pathogenicity and tumorigenesis remains to be established.

1.4.2 Switch to Viral Lytic Reactivation

Reactivation from latency is an important step in the pathogenesis of KSHV and is necessary for viral spread and transmission. The switch from latency to lytic replication, in Rhadinoviruses, is controlled by the replication and transcription activator (RTA) protein that is encoded by the open reading frame ORF50. Expression of RTA is necessary and sufficient to initiate lytic gene transcription, virion formation, and death of the host cell. To date, studies of RTA induction and function have identified signals that contribute to viral reactivation, such as chemical treatment with phorbol esters [142] and histone deacetylase inhibitors [143], calcium inhibition [144], hypoxia [145], viral infection [146], and BCR stimulation [147].

The first transcript to be induced after stimuli is the 3.6 kb ORF50 transcript, which is resistant to protein synthesis inhibition with cyclohexamide (CHX), identifying this protein as the KSHV immediate early (IE) protein [148,149]. RTA, a sequence-specific DNA binding protein, regulates the transcription of viral early (E) genes and positively autoregulates its transcription through complex mechanisms [150-154]. The early genes include genes involved in the synthesis of viral DNA and genes required for the expression of the late (L) structural genes. Overall, the genes expressed during lytic reactivation include those required for genome replication and virion assembly, as well as genes involved in the evasion of cellular death and innate immune responses.

1.4.2.1 RTA-Mediated Transcriptional Regulation

RTA is a 691 amino acid nuclear protein that binds to RTA-responsive elements (RRE) located in viral gene promoters and activates gene transcription [149,155]. Additionally, RTA can interact with the cellular protein RBP-J-κ, thereby regulating RBP-J-κ dependent cellular gene expression. The specificity of RTA to the promoters is determined by its direct binding to DNA or by its interaction with other cellular and viral DNA binding proteins. Upon recognition of RRE sequences, RTA oligomers induce gene expression [156] of a specific set of viral genes [157].

Thus far, there are no obvious RRE consensus motifs identified between the regions bound by RTA in various gene promoters. RTA can bind to a 5'-AACAATATAATGTT-3' sequence found in the promoters of both ORF57 and K8, which is distinct from the 5'-AAATGGGTGGCTAACCCCTACATAA-3' sequence found in the PAN (nut-1) and K12 promoters [158], or the RRE found in the v-IL6 promoter 5'-

AAACCCCGCCCCCTGGTGCTCACTTT-3' [159]. A second adjacent RRE has been described in ORF57 (5'-ATTTTTCGTTTGTG-3'), which is bound by both RTA and IRF7. IRF7 binding to this sequence results in the competitive inhibition of RTA-mediated ORF57 induction [160]. The inhibition posed by IRF7 is overcome by direct ubiquitination and proteosomal degradation of IRF7 by RTA [161,162]. It has also been shown that RTA can regulate both viral (K14) and cellular gene expression (ISGs) by binding to ISRE-like sequences contained in the promoters of these genes [163]. Intriguingly, analysis of the RTA DNA-binding domain primary structure revealed conserved amino acids shared between RTA and the IRF family of proteins. Mutations at the conserved lysine residue 152, which is homologous to the essential K92 residue in IRF7, resulted in impaired binding to ISRE sequences and loss of transcriptional activation capacity of RTA [163]. These results suggest that RTA may hijack the IRF signaling pathway in order to evade immune responses and that IRF proteins potentially exert a regulatory function on viral gene expression shaping the establishment of latency in KSHV infected cells.

1.5 RATIONALE AND HYPOTHESIS

The functional role of IRF4 in KSHV-associated B cell malignancies has not yet been explored. Little information regarding the signaling events controlled by the IRF transcription factors that contribute to immune evasion, viral persistence, and cellular growth and proliferation. Previous studies have shown that IRF4 acts as both an activator and repressor of ISRE driven promoter activation and this is largely dependent on the interactions of IRF4 with other transcription factors. However, the potential regulation of interferon-stimulated genes by IRF4 in the absence of co-factors remains to be examined. Furthermore, latency-associated innate immune

modulators expressed in KSHV infected cells are capable of shaping the transcriptional potential of IRF proteins by directly interacting with these proteins, their transcriptional co-factors or the DNA sequences they recognize. It is likely, that these proteins act as regulators of IRF4 mediated gene expression in order to ensure viral persistence. Lastly, given the sequence similarities between the IRF4 and RTA binding domains, there is a potential that IRF4, like IRF7, could bind to ISRE-like sequence modulating RTA-mediated gene transcription. Thus, we hypothesize that IRF4 expression in PEL cells results in the regulation of ISRE and ISRE-like driven cellular and viral gene expression and contributes to the pathogenesis of KSHV.

2.0 REGULATION OF IFN-STIMULATED GENE EXPRESSION BY IRF4

Work described in this section was partly published in the Journal of Immunology

(J of Immunol. 2013 Aug 1;191(3):1476-85) by authors

Adriana Forero,

Patrick S. Moore, and Saumendra N. Sarkar.

2.1 INTRODUCTION

IRF4 is a tissue specific transcription factor involved in the regulation of immune responses that result in the maturation and differentiation of lymphocytes [22]. Interestingly, the expression of IRF4 has also been suggested to have transformative potential [34,164] and has been correlated with the development of several B- and T-cell lymphoproliferative diseases [18,30,32,33,36]. One such malignancy is primary effusion lymphoma (PEL), a KSHV-associated B cell neoplasm [88,97]. PEL cells have the appearance of immunoblastic or plasmablastic cells in that these cells express high levels of IRF4 and CD138-positive [29,30]. While the transcriptional regulatory role of IRF4 in other plasmablastic malignancies has been previously studied, the significance of IRF4 in the context of PEL cells has yet to be explored.

Aside from having a plasma cell-like phenotype, PEL cells are characterized by being latently infected with KSHV. IRF proteins are well known for their role in mediating immune responses to viral invasion. The unifying feature of this family of proteins is the similarity of their N-terminal DBD domain, containing a pentad of tryptophans, crucial for the recognition of the ISRE sequence generally found in the promoters of IFN and the effector proteins upregulated in response to IFN [165,166]. Thus, it is likely that IRF4 also plays a role in shaping the cellular response to viral infection by targeting the expression of IFN-stimulated genes (ISG).

By forming distinct transcriptional complex with other transcription factors, IRF4 acts as both a positive and negative regulator of ISG expression [22]. Dimerization between IRF4 and PU.1 results in the potent activation of ISG by binding to EICE enhancer elements [13]. On the

other hand, interactions with IRF8, results in the inhibition of ISG15 expression by binding to the ISRE motif [25]. However, PEL has been demonstrated to have a disrupted B cell phenotype, lacking the expression of PU.1, IRF8, and Oct-2 [167]. Given that IRF4 itself can directly bind DNA [168] and this unique condition in which its co-transcriptional regulators are downregulated, it is relevant to better understand the transcriptional potential of IRF4 in innate immunity.

In this chapter, we investigate the role of IRF4 in controlling ISRE-driven promoter activity through promoter reporter assays, qRT-PCR, and ChIP analysis in model cell lines as well as PEL cell lines. The transcriptional control of ISGs by IRF4 is intricate. We show that IRF4 can directly target the ISG60 and Cig5 promoters and positively regulate their gene expression while also resulting in the downregulation of the IFN-responsive gene, MxA. These studies have contributed to further clarify the involvement of IRF4 on the distinct regulation of ISRE-mediated gene transcription and have allowed us to establish an assay for future studies on identifying modulators of IRF4 function.

2.2 MATERIALS AND METHODS

2.2.1 Cell Lines and Reagents

The cell lines used in this study have been described on Table 3. HEK293 cells, 293FT, and HEK293-derived cell lines, 293*i*4, RL24*i*4, and RL24, were cultured in Dulbecco's Modified Eagle Medium (Lonza) containing 10% fetal bovine serum (Atlanta Biologicals) and 100 I.U./ml penicillin and 100 mg/ml streptomycin (Lonza). BCBL-1, BC-1, and BC-3 cells were cultured in RPMI medium (Lonza) supplemented with 10% fetal bovine serum (FBS) (Atlanta Biologicals) and 100 I.U./ml penicillin and 100 mg/ml streptomycin (Lonza). BCP-1 cells were cultured with similar medium conditions but FBS levels were adjusted to 20%. EBV-negative Burkitt lymphoma cell line, BJAB, was used as a KSHV negative control cell line. BJAB and BJAB derived cells were cultured in RPMI medium supplemented with 10% fetal bovine serum and 100 I.U./ml penicillin and 100 mg/ml streptomycin (Lonza). Doxycycline (Clonetech) was resuspended in a 1 mg/ml stock in H_20 and used at the reported concentrations.

Table 3. Chapter 2 - Cell Lines.

Cell Line	Description	Source	Reference
HEK293	Human embryonic kidney cells, immortalized/ transformed by adenovirus transduction.	ATCC® CRL-1573	
293FT	HEK293 transformed with the SV40 Large T antigen	Invitrogen (Cat no. R700-07)	
293*i*4	HEK293-derived doxycycline-inducible IRF4 expressing cell line generated by lentiviral tranduction with pInducer20/IRF4-V5	Sarkar Lab (University of Pittsburgh)	[169]
293/pLenti	HEK293-derived vector control cell line generated by lentiviral transduction with pLenti/CMV/Puro	Sarkar Lab	[169]
293/pLenti-IRF4-V5	HEK293-derived cell line generated by lentiviral tranduction with pLenti/CMV/Puro/IRF4-V5	Sarkar Lab	[169]
RL24	HEK293 derived stably expressing TLR3, ISG56-FLuc and pTK-Rluc	Sarkar Lab	[170]
RL24*i*4	RL24 derived doxycycline-inducible IRF4 expressing cell line generated by lentiviral tranduction with pInducer22/IRF4-V5	Sarkar Lab	
BCBL-1	KSHV +ve, EBV –ve, p53 wt PEL cell line derived from a male patient	Chang-Moore lab (University of Pittsburgh)	[171]
BC-1	KSHV +ve, EBV +ve, p53 wt PEL cell line derived from a male patient	Chang-Moore lab (ATCC® CRL-2230)	[91]
BC-3	KSHV +ve, EBV –ve, p53 wt PEL cell line derived from a male patient	Chang-Moore lab (ATCC® CRL-2277)	[172]
BCP-1	KSHV +ve, EBV –ve, p53 wt PEL cell line derived from a male patient	Chang-Moore Lab (ATCC® CRL-2294)	[173]
BJAB	EBV –ve human Burkitt's lymphoma cell line	Chang-Moore Lab	[174]
BJAB*i*4	BJAB –derived doxycycline-inducible IRF4 expressing cell line generated by lentiviral tranduction with pInducer20/IRF4-V5	Sarkar Lab	[169]

2.2.2 Plasmids and Lentiviral Vectors

IRF4, transcript variant 1 (NM_002460), was PCR amplified with an N-Terminal V5 tag from the pCMV6-IRF4 plasmid (Origene) using the following primers: 5'-CACCGAATTCCACCATGGGTAAGCCTATCCCTAACCCTCTCCTCGGTCTCGATTCTACGAACCTGGAGGGCGGCGGC-3'; 5'- CGCCATTCCTCTATTCAAGAATGACTCGAG-3'. The PCR product was then cloned into pENTR-D/TOPO (Invitrogen) following manufacturer's guidelines. The expression vector pcDNA/IRF4-V5 was generated by recombination between pENTR/D-TOPO IRF4-V5 and pcDNA/DEST47 using Gateway LR Clonase II enzyme mix (Invitrogen) according to manufacturer's guidelines.

Doxycycline-inducible, cDNA expressing lentiviral vectors were generated by performing LR recombination between pENTR/D-TOPO IRF4-V5 with pInducer 20 or pInducer 22 [175] vectors using the Gateway LR Clonase II enzyme mix (Invitrogen) following manufacturer's guideline. Constitutive IRF4 expressing lentiviral vector was generated by LR recombination of pENTR/D-TOPO IRF4-V5 with pLenti/CMV/Puro DEST (W118-1) (Addgene). Control pInducer20 and pLenti/CMV/Puro vectors were generated by recombination with empty pENTR-V5 plasmid (Addgene).

2.2.3 Lentivirus Packaging and Transduction of Cells

Lentiviruses were packaged in 293FT by transfection of 5 μg of lentiviral vector, 2.5 μg packaging plasmid pCMVΔ89.2 (gag/pol), and 2.5 μg of envelope plasmid pCMV-VSV-G were

transfected into $1x10^7$ 293FT cells using Fugene 6 at a 1:3 DNA to Fugene 6 ratio. After 24 hrs, medium was changed to 10 ml fresh growth medium (DMEM, 10% FBS, Pennicillin/Streptomycin). Supernatants were harvested 48 hrs post transfection and cellular debris was removed by centrifugation at 1200 RPM for 5 minutes. Clarified supernatants were then filtered using a 0.45 μM syringe filter and concentrated using Lenti-X concentrator (Clontech). Briefly, virus supernatants were incubated with 4X Lenti-X Concentrator overnight at 4 °C. Samples were spun at 1,500 x g for 45 minutes at 4°C. Pellets were resuspended and concentrated to 1/10 original volume. Virus preparations were kept frozen at -80°C until further use.

HEK293-derived 293*i*4 cells were generated by overnight lentiviral infection of $1x10^6$ cells with 500 μl virus packaged from pInducer20/IRF-V5 (previously described) in the presence of 5 μg/ml polybrene (Sigma-Aldrich). 48 hrs post-infection, cells were selected with 500 μg/ml G418 (InvivoGen) for 7 days. G418-resistant cells were pooled and used for further studies. RL24*i*4 cells were generated by overnight infection of $1x10^6$ RL24 cells with 500 μl concentrated pInducer22/IRF4-V5 virus. Pools of infected cells were used for further studies. 293FT-derived pLenti-IRF4 cells were generated by overnight lentiviral infection of $1x10^6$ cells with 500 μl virus packaged from pLenti/CMV/Puro/IRF4-V5 or empty pLenti/CMV/Puro (previously described). At 48 hrs post-infection, cells were selected with 1 μg/ml Puromycin (InvivoGen) for 7 days. Puromycin-resistant cells were pooled and used for further studies. BJAB*i*4 cells were generated lentiviral infection with pInducer20/IRF4-V5 virus. In brief, $1x10^6$ cells were infected by spin inoculation (30 min. at 2500 RPM, room temperature) with 1 ml of concentrated virus resuspended in RPMI. Cells were selected with 500 μg/ml G418 for 7 days. G418-resistant pools of cells were used in these studies.

2.2.4 RNA Isolation and qRT-PCR

RNA was isolated from cells using TRIzol® reagent (Invitrogen) following manufacturer's protocol. Briefly, cells were lysed in 1 ml TRIzol® reagent and incubated 5 minutes at RT prior to addition of 200 μl of chloroform. Samples were spun down and the aqueous portion as harvested and incubated with equal volume of isopropanol for 10 minutes at room temperature. RNA was harvested by centrifugation and washed with 70% ethanol. RNA pellets were resuspended in DEPC-treated nuclease free water. Total RNA extractions were treated with DNA-free (Ambion) to remove DNA contamination. In brief, 5 μg of RNA were dissolved in 24 μl of water with DNAse I buffer and 1 μl of DNAse I. Samples were incubated at 37°C for 1hr. 1 μl total RNA was used for reverse transcription using iScript cDNA synthesis kit (Bio-Rad) according to manufacturer's instructions. cDNA was diluted in water 1:3 and 1 μl per sample was subjected to SYBR green real-time PCR using a CFX96 real time system (Bio-Rad). Samples were denatured at 98^{o}C for 2 minutes, followed by 40 cycles of amplification as follows: 98^{o}C for 2s, 56^{o}C for 5s with reading of plate. Samples were the incubated at 95^{o}C for 10 min. Melt curves were produced by exposing the final PCR product to a temperature gradient from 65^{o}C to 95^{o}C, in 0.5^{o}C increments with constant fluorescent readouts collected between each increment. Primers used for target gene amplification can be found in Table 2. Each sample was normalized to RPL32 and expressed as fold change with respect to vector expressing cells or non-stimulated cells (Value 1).

Table 4. IFN-Stimulated Gene Primer Set.

Gene	Orientation	Sequence
RPL32	Forward	5' - CAACATTGGTTATGGAAGCAACA - 3'
	Reverse	5' - TGACGTTGTGGACCAGGAACT - 3'
IRF4	Forward	5' - ACCCGCAGATGTCCATGAG - 3'
	Reverse	5' - GTGGCATCATGTAGTTGTGAACCT - 3'
ISG60	Forward	5'-AGTCTAGTCACTTGGGGAAAC-3'
	Reverse	5'-ATAAATCTGAGCATCTGAGAGTC-3'
Cig5/Viperin	Forward	5' - CAGTGCTTGCATTGCTTTGT - 3'
	Reverse	5' - CAAGGTTCCAGCGTGATTTT - 3'
OasL	Forward	5' - GGACCGTGGAGGAGTTTCTG - 3'
	Reverse	5' - GAGCCCACCTTGACTACCTTC - 3'
IFNβ	Forward	5' - TGGGAGGATTCTGCATTACC - 3'
	Reverse	5' - CAGCATCTGCTGGTTGAAGA - 3'
IFNα	Forward	5'- GTGAGGAAATACTTCCAAAGAATCAC - 3'
	Reverse	5' - TCTCATGATTTCTGCTCTGACAA - 3'
IRF7	Forward	5' - TACCATCTACCTGGGCTTCG - 3'
	Reverse	5' - AGGGTTCCAGCTTCACCA - 3'
MxA	Forward	5' - AGGTCAGTTACCAGGACTAC - 3'
	Reverse	5' - ATGGCATTCTGGGCTTTATT - 3'
ISG15	Forward	5' - ACTCATCTTTGCCAGTACAGGAG - 3'
	Reverse	5' - CAGCATCTTCACCGTCAGGTC - 3'
PKR	Forward	5' - TCTGACTACCTGTCCTCTGGTTCTT - 3'
	Reverse	5' - GCGAGTGTGCTGGTCACTAAAG - 3'

2.2.5 Luciferase Assays

RL24 cells (1.5×10^5 cells/well) in 24-well plate were transfected with 0, 100, 250, 500 ng of pcDNA/IRF4-V5 or empty vector using Fugene 6 at a 1:3 DNA: Fugene 6 ratio. DNA concentrations were kept consistent amongst all wells (500 ng). At 24 hours post transfection, cells were collected by trypsin-EDTA digestion and seeded into 6 wells in a white walled 96-well plate. At 48 hours post transfection, luciferase activity was measured using the Dual-Glo

luciferase assay system (Promega). Briefly, 15 μl of Dual-Glo reagents were added to 100 μl of cell culture medium. Cells were incubated for 10 minutes and firefly luciferase (Fluc) activity was measured. The reaction was stopped using 15 μl of Stop-Glo reagent and renilla luciferase (Rluc) activity was measured. Fluc activity was normalized of Rluc activity and the normalized once again to the negative control. Changes in promoter activity were determined as fold change with respect to vector expressing cells. Alternatively, $2.5x10^4$ RL24*i*4 cells were seeded in 96-well plates and stimulated with increasing doses of doxycycline for 24 hrs. Luciferase activity was measured using the Dual luciferase assay system (Promega). Briefly, cells were lysed for 10 minutes at room temperature with 20 μl 1x PLB. After lysis, 7 μl of lysate was placed on a white walled 96-well plate. Firefly luciferase (Fluc) activity was measured by adding 20 μl of LARII reagent. Following luminescence readings, 20 μl of Stop and Glo reagent were added to quench the reaction and measure renilla luciferase activity (Rluc). Relative luciferase activity was determined by normalizing the Fluc/Rluc values relative to untreated cells.

2.2.6 Chromatin Immunoprecipitation assays

Chromatin immunoprecipitation (ChIP) was performed using the ChIP-IT Express kit from Active Motif according to the manufacturer's protocols. Briefly, $1x□10^7$ HEK293 cells stably expressing pLenti/CMV/Puro vector control or pLenti/CMV/Puro IRF4-V5 or $1x□10^7$ BCBL-1 cells were cross-linked with 1% formaldehyde in PBS for 10 min. Cells were then placed in lysis buffer and homogenized with a dounce homogenizer. Nuclei were harvested and resuspended in shearing buffer containing PMSF and protease inhibitors. Chromatin was sheared into 200-600 bp fragments by sonication. To examine binding of IRF4 to ISRE elements in 293 cells, 25 μg of

cross-linked chromatin was incubated with 25 μl protein G magnetic beads and 3 μl anti-V5 (Invitrogen), anti-Pol II (8WG16) (Millipore), or control IgG antibody overnight to immunoprecipitate each target protein. In the case of PEL cells, 20 μg of chromatin were incubated with protein 25 μl of protein G magnetic beads and 4.9 μg anti-IRF4 (#4964) (Cell Signaling), anti-Pol II (8WG16), or control IgG antibody. DNA was purified after reversing protein/DNA cross-linking; equal amounts of the purified ChIP DNA were subjected to quantitative PCR analysis, as previously described, using primers ISG60 ISRE (5′-GGTCTCAAGCCGTTAGGTTTCATTT-3′; 5′-GAAGTCTTCCTGTCTGCCTCAAGTA-3′) and Cig 5 ISRE (5'- CCCGATCTCTAGTCTTCAGTCTTGG -3'; 5'-GCAGGACACACCTTCTTTGACTAAC-3′). Each sample was normalized to the negative control and expressed as fold change with respect to vector expressing cells (Value 1).

2.2.7 Subcellular Fractionations

293*i*4 and BCBL-1 cells were harvested and washed with PBS. Cell pellets were suspended in hypotonic buffer (20 mM HEPES pH8.0, 10 mM KCl, 1 mM $MgCl_2$, 20% glycerol, 0.1% Triton-X 100) with protease inhibitors. The cell suspensions (100 μl) were vortexed for 30s, incubated on ice for 15 min, and centrifuged (16,000g for 10 min at 4 °C). The supernatants were collected as soluble cytoplasmic fractions. The remaining nuclear pellets were thoroughly washed in 10 volumes of hypotonic buffer and then resuspended in 100 μl RIPA buffer (50mM Tris-HCl [pH7.4], 150mM NaCl, 1% NP-40, 0.25% sodium deoxycholate, 1mM EDTA, 1mM PMSF, 1X Protease inhibitor cocktail) and incubated in ice for 30 minutes prior to SDS-PAGE. Equal volumes of soluble cytoplasmic fraction and total nuclear fraction were resolved and

immunoblotted with anti-IRF4 (Cell Signaling), DRBP76 [176], and Tubulin antibodies (Santa Cruz). Density analysis was done using ImageJ.

2.2.8 Immunoblotting

Protein concentration from cell lysates was determined using the Bio-Rad Protein Assay (Bio-Rad). Equal amount of protein extracts were resolved on either 8.5% or 12% SDS–polyacrylamide gels, and proteins were transferred to PVDF membranes. Membranes were stained with Ponceau S stain for 5 minutes to assess even transfer, washed twice in Tris-buffered saline with Tween 20 (TBS-T; 20 mM Tris, 0.5 M NaCl [pH 7.5] plus 0.5% Tween 20) and blocked for 1 hr in 10% nonfat dry milk TBS-T. Primary antibody incubation was done overnight in 10% nonfat dry milk. Antibodies used anti-IRF4 (Cell Signaling), anti-ISG60, anti-ORF50, anti-LANA, anti-LANA2 were used at a concentration of 1:1000 and have been previously described [169]. Membranes were then washed twice with TBS-T and incubated with horseradish peroxidase-conjugated anti-mouse or anti-rabbit immunoglobulin G (IgG) (Rockland) diluted at 1:10000 in TBS-T plus 10% nonfat dry milk. Blots were developed by enhanced chemiluminescence using Hy-Glo reagent (Denville) according to manufacturer's protocol.

2.2.9 VSV Infection and Growth Assessment

293 cells were stably transduced by viral infection with either pLenti/CMV/Puro/IRF4-V5 or empty pLenti/CMV/Puro. Puromycin resistant cell pools were infected with VSV-GFP [177] at a

multiplicity of infection (m.o.i) of 0.001. 24 hrs after transfection, cellular supernatants were harvested and viral yield was measured by plaque assay on BHK21 cells.

2.2.10 Statistical analysis

Data were analyzed using two-tailed paired Student's t-test. Values were considered significant at $p < 0.05$.

2.3 RESULTS

The PEL cell line BCBL-1 expressed increased levels of IRF4 mRNA (Figure 2-1A) and protein concomitant with the expression of LANA and LANA2, KSHV latency associated proteins (Figure 2-1B) as has been previously described [29,30]. The transcriptional activities of IRF proteins are associated with their activation and nuclear translocation [1], thus we examined the cellular localization of IRF4 in PEL cells. We prepared both soluble cytoplasmic and nuclear fractions and subjected them to immunoblot analysis to probe for IRF4 subcellular localization. A major portion of IRF4 protein in BCBL-1 cells was localized to the DRBP76-positive nuclear fraction, characteristic of an activated IRF. A significantly smaller percentage of the total detected IRF4 protein was localized to the Tubulin-positive cytoplasmic fraction (Figure 2-1C). Given that IRF4 is found in a presumably activated form in PEL cells, a better understanding of the affected target genes could prove beneficial to expand our knowledge on the contributions of IRF4 to KSHV pathogenesis.

PEL cells have been described to display an incomplete B-cell transcriptional program due to the lack of PU.1, IRF8, and Oct-2 expression [167]. We measured the expression of PU.1 transcripts in the PEL cell line BCBL-1 and Burkitt's lymphoma cell line, BJAB, relative to 293 cells, which are devoid of PU.1 expression. In accordance with previous reports, BCBL-1 cells expressed similar levels of PU.1 relative to 293 cells. BJAB cells however, showed over 20-fold higher PU.1 mRNA transcript relative to 293 cells (Figure 2-1D). Thus, to understand the transcriptional potential of IRF4 in the absence of PU.1 or other B-cell specific transcription factors, we generated IRF4 expression systems that would allow us to examine IRF4 function in several experimentally manipulatable cell lines as well as in PEL cell lines.

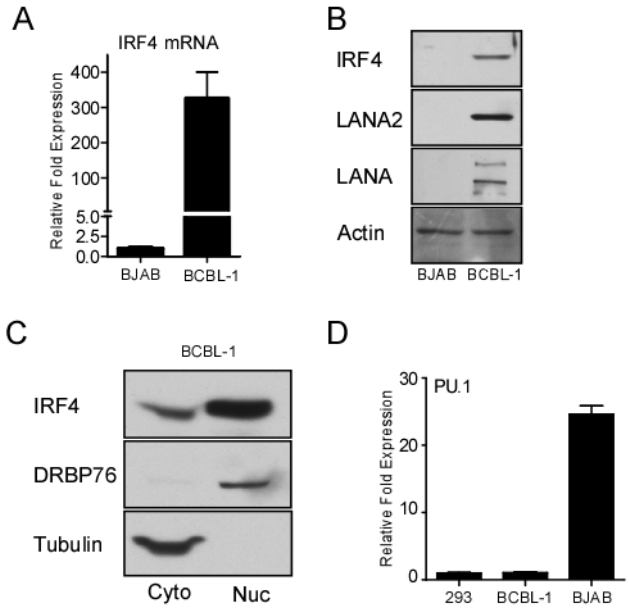

Figure 2-1. PEL Cell Lines Express IRF4.

(A) IRF4 mRNA analysis in BJAB and BCBL-1 cells. Total RNA was harvested and subjected to qRT-PCR using primers against IRF4 and RPL32 as indicated in materials and methods. Expression of IRF4 was normalized to RPL32 and expressed as fold change with respect to BJAB cells (value 1).
(B) Analysis of IRF4 protein levels in BJAB and BCBL-1 cells. Lysates were prepared from PEL cell lines and probed with anti-IRF4, anti-LANA, anti-LANA2, and anti-Actin antibodies.
(C) Sub-cellular localization of IRF4 in PEL cell lines. Cytoplasmic and nuclear fractions were prepared from 1×10^7 BCBL-1 cells and immunoblotted with IRF4, Tubulin, and DRBP76 antibodies.
(D) Analysis of PU.1 expression in PEL cell line, BCBL-1. Total RNA was harvested from BJAB, BCBL-1 and 293 cells and subjected to qRT-PCR using primers against PU.1 and RPL32 as indicated in materials and methods. Expression of PU.1was normalized to RPL32 and expressed as fold change with respect to 293 cells (value 1).

IRF4 cDNA was subcloned by PCR amplification from pCMV-XL6/IRF4. An N-terminal V5 tag was cloned in frame with the IRF4 coding sequence in the PCR reaction. The generated PCR fragments were TOPO cloned into the pENTR/D-TOPO vector, thus generating the pENTR-D/TOPO IRF4-V5 expression vector. The plasmid was isolated from single colonies, amplified, and sequenced to verify PCR fidelity and tag insertion. The obtained nucleotide sequence was then translated *in silico* to assess that the proper framing of our newly generated protein-coding sequence (CDS). The amino acid sequence showed V5 tag located to the N-terminus (highlighted in pink) and the corresponding to the IRF4 mRNA transcript variant 1 (Figure 2-2). pENTR-D/TOPO IRF4-V5 was then further used to generate both lentivirus-based expression vectors and eukaryotic expression vectors described in Chapter 2 Materials and Methods.

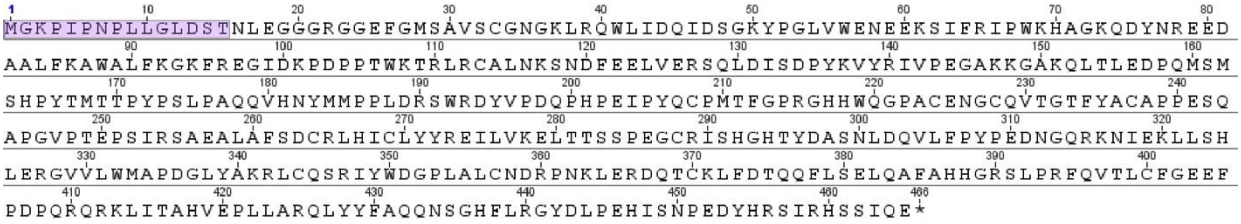

Figure 2-2. Amino Acid Sequence of IRF4-V5.

Amino acid sequence for N-terminal V5 tagged IRF4. V5 sequence has been highlighted in pink. Amino acids 16-466 correspond to the primary structure of IRF4 (transcript variant 1). Asterisk denotes stop codon.

Previous reports have suggested that IRF4 has the ability to promote the weak induction of promoters encoding ISRE elements. In order to explore whether ectopic expression of IRF4 can drive the activation of ISRE mediated gene expression, we examined the effect of IRF4 expression in promoter reporter assays. First, we employed an IFNβ promoter reporter construct ($IFN\beta_{125}$-luc) containing two tandem IFNB enhancer elements each containing the ISRE-

elements (PRDIII/PRDI) known to be targeted by IRF proteins (Figure 2-3A). Transfection of 293T cells with increasing doses of IRF4 cDNA resulted in a dose dependent increase (up to 10-fold) of the IFNβ_{125} reporter construct activity relative to empty vector transfected cells (Figure 2-3B). Then, we examined whether IRF4 could induce the activation of a second well-characterized ISRE regulated promoter, ISG56. For this purpose, we used lentivirus from the pInducer22/IRF4-V5 vector to stably transduce the RL24 reporter cell lines with a doxycycline-inducible IRF4 expression vector (RL24*i*4). RL24 have been engineered to stably express an ISG56 promoter-driven firefly luciferase gene along with a renilla luciferase expression vector to serve as an internal control [170]. Stimulation of RL24*i*4 cells with 250 ng/ml of doxycycline (Dox) for 48 hrs led to the activation of the ISG56 promoter resulting in an almost 15-fold increase in luciferase activity (Figure 2-3C). Dox treatment resulted in the accumulation of IRF4 protein as determined by western blot analysis using antibodies against the V5 epitope and IRF4 that was accompanied by the detection of firefly luciferase protein synthesis and the induction of ISG60 protein expression (Figure 2-3D). To verify our luciferase reporter data, we transiently transfected pcDNA/IRF4-V5 in 293T cells and examined its effect on ISG60 protein expression. Again, IRF4 led to the induction of ISG60 protein 48 hrs after transfection (Figure 2-3E). Together, these results suggest that IRF4 acts as a positive regulator of ISRE-driven gene expression.

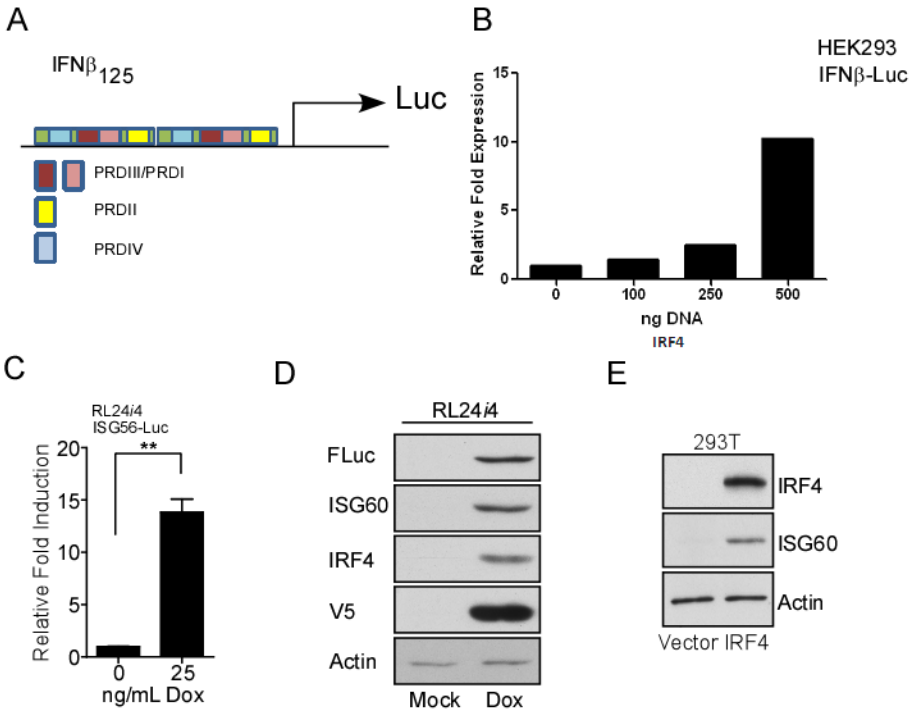

Figure 2-3. IRF4 Activates ISRE-driven Promoters.

(A) Induction of ISG60 expression by IRF4. 293T cells were transiently transfected with pcDNA/IRF4-V5 or vector control. Lysates were prepared and probed with antibodies against IRF4, ISG60, and Actin.
(B) Schematic representation of the IFNβ$_{125}$ luciferase reporter construct. Two tandem IFNβ enhanceosome sequences have been cloned upstream of the firefly luciferase gene. IRF binding domains PRDIII/PRDI are highlighted in red and pink. The NF-κB binding domain (PRDII), and the AP-1 binding domain (PRD IV) have also been depicted in yellow and blue respectively.
(C) IRF4 activates the IFNβ reporter construct. Increasing concentrations of IRF4 cDNA were co-transfected with IFNβ-Luc and pRL-null in 293 cells. Firefly luciferase activity was normalized to renilla luciferase activity and empty vector transfected cells (value 1).
(D) Analysis of ISG60 and ISG56 promoter-driven firefly luciferase protein expression in RL24*i*4 cells. Lysates were prepared from 1×10^5 cells stimulated with 250 ng/ml Dox for 48 hrs and probed with antibodies against firefly luciferase, IRF4, V5, ISG60, and Actin.
(E) Induction of ISG56-luc promoter activity by IRF4. Luciferase activity was measured from Dox-stimulated RL24*i*4 cells (48 hrs). Firefly luciferase activity was normalized to renilla luciferase activity and non-stimulated cells (value 1).

While ectopic expression of IRF4 was sufficient to activate ISRE-driven promoters and induce the expression of ISG60, we wanted to investigate the ability of IRF4 to broadly alter the transcriptional expression of ISGs. In order to investigate the effect of ectopic IRF4 expression in 293 cells, we engineered a dox-responsive cell line expressing IRF4-V5 (293*i*4). Stably transduced cells responded to 48 hr stimulation with Dox by inducing the expression of IRF4 mRNA (Figure 2-4A). Similarly, Dox stimulation also promoted dose-dependent IRF4 protein synthesis (Figure 2-4B). This upregulation in IRF4 protein expression was concomitant with a weak accumulation of ISG60, as previously observed both in Dox stimulated RL24*i*4 and 293 cells transiently transfected with IRF4 cDNA. We further examined the protein expression of Cig5 (RSAD2) and OASL proteins, two ISGs usually not expressed in normal uninfected cells but strongly upregulated upon both viral infection and interferon treatment (Figure 2-4C). Again, the both Cig5 and OASL protein synthesis was enhanced in cells expressing IRF4. To determine whether the increase in protein synthesis was due to the transcriptional activation of ISG60, Cig5, and OASL genes, as predicted from our reporter assays, we examined the levels of mRNA expression in Dox stimulated cells by qRT-PCR. As expected, IRF4 expression (Figure 2A and B) was associated with a significant increase in both ISG60 (p-value 0.005) and Cig5 (p-value 0.037) expression. Analysis of OASL mRNA expression showed a trend of upregulation, albeit not statistically significant (p-value 0.259), following Dox treatment (Figure 2-4D). Taken together, these results suggest that IRF4 can potentially mediate antiviral functions through the transcriptional upregulation of genes like ISG60, Cig5, and potentially OASL previously shown to have antiviral functions [178,179](Appendix B).

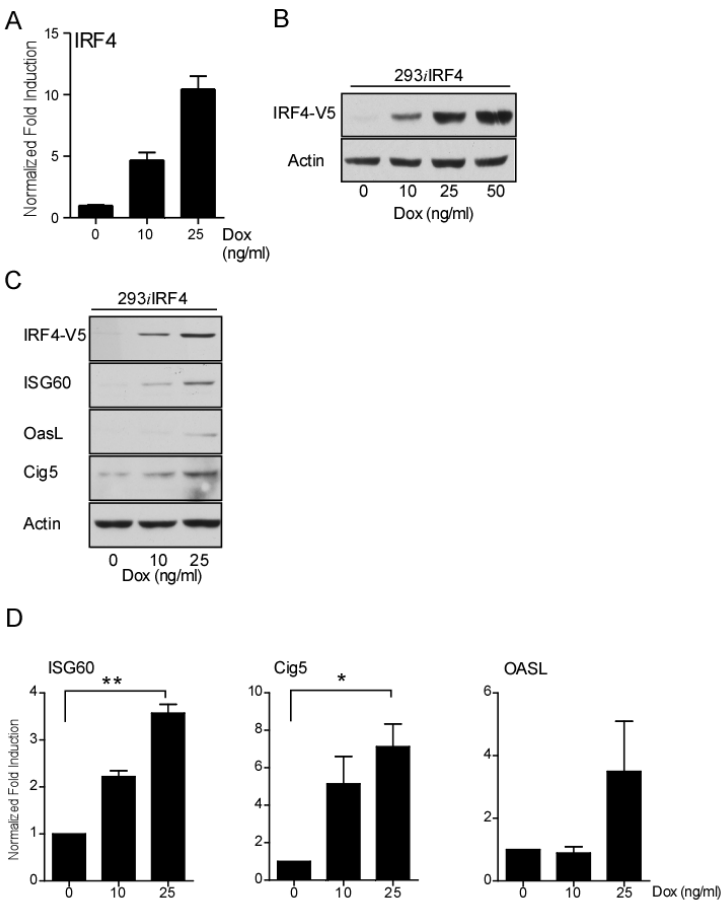

Figure 2-4. IRF4-Mediated Induction of Endogenous ISGs in Epithelial Cells.

(A) Analysis of IRF4 mRNA expression in 293*i*4. Total RNA was harvested from Dox-stimulated 293*i*4 cells and subjected to qRT-PCR using primers against IRF4 and RPL32 as indicated in materials and methods. Expression of IRF4 was normalized to RPL32 and expressed as fold change with respect to non-stimulated cells (value 1).
(B) IRF4 protein expression in 293*i*4 cells. 293*i*4 cells were stimulated with increasing doses of Dox for 48 hrs. Lysates were probed with antibodies against V5 and Actin.
(C) ISG protein expression in 293*i*4 cells. 293*i*4 cells were stimulated with increasing doses of Dox for 48 hrs. Lysates were prepared and probed with antibodies against V5, ISG60, Cig5, OASL, and Actin.
(D) Analysis of IRF4 mRNA expression in 293*i*4. Total RNA was harvested from Dox-stimulated 293*i*4 cells and subjected to qRT-PCR using primers against ISG60, Cig5, OASL and RPL32 as indicated in materials and methods. Expression of ISG mRNA was normalized to RPL32 and reported as fold change with respect to non-stimulated cells (value 1). ** $p<0.01$ and * $p< 0.05$

In order to assess whether IRF4 is a broad transactivator of ISG expression, we measured the mRNA expression levels of other ISGs induced by the activation of the IFN synthesis and signaling pathway. We first focused on the expression of ISG15 as IRF4 expression had been previously shown to activate an ISG15-promoter reporter construct [25]. As expected, the

expression of IRF4 by stimulation with Dox resulted in a modest (p-value 0.005) induction of ISG15 gene expression. Further analysis of ISG expression showed an absence of a significant transcriptional induction of PKR (p-value=0.074) and IRF7 (p-value 0.107) (Figure 2-5A). Having previously determined that IRF4 expression results in the activation of an IFNβ promoter reporter, we examined whether IRF4 expression could promote the expression of endogenous type I IFN. Interestingly, the detection of IFNβ mRNA (p-value 0.284) was not significantly affected by IRF4 expression in Dox treated 294*i*4 cells.

We then examined the effect of ectopic IRF4 expression on the transcriptional regulation of two genes associated with the late phase of the IFN response pathway, IFNα and the interferon-responsive gene, MxA. Interestingly, the stimulation of IRF4 expression by doxycycline treatment resulted in a trend of inhibition of these genes. We used pan-IFNα primers and saw a trend of inhibition by IRF4 expression. However, IRF4 led to a significant inhibition of MxA in Dox stimulated cells (p-value 0.0308) (Figure 2-5B). Given the differential regulation of ISG expression, we questioned whether the selective upregulation of ISG60, Cig5, and OASL or the selective inhibition of IFNα and MxA by IRF4 had a biological consequence in the context of a VSV infection in epithelial cells. We infected 293 cells ether stably expressing an empty control vector or 293 cells constitutively expressing IRF4 with VSV (m.o.i = 0.001). Although the gene product of the ISGs exert antiviral functions, the weak and selective induction of interferon–stimulated genes by IRF4 was not sufficient to block the viral replication of vesicular stomatitis virus (VSV) in 293 cells expressing IRF4 (Figure 2-5C). Taken together, these results suggest that although IRF4 has a potential transcriptional regulatory capacity to drive ISG expression, the transcriptional signature of IRF4 is limited relative to other IRF proteins, which can regulate the expression of ISRE responsive genes with greater intensity and

broader target specificity mediating strong antiviral responses. However, the mechanism of the selective ISG upregulation and its biological consequences still remain to be identified.

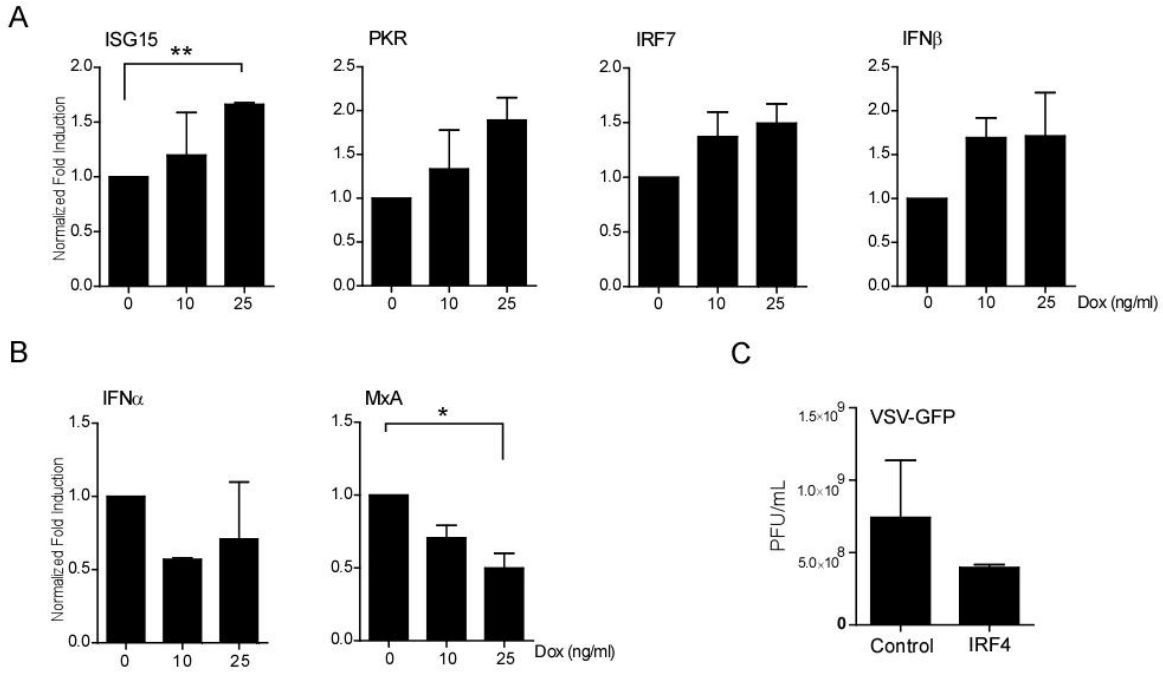

Figure 2-5. IRF4 Differentially Regulates ISG Transcription.

(A) Analysis of ISG mRNA induction by IRF4. Total RNA was harvested from Dox-stimulated 293*i*4 cells (48 hrs) and subjected to qRT-PCR using primers against ISG15, PKR, IRF7, and IFNβ and RPL32 as indicated in materials and methods. Expression of ISG mRNA was normalized to RPL32 and reported as fold change with respect to non-stimulated cells (value 1).
(B) Analysis of interferon-responsive gene mRNA induction by IRF4. Total RNA was harvested from Dox-stimulated 293*i*4 (48 hrs) cells and subjected to qRT-PCR using primers against Pan- IFNα, MxA, and RPL32. Expression of ISG mRNA was normalized to RPL32 and reported as fold change with respect to non-stimulated cells (value 1).
(C) IRF4 expression fails to protect 293 cells from viral infection. 293 cells stably expressing IRF4 or vector control were infected with VSV-GFP. Supernatants from infected cells were harvested and virus replication was measured by plaque assay on BHK21 cells.

In order to establish whether the alterations in ISG transcription caused by IRF4 expression were shared in B-cells, we generated a BJAB-derived cell line stably expressing Dox-responsive IRF4, BJAB*i*4. Forty-eight hour treatment with increasing doses of Dox resulted in the dose dependent induction of both IRF4 protein synthesis (Figure 2-6A) and mRNA

expression (Figure 2-6B). Analysis of ISG expression following Dox treatment showed that the increase in IRF4 expression was concomitant with an increase in ISG60 (Figure 2-6C) and Cig5 (Figure 2-6D) transcription and a decrease in MxA transcript (Figure 2-6E), as observed in epithelial cells. These results indicate the transcriptional regulatory functions of IRF4 are conserved across multiple cell types.

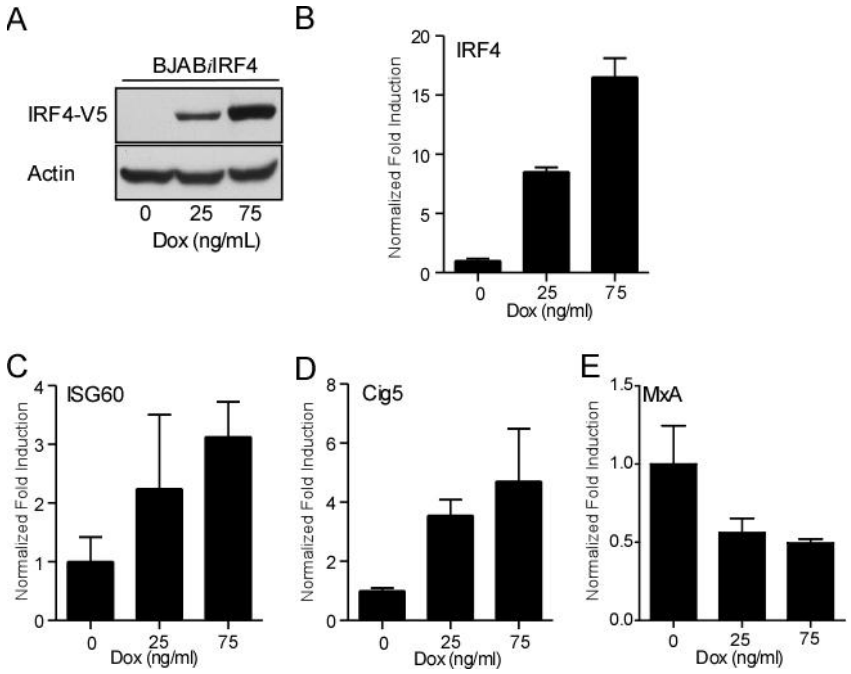

Figure 2-6. IRF4 Modulates ISG Transcription in BJAB cells.

(A) IRF4 protein expression in BJAB*i*4 cells. BJAB*i*4 cells were stimulated for 48 hrs with increasing doses of Dox as indicated. Lysates were prepared and probed with antibodies against V5 and Actin.
(B) Analysis of IRF4 mRNA expression in BJAB*i*4. Total RNA was harvested from 48 hr Dox-stimulated BJAB*i*4 cells and subjected to qRT-PCR using primers against IRF4 and RPL32 as previously described. Expression of IRF4 was normalized to RPL32 and expressed as fold change with respect to non-stimulated cells (value 1).
(C-E) ISG protein expression in BJAB*i*4 cells. BJAB*i*4 cells were stimulated with increasing doses of Dox for 48 hrs. Total RNA was harvested from 48 hr Dox-stimulated BJAB*i*4 cells and subjected to qRT-PCR using primers against ISG60 (C), Cig5 (D), MxA (E), and RPL32 as previously described. ISG mRNA expression was normalized to RPL32 and expressed as fold change with respect to non-stimulated cells (value 1).

In order to exclude the involvement of other IRF proteins in the transcriptional regulation of ISG60 and Cig5, we again employed our 293*i*4 cell-based system to examine alterations on both IRF protein synthesis and mRNA expression levels following Dox treatment. Immunoblot analysis of 48 hr Dox-stimulated cells, showed that IRF4 expression was induced in a dose dependent manner. However, when we examined the protein levels of IRF proteins, IRF-1, -3, -5, -7, -8, -9 there was no detectable increase in protein synthesis (Figure 2-7A). Similarly, there was no differential mRNA expression was observed after ectopic IRF4 expression (Figure 2-7B). Thus, it is likely that the transcriptional activation of ISG60 and Cig5 is due to direct binding of IRF4 to ISRE enhancers in their 5' promoter regions.

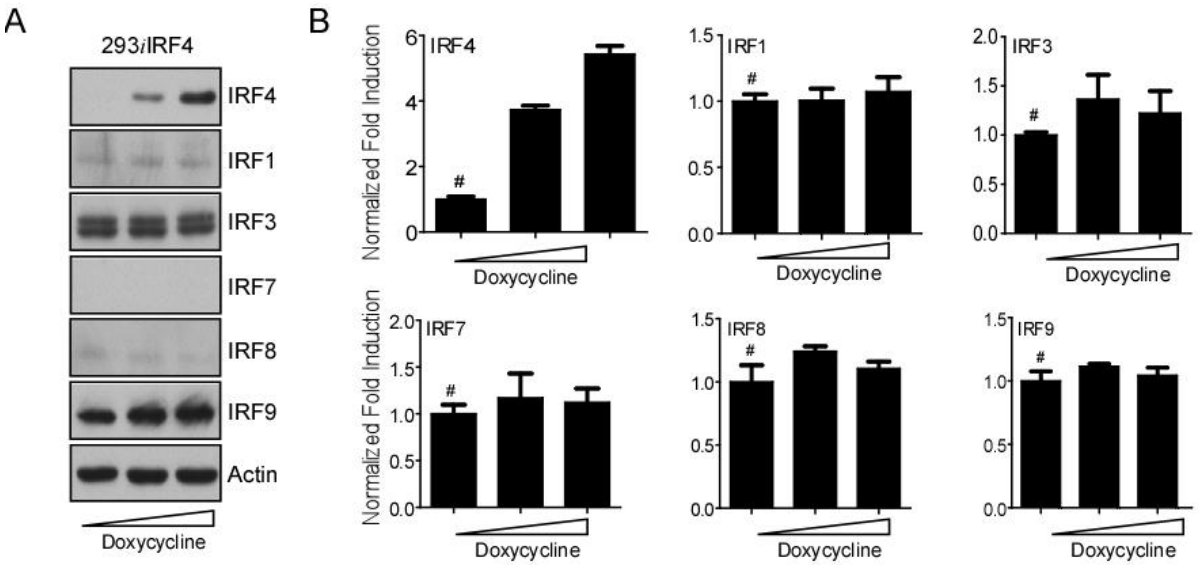

Figure 2-7. Expression of IRF Proteins in IRF4 Expressing Cells.

(A) Analysis of IRF protein expression in 293*i*4 cells. 293*i*4 cells were stimulated for 48 hrs with increasing doses of Dox as indicated. Lysates were prepared and probed with antibodies against IRF4, IRF1, IRF3, IRF7, IRF8, IRF9, and Actin.
(B) Analysis of IRF mRNA expression in 293*i*4. Total RNA was harvested from 48 hr Dox-stimulated 293*i*4 cells and subjected to qRT-PCR using primers against IRF4, IRF1, IRF3, IRF7, IRF8, IRF9, and RPL32 as previously described. The expression of IRFs was normalized to RPL32 and reported as fold change with respect to non-stimulated cells (#, value 1).

In order to dissect the *trans*- and *cis*- regulatory elements involved in the regulation of ISG60 and Cig5 expression in Dox-stimulated 293*i*4 cells, we first examined whether IRF4 localizes in the nucleus following 48 hr treatment of cells. Similar to the expression of IRF4 in BCBL-1 cells, IRF4 protein was predominantly detected in the nuclear compartment (~70%) confirming its potential role in direct transcriptional regulation of ISGs (Figure 2-8A). We then retrieved the 5' flanking sequences corresponding to nucleotides -1000 to 299 relative to the start of transcription of ISG60 and Cig5 using the Transcriptional Regulatory Element Database (TRED) database [180]. We used PROMO [181] to search for IRF transcription factor binding motifs in the DNA sequences corresponding to the promoter of ISG60 and Cig5, and to identify putative ISRE elements regulating the expression of these genes. Two putative sequences with less than 15% dissimilarity to IRF binding motifs were identified for ISG60, ISRE I (6.12%) and ISRE II (3.64%), and (Figure 2-8B and D) a potential ISRE site in Cig5 with a 1.92% sequence dissimilarity. These same putative enhancer elements were also identified as IRF response element through sequence analysis using TESS and TFSEARCH. Thus, to determine whether IRF4 binds to the identified ISRE elements, we performed chromatin immunoprecipitation (ChIP) assays on HEK293 cells constitutively expressing V5-tagged IRF4. ChIP with anti-V5 antibody showed enrichment for the regions encompassing both the ISREII/I elements of ISG60 (Figure 2-8C) and to the region containing the ISRE element on the Cig5 promoter (Figure 2-8E). These results show that ectopic expression of IRF4 in epithelial cells, results in its activation and nuclear translocation, where it can directly bind to the ISRE elements in the promoters of ISG60 and Cig5, resulting in their transcriptional activation.

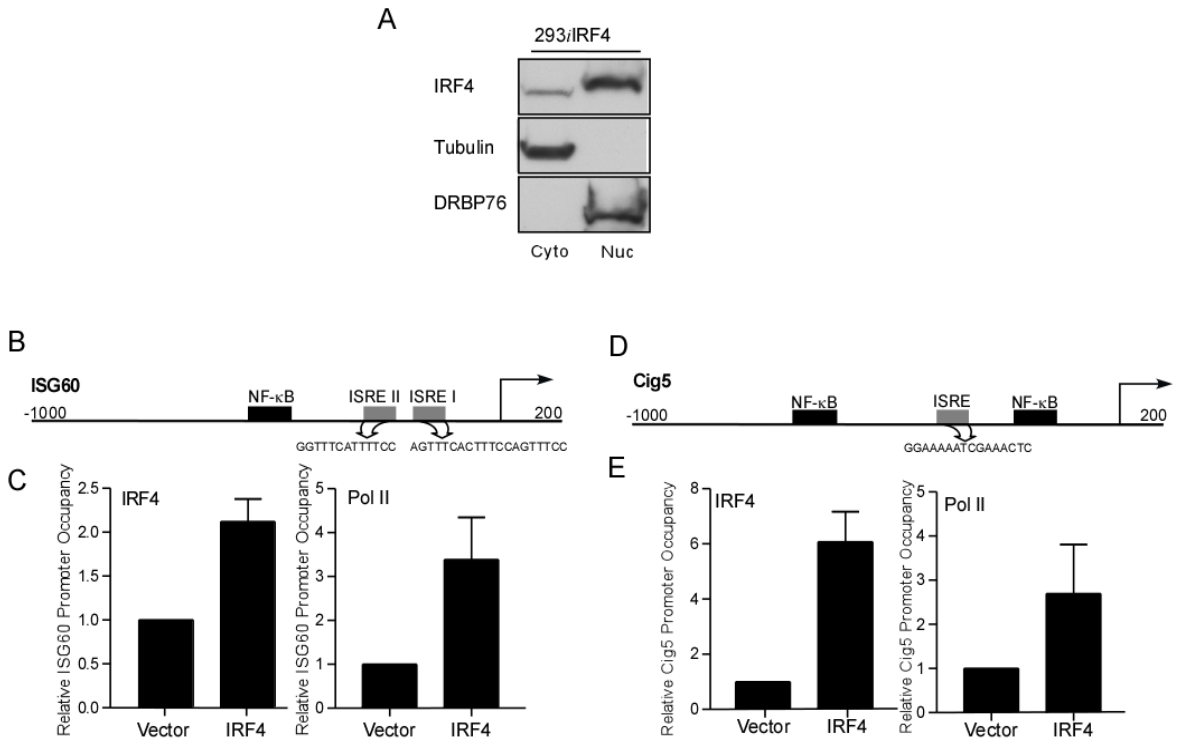

Figure 2-8. IRF4 Binds to ISRE Motifs in the ISG60 and Cig5 Promoters in Epithelial Cells.

(A) Subcellular localization of IRF4 in 293*i*4 cells. 293*i*4 cells were stimulated with Dox and cytoplasmic and nuclear protein fractions were extracted. Lysates were probed with antibodies against V5, DRBP76, and Tubulin. Expression of IRF4 was predominantly nuclear.
(B) Schematic representation of the ISG60 promoter-regulatory region depicting the positions of two ISRE sites (gray) and their sequences as predicted using the Transcriptional Regulatory Element Database (TRED). A putative -κB motif (black) was also identified.
(C) Chromatin-immunoprecipitation of IRF4 bound to ISG60 promoter. Chromatin was prepared from 1×10^7 HEK293 cells expressing IRF4-V5 (HEK293/pLenti-IRF4-V5) or vector control (HEK293/pLenti). IRF4 and Pol II binding to the promoters were assayed by ChIP assay using anti-V5 and anti-Pol II antibodies for immunoprecipitation. Relative promoter occupancy was determined relative to vector control cells as indicated in materials and methods.
(D) Schematic representation of the Cig5 promoter-regulatory region depicting position of the ISRE site (gray) and its sequence as predicted using the Transcriptional Regulatory Element Database (TRED). Two putative -κB motif (black) was also identified.
(E) Chromatin-immunoprecipitation of IRF4 bound to Cig5 promoter. ChIP assays were performed as described above. Relative promoter occupancy was determined relative to vector control cells as indicated in materials and

To define whether IRF4 participates in the regulation of ISG60 expression in PEL cell lines, we examined the association of IRF4 to the ISG60 promoter by ChIP assay in BCBL-1 cells. As previously observed in HEK293 cells, chromatin pulldown with IRF4 specific antibodies showed that IRF4 interacts with the DNA sequences corresponding to the ISREII/ISREI enhancer element in the ISG60 promoter. Specifically, there was a 7-fold enrichment in the expression of the sequences corresponding to the ISRE motifs relative to that observed after with IgG isotype control antibodies. Furthermore, ChIP analysis revealed that RNA PolII is also actively recruited to the ISG60 promoter in PEL cells. Together, these results suggest that the overexpression of IRF4 in PEL cell lines likely results in the increased expression of interferon-stimulated genes, particularly, ISG60 (Figure 2-9A). Thus we examined the expression of ISG60 proteins in whole cell lysates prepared from PEL cell lines BCBL-1, BC-1, and BCP-1. Immunoblot analysis confirmed that the expression of IRF4 across all lines. Interestingly, BCP-1 cells displayed a lower level of IRF4 expression compared to BCBL-1 and BC-1, which express similar levels of IRF4. This observation was consistent with previous analysis of IRF4 protein expression in PEL cell lines by Arguello et al. [167] (Figure 2-9B). On the other hand, the expression of ISG60 varied across all cell types tested. ISG60 protein was readily detected in cells BCBL-1 and BC-1 cells, with BCBL-1 cells expressing higher levels of ISG60 than BC-1. However, ISG60 expression was not detectable in BCP-1 cells consistent with the reduced expression of IRF4 protein. Together, these results suggest that IRF4 is a potential regulator of ISG60 expression in both epithelial and PEL cell lines.

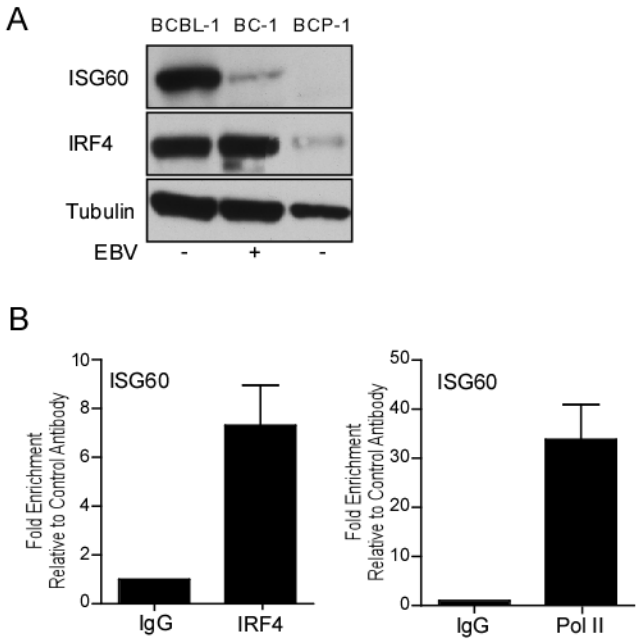

Figure 2-9. IRF4 Associates to the ISG60 Promoter in PEL cells

(A) Analysis of ISG60 protein expression in PEL cell lines BCBL-1, BC-1, and BCP-1. Whole cell lysates were prepared from 1×10^6 cells and probed with antibodies against IRF4, ISG60, and Tubulin.
(B) Chromatin-immunoprecipitation of endogenous IRF4 bound to ISG60 promoter in BCBL-1 cells. IRF4 (left) and Pol II (right) binding to the ISG60 promoter was analyzed by ChIP assay as previously described. Relative promoter occupancy was determined relative to isotype control antibody (value 1).

2.4 DISCUSSION

The induction of type I IFN secretion and downstream upregulation of ISG expression is a potent antiviral mechanism. Efforts to comprehend the regulation of this complex signaling pathway have largely described the IRF family of transcription factors as the major regulators of antiviral gene expression [2]. However, few studies on the specific contribution of IRF4 to innate immunity and the regulation of effector gene expression have been reported. On one hand, IRF4 is known to directly interact with the adaptors molecules of Toll-like receptors, MyD88, effectively inhibiting IRF5 activation after ligand stimulation [182]. On the other hand IRF4 can

bind DNA and act as both a positive and negative transcriptional regulator of antiviral effector genes [23,25,183]. The association of IRF4 with IRF and non-IRF proteins awards distinct DNA-binding specificities to the IRF4 heterodimeric complexes. Furthermore, increasing evidence suggests that components of the antiviral innate immune response regulate gammaherpesvirus gene expression and reactivation from latency [146,184-187]. While IRF4 expression is uprgulated in KSHV infected PEL cells, the role of IRF4 in regulating either cellular or viral gene expression in this malignancy has yet to be explored.

In this chapter, we have examined the transcriptional capacities of IRF4 in a biological context lacking expression of PU.1 and IRF8 and where there is an absence of exogenous stimuli (viral infection). Thus, we are looking at the inherent ability of IRF4 to regulate cellular ISG expression, through ISRE enhancer binding. Using an epithelial cell system, we identified IRF4 as a dual regulator of ISG expression. First, we observed an IFN-independent induction of ISG60 and Cig5 mRNA expression and protein synthesis post-expression of IRF4. It should be noted however, that the transcriptional signature of IRF4 was restricted to a subset of the ISGs examined and the induction of ISG60 and Cig5 was weaker than that generally observed after virus infection. Thus, IRF4 mediated ISG induction was not sufficient to confer 293 cells with protection against VSV. This is to be expected given that IRF4 expression does not induce the expression of IFNβ and thus, the activation of IFN responsive transcription complexes (ISGF3) and IFN-inducible IRF proteins (IRF1, IRF7, and IRF5) that can confer protection from viral infection by increasing the magnitude of ISG transcription is absent.

Needless to say, the biological significance of the ISG induction by IRF4 should not be understated by the failure to award protection against VSV. Enhanced ISG expression has previously been observed in certain tumor types [5,188-196]. Furthermore, the expression of

ISG60 results in the inhibition of ISG54 mediated caspase-3 activation and apoptotic cell death [197]. Other studies have shown that ISG15 expression, also weakly induced by IRF4, is increased in bladder and prostate cancers [195,196]. The degree of ISG15 expression also correlated with tumor invasiveness [195]. Thus IRF4-mediated gene induction could contribute to the disruption of homeostasis that leads to cellular transformation and oncogenesis in PEL.

We also observed a trend of inhibition of IFNα and MxA basal expression. This raises a question as to the potential mechanism by which IRF4 inhibits gene expression. It is likely that IRF4 can also bind to the ISRE elements, generally targeted by ISGF3 complex (STAT1, STAT2, IRF9), inhibiting the transcription of MxA. Support for this hypothesis is found in IRF4 ChIP-seq assays performed by Richard Myers' group (Hudson Alpha Institute for Biotechnology) and deposited in the UCSC Genome Bioinformatics database. Their results show a potential binding of IRF4 to the MxA promoter as well as those of genes involved in the relay of IFNAR/JAK/STAT signaling pathway [198]. Together, these results suggest that IRF4 might be a negative regulator of the IFN response pathway, dampening anti-apoptotic and antiviral responses against KSHV.

Lastly, we examined the protein expression levels of ISG60 across PEL cell lines, we found that high levels of IRF4 expression correlated with the induction of ISG60. Interestingly, we observed a discrepancy in expression of ISG60 between BCBL-1 and BC-1 cells. BCBL-1 cells are KSHV +ve and EBV -ve while BC-1 cells are both KSHV and EBV +ve [171,173]. This discrepancy in ISG60 expression could be attributed to the presence of EBV encoded viral proteins that can interfere with the functions of IRF4. Furthermore, the decrease in IRF4 expression in BCP-1 cells, relative to BCBL-1 cells, has been previously reported [167]. Therefore, comparative genome profiling between the established PEL cell lines could provide

useful information in identifying the distinct regulators of IRF4 expression and target gene regulation.

3.0 MODULATION OF IRF4 MEDIATED SIGNALING BY KSHV ENCODED VIRAL FLICE INHIBITORY PROTEIN

Work described in this section was partly published in the Journal of Immunology (J of Immunol. 2013 Aug 1;191(3):1476-85) by authors Adriana Forero, Patrick S. Moore, and Saumendra N. Sarkar.

3.1 INTRODUCTION

Primary effusion lymphomas are defined by being latently infected with KSHV [88]. In the infected cells, the virus persists as a naked episome (50-100 copies/cell) and expresses only a limited subset of viral genes [104,106,107,199]. These genes, known as latency-associated genes, encode KSHV vFLIP (vFLIP), viral cyclin (vCYC), latency-associated nuclear antigen LANA, LANA2 (also known as vIRF3), K12, and miRNA encoding genes [200]. The function of these proteins has been the subject of extensive study given that they are the viral mediators that promote viral persistence and tumorigenesis. Indeed, the expression of these proteins is crucial for maintenance of latency, episome tethering to the chromosomes, viral DNA replication, and segregation to daughter cells. Furthermore, these genes have been demonstrated to encode potent oncogenes capable of interacting with cellular proteins resulting in the deregulation of various cellular processes. Thus, KSHV can promote sustained cellular proliferation amidst diminished apoptotic responses and promote inflammation while evading immune clearance [104,200].

Studies focused on understanding how latency-associated proteins shape the immune responses in PEL cells have identified specific escape mechanisms including the inhibition of antigen presentation [201-203], prevention of cellular apoptosis [116,204], and the inhibition of type I IFN mediated antiviral responses [109]. Two of the latency-associated nuclear antigens, LANA and LANA2 (vIRF3) have conclusively been shown to negatively regulate the transcriptional functions of IRF3 and IRF7, as well as IRF5 resulting in the inhibition of IFNβ,

ISG expression, and cell death [111,123]. On the other hand, the activation of NF-κB by the latency protein vFLIP, results in synergistic enhancements of IRF3 and IRF7 mediated IFNβ promoter activation [141]. Studies examining the importance of vFLIP in the shaping the cellular response to viral infection with KSHV, determined vFLIP to be required for the induction of interferon stimulated gene expression [140].

In this chapter, we investigate the effect of latency-associated proteins in regulating the expression of IRF4 mediated gene transcription. Co-expression of v-FLIP enhanced transcriptional activation of ISGs by IRF4. We demonstrated that the synergistic enhancement of ISG60 transcription following IRF4 and v-FLIP co-expression is dependent on the activation of NF-κB. Thus, these studies illustrate the interplay between host factors and viral proteins in regulating gene expression and shed light into the signals that control ISG expression.

3.2 MATERIALS AND METHODS

3.2.1 Cell Lines and Reagents

Cells lines HEK293, 293FT, 293*i*4, BJAB and BCBL-1 were described in the materials and methods section in Chapter 2. WT11 cells, are HEK293-derived cell lines stably expressing Flag-tagged TLR3 [176]. 293*i*4S446D cells are HEK293-derived cells stably transduced with pInducer20/IRF4 S446D [169]. 293-derived cells were cultured in Dulbecco's Modified Eagle Medium (Lonza) containing 10% fetal bovine serum (Atlanta Biologicals) and 100 I.U./ml penicillin and 100 mg/ml streptomycin (Lonza). Sendai Virus (Cantell Strain) was purchased from Charles River Laboratories. Doxycycline (Clonetech) was resuspended in a 1 mg/ml stock

in H_20 and used at the reported concentrations. TNFα (10 ng/ml) and IL1-β (100ng/ml) were purchased from PeproTech.

3.2.2 Plasmids and Lentiviral Vectors

The expression vector pcDNA/IRF4-V5 was generated as previously described in Chapter 2. Phosphomimetic mutant of IRF4 S446D was generated by substitution of serine (TCC) to aspartic acid (GAC) by site-directed amino acid substitution of pENTR/D-TOPO IRF4-V5 using QuikChange II site-directed mutagenesis kit (Stratagene) following manufacturer's protocols using primers: 5'- CCACAGATCTATCCGCCATGACTCTATTCAAGAATGACTC-3' and 5'- GAGTCATTCTTGAATAGAGTCATGGCGGATAGATCTGTGG-3'. Mutagenesis was verified by sequence analysis. Doxycycline-inducible lentiviral vectors were generated by performing LR recombination between pENTR/D-TOPO IRF4-S446D-V5 with pInducer 20 destination vector [175].

To generate vFLIP (K13) eukaryotic expression vectors pcDNA/K13-HA was generated by PCR amplification of K13 cDNA with a C-terminal HA tag from pMSCV/K13 (Kindly provided by Dr. Preet Chaudhary, USC Norris) using primers: 5' CACCGAATTCACACCATGGCCACTTACGAG GTTCT- 3' and 5'- ATTATCTAGACTAAGGTCCTCCCAGGCTGGCATAGTCAGGCACGT CATAAGGATACTCGAGTGGTGTATGGCGATAGTGTTGG - 3'. The PCR product was then cloned into pENTR/D-TOPO (Invitrogen), sequence verified, and K13-HA was subcloned into the EcoRI-XbaI sites in pcDNA3.1(+)/Hygro (Invitrogen). The vFLIP mutant, A57L, was generated by subsititution of the alanine (TCC) codon to leucine (GAC) from the pcDNA/K13-

HA using QuickChange II site-directed mutagenesis kit using the following mutangenesis primers: 5'-CGTTTCCCCTGTTACTGGAATGTCTGTTTCGTG-3' and 5' -CACGAAACAGACATTCCAGTAACAGGGGAAACG-3'. The IκB super-repressor mutant S32A/S36A was kindly provided by Dr. Kathy Shair (University of Pittsburgh) and has been described before [205]. The pcDNA3.1-HisC/vIRF1 was generated by cloning full length vIRF1 CDS into the EcoRI and XhoI sites of pcDNA3.1-HisC vector [206]. pMET.vIL-6, was generated by cloning vIL-6 from BC-1 cells into the pMET7 expression vector [207]. pcDNA3.1-HisA/K3 was generated by cloning K3 form BC-1 cells into pcDNA3.1-TOPO. K3 was then subcloned into the BstXI site of pcDNA3.1-HisA. The pcDNA/ORF50, pcDNA-His/LANA, and pcDNA3.1-HisB/LANA2 vectors have been previously described [116,169,202]. The pcDNA3.1/vIRF1, vIL-6, pcDNA/ORF50, pcDNA3.1/K3, pcDNA-His/LANA, and pcDNA/LANA2 vectors were a kind gift of Drs. Yuan Chang and Patrick Moore (University of Pittsburgh) and have been previously described.

3.2.3 Modulation of IRF4 Activity by KSHV Proteins

293*i*4 ($8x10^5$) cells were seeded on a 6-well plate. 24 hours later, cells were transfected with 800 μg of LANA, LANA2, and vFLIP cDNA of vector control. Eight hrs post transfection, cells were trypsinized and plated on 6-wells from a 12-well plate. Cells were then stimulated with increasing doses of doxycycline (0-500 ng/ml) at 24 hrs post plating. Total RNA was harvested from cells 48 hrs post stimulation as mentioned below.

3.2.4 RNA Isolation and qRT-PCR Analysis

RNA isolation, cDNA synthesis, and qRT-PCR analysis were performed as previously described in Chapter 2 Materials and Methods. The qRT-PCR primer sets utilized in this study have been described in Table 5. ISG60 and Cig5 specific primers were described in Table 4.

Table 5. KSHV Latency-Associated Genes Set.

Gene	Orientation	Sequence
RPL32	Forward	5' - CAACATTGGTTATGGAAGCAACA - 3'
	Reverse	5' - TGACGTTGTGGACCAGGAACT - 3'
LANA (ORF73)	Forward	5'-ATACTCATTCTCCATCTCCTGCATTGC-3'
	Reverse	5'-TTCCTGTAGGACTTGAAAGCGGT-3'
LANA2 (K10.5)	Forward	5'-CTCTTTGATCTGCTTGGCATCC-3'
	Reverse	5'-TTGCATCCGTGTCGCCT-3'
vFLIP (K13)	Forward	5'-GGATGCCCTAATGTCAATGC-3'
	Reverse	5'-GGCGATAGTGTTGGAGTGT-3'

3.2.5 Subcellular Fractionations

Subcellular fractionations were done as previously described in Chapter 2 Materials and Methods. Densitometric analysis of band intensity was done using ImageJ.

3.2.6 Immunoblotting

Protein concentration from cell lysates was determined using the Bio-Rad Protein Assay (Bio-Rad). Equal amount of protein extracts were separated on 8.5% to 12% SDS–polyacrylamide gels, and proteins were transferred to PVDF membranes. Membranes were stained with Ponceau S stain for 5 minutes to assess even transfer, washed twice in Tris-buffered saline with Tween 20

(TBS-T; 20 mM Tris, 0.5 M NaCl [pH 7.5] plus 0.5% Tween 20) and blocked for 1hrs in 10% nonfat dry milk TBS-T. Primary antibody incubation was done overnight in 10% nonfat dry milk. Antibodies used anti-V5 (Invitrogen), anti-Tubulin, anti-DRBP76 were used at a concentration of 1:1000 and have been previously described [169]. Membranes were then washed twice with TBS-T and incubated with horseradish peroxidase-conjugated anti-mouse or anti-rabbit immunoglobulin G (IgG) (Rockland) diluted at 1:10,000 in TBS-T plus 10% nonfat dry milk. Blots were revealed by enhanced chemiluminescence using Hy-Glo reagent (Denville) according to manufacturer's protocol.

3.2.7 Luciferase Assays

$1x10^5$ WT11 cells were seeded in a 24-well plate. Cells were transfected with 0.5 or 1μg viral gene cDNA, 0.5 μg IFNβ_{125}-luc, and ng of renilla luciferase reporter construct. DNA quantity was kept constant using empty vector. 24 hrs post transfection, cell were seeded on 96-well white-walled plates and infected with Sendai virus (200 HAU/ml) for 8 hrs. Luciferase activity was measured by Dual-Glo Assay (Promega) as previously described in Chapter 2 Materials and Methods. Firefly luciferase activity was normalized to renilla luciferase activity and expressed as fold change relative to vector control transfected cells (value 1).

3.3 RESULTS

KSHV encodes over 80 genes, which are necessary for the control of viral gene expression, DNA replication, packaging, and assembly of virions. Several of the viral encoded genes serve to

manipulate the cellular landscape in order to counteract the host response to and favor viral genome persistence and propagation. Infection with Sendai virus (SeV), triggers the activation of RIG-I resulting in the activation of IRF3 and transactivation of the antiviral cytokine, IFNβ, and IRF3-target genes that mediate antiviral responses. In order to identify KHSV-encoded genes that could either positively or negatively modulate IRF3 functions, we employed an IFNβ promoter luciferase reporter construct. Briefly, WT11 cells were co-transfected with increasing concentration of KSHV gene expression plasmids, IFNβ_{125}-Luc, and a renilla luciferase reporter for normalization. After 48 hrs, cells were infected with 200HAU/mL SeV for 8 hrs prior to analysis of luciferase activity. Both LANA and vIRF1 inhibited IFNβ promoter activity. These results were in accordance with previously published results suggesting that both LANA and vIRF1inhibit IRF3 mediated gene transcription through distinct pathways [111,208]. On the other hand, expression of LANA2 (vIRF3) resulted in an increase in promoter activity, suggesting that LANA2 is an enhancer of IRF3 mediated transcription as previously reported [121]. Interestingly, we observed an increase in promoter activity in mock-infected RTA expressing cells, suggesting that RTA is an inducer of IFNβ (Figure 3-1). Expression of vIL6 and K3 had no significant effect on the activation of the IFNβ reporter construct. Together, these results demonstrate the mechanistic versatility by which KSHV can deregulate the antiviral responses mediated by IRF3.

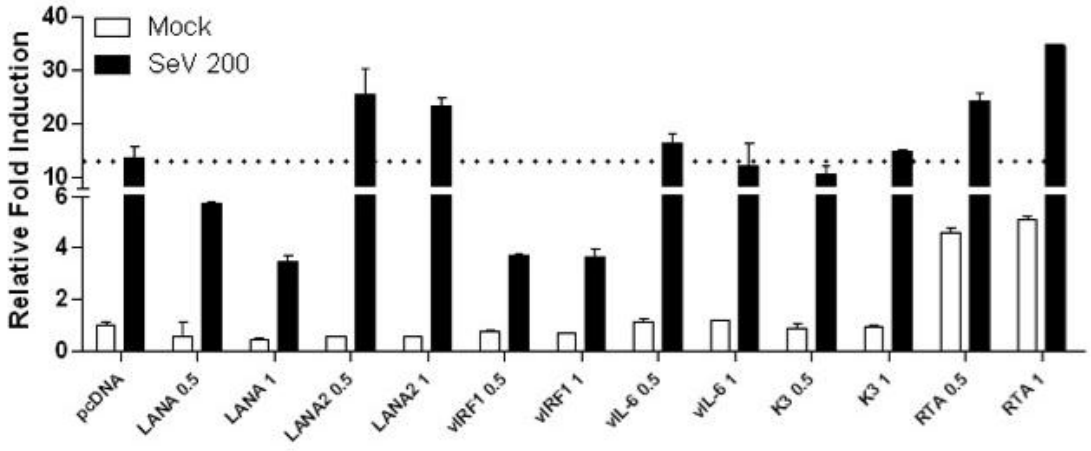

Figure 3-1. KSHV Modulators of IRF3-Mediated Gene Expression.

Identification of IRF3-mediated transcriptional modulators. WT11 cells were tranfected with cDNA corresponding to LANA, LANA2, vIRF1, vIL-6, K3, or RTA along with IFNβ125-luciferase reporter construct and a renilla luciferase expressing vector. 48 hrs post transfection, cells were infected with 200HAU/ml Sendai virus for 8 hrs. Firefly luciferase activity was measured and normalized to renilla luciferase activity. Promoter activation was reported relative to the activity of mock-infected empty vector transfected cells (value 1).

Given that the mechanisms by which LANA and LANA2 regulate IRF3-mediated gene induction have been elucidated, and taking into consideration that both LANA and LANA2 are co-expressed during latency along with IRF4 (Figure 3-2 and Figure 2-1B), we asked whether the expression of these genes had similar regulatory effects on IRF4-mediated transcription. For this purpose we focused on the ability of LANA and LANA2 to regulate the transcription of ISG60, a direct target of IRF4, in our 293*i*4 cellular system.

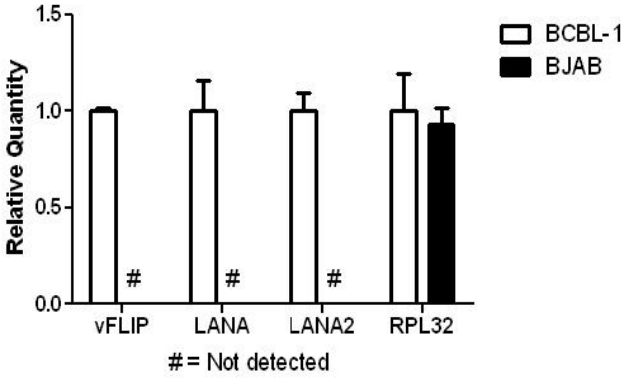

Figure 3-2. Detection of KSHV Genes in PEL Cells.

Analysis of KSHV latency associated gene transcription in BCBL-1 cells. Total RNA was harvested from 1x106 KSHV negative cell line BJAB and PEL cell line, BCBL-1. Transciption of LANA, LANA2, and v-FLIP was assessed by qRT-PCR analysis. Latency associated gene expression was reported relative to the detection in BCBL-1 cells (value 1). # represents a lack of detection of transcripts.

Transient transfection of LANA cDNA in 293*i*4 cells did not affect the induction of IRF4 following Dox treatment of 293*i*4 cells (Figure 3-3A, left). Furthermore, co-expression of LANA and IRF4 resulted in equivalent induction of ISG60 transcription in 293*i*4 cells (Figure 3-3A, right). Similarly, the expression of LANA2 neither affected the induction of IRF4 mRNA following Dox treatment (Figure 3-3B, left) nor the IRF4 mediated transcription of ISG60 (Figure 3-3B, right). These results suggest then, that the LANA and LANA2 proteins differentially target individual IRF proteins. A third latency-associated gene, vFLIP, has also been shown to synergistically enhance of IRF mediated target gene expression [141]. Thus, we investigated whether vFLIP could also enhance IRF4 mediated gene expression. Transfection of 293*i*4 cells with vFLIP did not affect the induction of IRF4 by Dox treatment (Figure 3-3C, right) however the co-expression of IRF4 and vFLIP resulted in a synergistic enhancement in ISG60 transcription in cells stimulated with Dox (Figure 3-3C, right). Expression of vFLIP alone was not sufficient for the induction of ISG60 mRNA. These results suggest that the expression of ISGs is primarily controlled by the activation of IRF proteins.

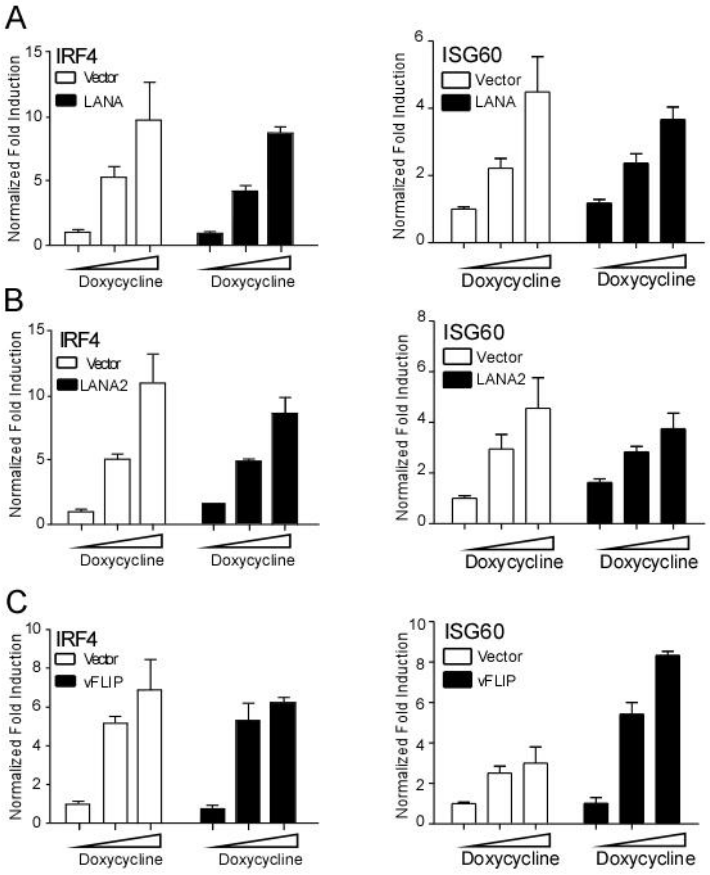

Figure 3-3. Effect of KSHV Latency-Associated Genes on IRF4-mediated Transcription.

(A), (B) and (C) Quantitation of ISG60 mRNA induction in 293*i*IRF4 cells transfected with KSHV latency-associated viral proteins. 8×10^5 cells were transfected in a 6-well plate with 800ng of vFLIP (A), LANA (B), LANA2 (C) expression vectors or their respective empty vector controls. Eight hours post transfection, cells were transferred to 24-well plates and stimulated with increasing doses of Dox. Total RNA was harvested 48 hrs post stimulation. IRF4 (left panel) and ISG60 (right panel) mRNA induction was quantified by qRT-PCR. Samples were normalized to RPL32 and expressed as fold change with respect to untreated vector control cells (value 1).

The function of IRF proteins is regulated by their temporal expression, their dimerization and translocation to the nucleus, and the phosphorylation of serine and threonine residues in the AIE domains located in the C-terminus of IRF proteins (Figure 3-4A). In order to identify the mechanism by which vFLIP co-expression enhances IRF4-mediated transcription we used two distinct approaches. First, we examined whether the expression of vFLIP resulted in increased IRF4 nuclear localization 293*i*4 cells stimulated with Dox. Analysis of IRF4 subcellular

translocation confirmed that as previously observed in Figure 2-8, Dox treatment of 293*i*4 resulted in the localization of over 70% of the total IRF4 protein expression to the DRBP76 positive nuclear fraction in vector transfected cells. Expression of vFLIP did not affect the subcellular localization of IRF4 (Figure 3-4B). Secondly, we examined the effect of vFLIP expression on the C-terminal phosphorylation of IRF4 at Serine 446, which is phosphorylated by ROCK2 in T-cells and required for the transcriptional activation of IRF4 [20]. For this purpose, we generated a phosphomimetic mutant of IRF4 by substituting the serine residue for an aspartic acid residue by site-directed mutagenesis. We then generated the stable cell line 293*i*IRF4/S446D, which expressed the phosphomimetic mutant of IRF4 in response to Dox treatment (Figure 3-4C). vFLIP was then co-expressed by transfecting 800 ng of cDNA and stimulating cells with Dox. Both vector and vFLIP transfected cells expressed comparable levels of IRF4 mRNA after 48 hrs of Dox stimulation at the indicated doses (Figure 3-4D). Furthermore, stimulation of 293*i*4/S446D cells with Dox showed expected increase in ISG60 mRNA in empty vector transfected cells and the transcription of ISG60 was further enhanced by the co-expression of vFLIP (Figure 3-4E). Should vFLIP affect the phosphorylation at S446, we would have expected to see a loss in the enhancement of ISG60 transcription. Taken together these data suggests that the effect of vFLIP on IRF4-mediated transcription is independent of phosphorylation of S446 or IRF4 nuclear translocation, suggesting that the observed transcriptional enhancement is likely due to mechanisms independent of IRF4 activation and function.

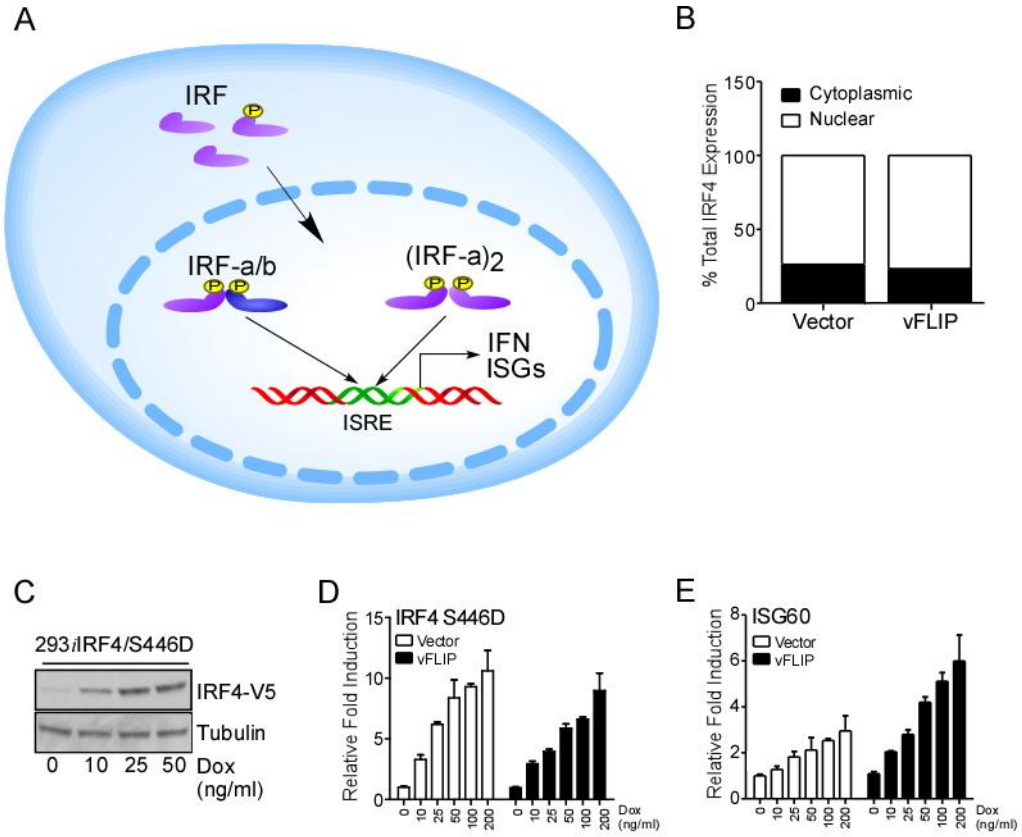

Figure 3-4. IRF4 Activation is Unchanged by vFLIP Co-Expression.

(A) Schematic representation of IRF protein activation. IRF proteins are generally found in a monomeric hypophosphorylated form in the cytoplasm. Upon serine phosphorylation in the C-terminus (yellow circles), IRF proteins form dimers and translocate to the nucleus where they regulate ISRE-driven gene expression.
(B) Effect of vFLIP on IRF4 subcellular localization. 293*i*4 cells were transfected with pcDNA-K13 and stimulated with 0.5μg/ml Dox for 48 h. Cells lysates were fractioned and subjected to immunoblotting with antibodies against V5. Immunoblots were quantified by densitometry and plotted as total IRF4 localized between the cytoplasmic and nuclear fractions.
(C) Western blot analysis of IRF4 protein induction following Dox stimulation in 293*i*IRF4/S446D cells. Cells were stimulated for 48 h with Dox as indicated. Lysates were prepared and subjected to immunoblotting using antibodies against V5 and Tubulin.
(D and E) Effect of IRF4-S446D on vFLIP-mediated enhancement of ISG60 mRNA induction. 293*i*4 and 293*i*4/S446D were transfected and stimulated as previously described. IRF4 (D) and ISG60 (E) mRNA induction was quantified by qRT-PCR. Samples were normalized to RPL32 and expressed as fold change with respect to untreated vector control cells (value 1).

Unlike other viral encoded FLIPs, a unique feature of KSHV encoded vFLIP is the ability to activate NF-κB by direct interaction with the IKK complex [137], which was shown to be necessary for the transcriptional enhancement of the IFNβ promoter in cells ectopically expressing vFLIP [141]. Thus we examined whether the requirement for NF-κB activation was necessary for the transcriptional enhancement of ISG60 mediated by the expression of vFLIP. First, we treated vFLIP-transfected 293*i*4 cells with NF-κB inhibitor, Bay 11-7082. Briefly, 8 hrs post transfection with vFLIP or empty vector, cells were stimulated with 5 μM of Bay 11-7082 and Dox or DMSO for an additional 48 hrs. Treatment with Bay 11-7082 resulted in a 2-fold reduction of the transcriptional enhancement of ISG60 (Figure 3-5A). We confirmed the results observed by using chemical inhibitors by employing a dominant negative IκBα (SR-IκBα). IκBα phosphosphorylation at serine residues 32/36 results in its proteolytic degradation releasing NF-κB subunits[209]. Substitution of Ser 32/36 to Ala in IκBα results in constitutive repression of NF-κB [210]. Co-transfection of cells with SR-IκBα and vFLIP results in a 7-fold reduction of the transcriptional enhancement of ISG60, confirming the requirement for NF-κB activation (Figure 3-5B). Lastly, we tested the role for NF-κB in vFLIP-mediated ISG enhancement using a genetic mutant of vFLIP impaired in its ability to activate NF-κB. Activation of NF-κB by vFLIP is mediated by the direct contact between vFLIP and IKKγ. This relies on a binding cleft in the death domain of vFLIP containing a critical Alanine residue in position 57 [211]. Substitution of Ala 57 to Leu by site-directed mutagenesis, renders vFLIP unable to activate NF-κB as determined by using a NF-κB-responsive promoter reporter assay. Transient transfection of 293T cells with wt vFLIP resulted in a seven-fold increase in the NF-κB responsive promoter activity relative to empty vector transfected cells. On the other hand, expression of vFLIP A57L

did not activate the reporter promoter (Figure 3-5C). Thus, we asked whether co-expression of IRF4 and the mutant vFLIP would result in changes in ISG60 transcription in 293*i*4 cells treated with Dox. As expected, expression of vFLIP wt or A57L did not affect the induction of IRF4 after stimulation with Dox (Figure 3-5D, left). Synergistic enhancement of IRF4-mediated ISG60 induction, however, was absent in A57L compared to wild-type vFLIP transfected cells (Figure 3-5D, right). Again, no induction of ISG60 was observed in cells transfected with either WT or mutant vFLIP expression vectors in the absence of Dox treatment. These results suggest that vFLIP upregulates IRF4 mediated ISG60 induction in a NF-κB dependent manner.

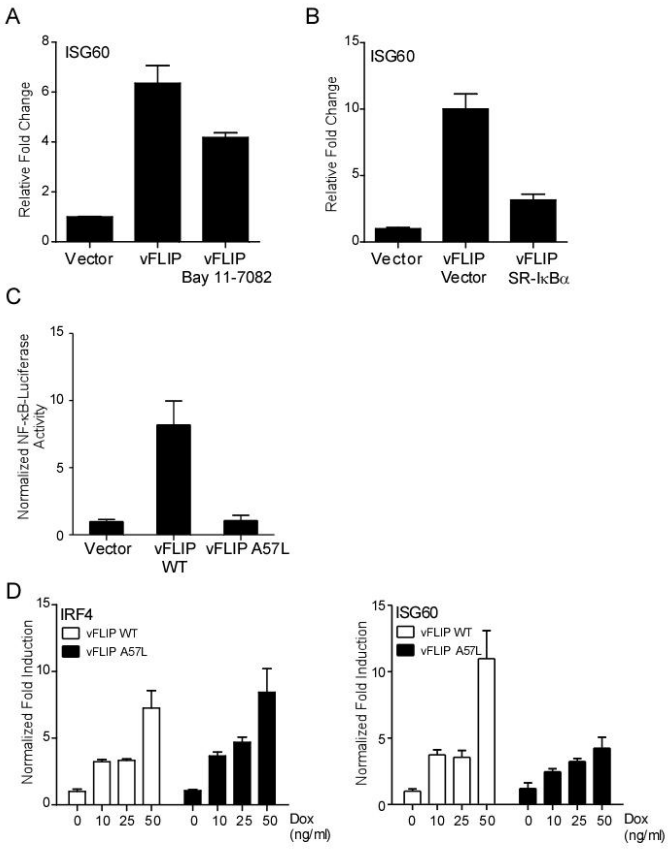

Figure 3-5. vFLIP Enhances ISG60 Induction in an NF-κB Dependent Manner.

(A) Effect of Bay 11-7082 on ISG induction by IRF4 and vFLIP. 293*i*IRF4 were transfected with vector control or vFLIP for 8 h. After transfection, cells were stimulated with Dox in the presence or absence of 5μM Bay 11-7082 for an additional 48 h. ISG60 mRNA induction was analyzed by qRT-PCR as described before. Samples were normalized to RPL32 and expressed as fold change with respect to untreated vector control cells (value 1)
(B) Effect of SR-IκBα expression on ISG induction by IRF4 and vFLIP. 293*i*IRF4 were co-transfected with vFLIP and SR-IκBα or the respective vector controls for 24 h. After transfection, cells were stimulated with Dox for an additional 48 h. ISG60 mRNA induction was analyzed by qRT-PCR as described before. Samples were normalized to RPL32 and expressed as fold change with respect to untreated vector control cells (value 1).
(C) NF-κB luciferase reporter assays from 293T cells transfected with wild-type vFLIP, vFLIP A57L, or empty vector control. 293T cells were co-transfected with 1μg of cDNA, 0.4 μg of NF-κB luciferase reporter construct and 12 ng of pRL-null. Firefly luciferase activity was measured 48 h post transcription and normalized to renilla luciferase.
(D) qRT-PCR analysis of IRF4 and ISG60 induction in 293*i*IRF4 cells transfected with wild-type or A57L mutant vFLIP. RNA was extracted after transfection of WT or mutant vFLIP cDNA for 8 h followed by 48 h of Dox stimulation. IRF4 (left) and ISG60 (right) mRNA induction was quantified by qRT-PCR. Samples were normalized to RPL32 and expressed as fold change with respect to untreated cells (value 1).

Finally, to confirm the involvement of NF-κB in IRF4 mediated ISG60 upregulation, we treated cells with an NF-κB activating cytokines, tumor necrosis factor α (TNFα) and Interleukin-1β (IL-1β), and examined ISG60 and Cig5 transcript levels in presence of IRF4. 293*i*4 cells were stimulated with increasing doses of Dox for 48 h followed by 12 h stimulation with 10 ng/ml TNFα or 1□□□ng/ml IL-1β. The levels of IRF4 transcription following Dox stimulation was equivalent amongst the cells treated with DMSO, TNFα, or IL-1β (Figure 3-6A). Co-stimulation with TNFα in presence of IRF4 resulted in markedly increased ISG60 and Cig5 transcription. To be noted, treatment with TNFα alone did not result in a significant induction of either ISG60 or Cig5 mRNA (Figure 3-6B). Similarly, treatment with IL-1β resulted in a significant synergistic enhancement of ISG60 and Cig5 mRNA transcription in cells expressing IRF4, without inducing the expression of either gene in the absence of Dox stimulation (Figure 3-6C). Taken together, these results indicate that activation of NF-κB by vFLIP or pro-inflammatory cytokines TNFα or IL-1β is necessary but not sufficient to get the maximal induction of IRF4-dependent ISG gene expression. Thus, the transcriptional regulation of these ISGs is primarily mediated by IRF4 binding to the ISRE and further enhanced by the recruitment of other transcription factors, like NF-κB, to the 5' promoter regulatory region.

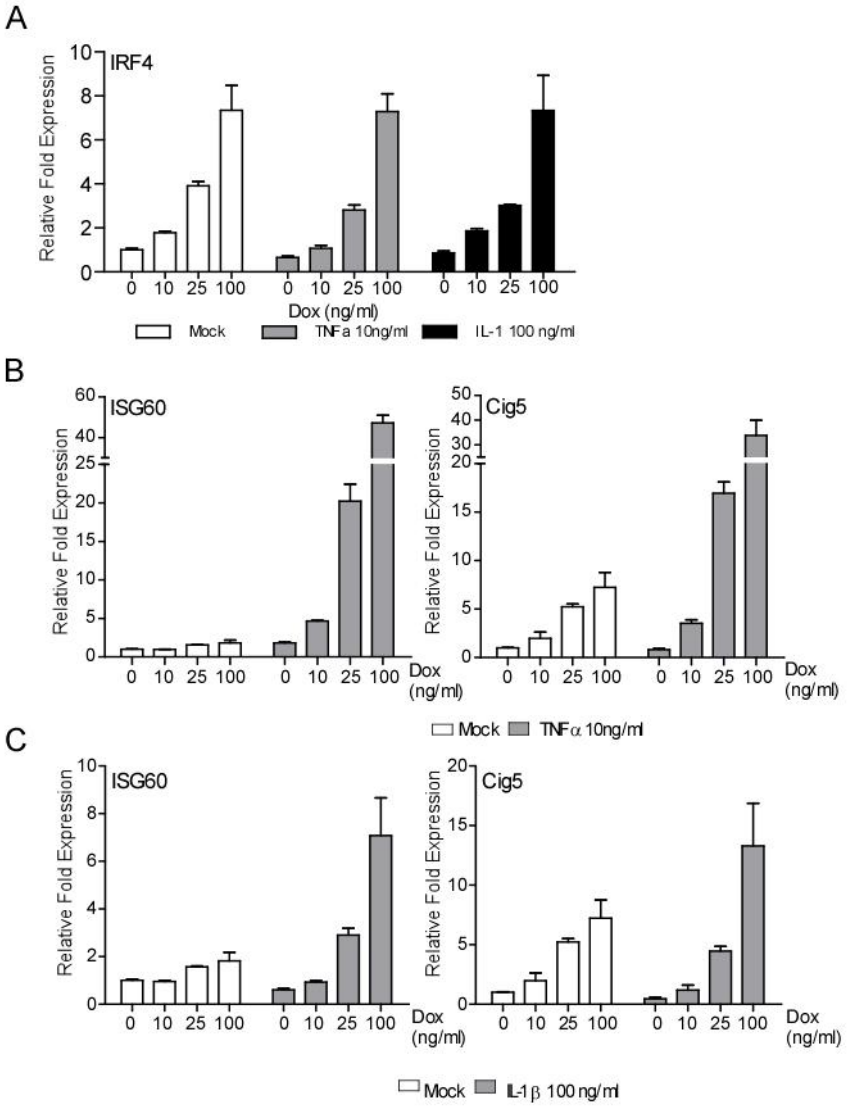

Figure 3-6. Proinflammatory Cytokines Enhance ISG Induction by IRF4.

(A) Analysis of IRF4 induction in Dox-stimulated 293*i*IRF4 cells. Cells were co-stimulated with Dox for 48 hrs and DMSO, TNFα (10 ng/ml), or IL-1β (100 ng/ml) for 12 hrs. Samples were normalized to RPL32 and expressed as fold change with respect to untreated cells (value 1).
(B) Analysis of ISG60 induction in TNFα stimulated cells. RNA was harvested from 293*i*4 cells treated as mentioned above. Samples were normalized to RPL32 and expressed as fold change with respect to untreated cells (value 1).
(C) Analysis of ISG60 induction in IL-1β stimulated cells. RNA was harvested from 293*i*4 cells treated as mentioned above. Samples were normalized to RPL32 and expressed as fold change with respect to untreated cells (value 1).

3.4 DISCUSSION

IRF4 expression leads to the induction of genes previously described to mediate antiviral responses as well as inhibit anti-proliferative cellular responses. Thus, we asked whether KSHV encodes modulators of IRF mediated responses resulting in the inhibition of anti-viral responses or enhancing the expression of genes that potentially promote tumorigenesis and viral persistence. For this purpose, we employed two cell-based assays to allow for the efficient screening of genetic modulators of both IRF3-mediated immune responses (WT11) and IRF4 transcriptional functions (293*i*4). The goal of this approach is to identify modulators and classify them in three different categories: activators, enhancers, and inhibitors. The activators are genes that result in the induction of promoter activity or mRNA transcription, in the absence of external stimuli, as observed for the induction of ISG60 by ectopic IRF4 expression. Transcription enhancers are genes that do not affect basal target gene expression upon being expressed, but lead to increased transcriptional activation when co-expressed along with the stimulus. Lastly, we have transcriptional inhibitors, which as their name indicates, inhibit the transcriptional activation of genes upon being expressed.

Using our WT11-based cellular system we screened KSHV encoded proteins previously implicated in the regulation of immune evasion strategies to identify modulators of IRF-mediated transcription. We identified all three classes of modulators of IRF3 mediated transcription (Figure 3-1). LANA expression led to an inhibition of IFNβ–promoter activation following infection with SeV. The mechanism of inhibition has been reported to correspond to the binding of LANA to the PRDI/PRDIII domains in the IFNβ enhancer, thus preventing recruitment of IRF3 [111]. vIRF1 was also an inhibitor of transactivation and it is thought that this is due to

p300 binding by vIRF1 preventing the formation of the CBP/p300-IRF3 transcriptional complex [208]. On the other hand, we found that LANA2 (vIRF3) was an IRF3 enhancer, given that no changes in basal luciferase activity were observed upon its expression, yet after stimulation, co-expression of LANA2 led to a 1.9-fold increase in IFNβ promoter activity. Interestingly, the effects of LANA2 on the transcriptional functions of IRF3 still remain unclear. Our observation is in accordance with previous reports suggesting that LANA2 enhances IRF3 mediated responses [121]. Lastly, we identified RTA, the major regulator of KSHV lytic reactivation, as an activator of IFNβ expression. Ectopic expression of RTA led to an almost 5-fold increase in IFNβ transcription and the promoter activity was further enhanced upon SeV infection. The mechanisms and implications of these observations will be further discussed in Chapter 4.

Using or 293*i*4 based system, we examined the modulatory function of genes expressed during viral latency using ISG60 target gene. We focused on LANA and LANA2 as we had previously shown they acted as modulators of IRF3, and we examined the effect of vFLIP, which had been shown to enhance the expression of IRF3/7 induction of IFNβ promoter reporters. To our surprise neither LANA nor LANA2 affected the expression of ISG60 mRNA. The difference in IRF3 versus IRF4 targeting likely due to the fact that IRF3 mediates strong antiviral and anti-proliferative responses. We then examined the effect of vFLIP expression and found that vFLIP enhances ISG60 transcription by activating NF-κB. This result is in accordance to previous reports showing that vFLIP enhances IFNβ transcription by stimulating the activation of NF-κB.

We have shown that the effect of vFLIP is independent from the activation of IRF4. Thus, we speculate that the induction of NF-κB subunits results in their recruitment to enhancer element in the promoters of IRF4 target genes. While the transcription of IFNβ has been widely shown to be regulated by binding of IRF3/7 to PRDI/PRDIII and further enhanced by binding of

NF-κB to PRDII [212], the role of NF-κB in the enhancement of ISG transcription has not received much attention. Recent bioinformatics analysis has shown that c-REL, an NF-κB transcription factor, is involved in the regulation of a subset of ISGs. Chromatin immunoprecipitations and gene expression analysis confirmed that c-REL binds to the promoter of ISG60 following treatment with IFN [213]. In this study we show, that indeed ISG60 and Cig5 are regulated both by IRF4 and NF-κB activation in a physiological context. Although further studies are still required to identify NF-κB subunits activated by vFLIP that bind the IRF4 target promoters, our study has establishes the hierarchical contributions of these two transcription factors to conclude that IRF4 expression is necessary and sufficient for the activation of ISG60 expression, whereas NF-κB requires the prior assembly of IRF4 complexes in order to bind to the target gene promoter [214].

4.0 IRF4 IS REQUIRED FOR THE MAINTENANCE OF KSHV LATENCY IN PRIMARY EFFUSION LYMPHOMA CELLS

Work described in this section was partly published in the Journal of Immunology (J of Immunol. 2013 Aug 1;191(3):1476-85) by authors Adriana Forero, Patrick S. Moore, and Saumendra N. Sarkar.

and

Submitted for publication by authors Adriana Forero, Frank Jenkins, and Saumendra N. Sarkar.

4.1 INTRODUCTION

The replication and transcription activator (RTA) protein, encoded by ORF50, mediates the switch from latency into lytic reactivation [152]. RTA is a sequence specific DNA-binding immediate early (IE) protein that regulates the expression of the early (E) genes encoded by KSHV. Like most proteins involved in the regulation of gene transcription, RTA is regulated through its temporal expression, posttranslational modifications that result in its activation, and the ability to oligomerize and interact with cellular regulators of gene expression [156]. This last step in regulation is important for the diverse target gene expression regulation by RTA.

Studies of RTA structure and function have uncovered an interesting relationship between RTA and IFN-regulatory factors (IRFs), which regulate the transcription of antiviral genes. Primary structure analysis of the RTA DNA-binding domain, revealed a partial homology with the IRF binding domain [163]. Four specific residues were distinguished as being conserved between all the cellular IRFs and RTA (RTA P102, F120, K152, A158). Mutation of any of these residues decreased the transactivation of genes by RTA. A mutation in IRF7 K97, which is homologous to K152 of RTA impairs its ability to induce target gene expression [215]. These results suggest that both cellular IRF proteins and RTA can potentially recognize similar motifs found in the promoters of innate immune effectors and viral genes.

Furthermore, a relationship between RTA and the IRF proteins DNA binding has also been described. While no obvious RRE consensus sequences have been identified, RTA has been shown to bind to RTA-responsive element (RRE) that shares sequence similarity to the ISRE

sequences located in the promoters of ISGs [163]. One of these target sites (5'-ATTTTTCGTTTGTG-3') is found in the ORF57 promoter. These ISRE-like sequences are found in various early genes and IRF7 has been shown to be able to bind to the ORF57 ISRE-like site resulting in dampened ORF57 after reactivation. These studies raise a question as to the potential contribution of innate immune cellular factors in the negative regulation of viral gene expression. Having established in Chapter 2 that IRF4 binds to DNA and acts as either a positive or a negative regulator of gene expression and given the sequence similarities between ISRE and RRE, it is likely that IRF4 regulates KSHV viral gene expression.

In this chapter, we explore the role of IRF4 in controlling KSHV gene expression in primary effusion lymphoma cells. We explore the ability of IRF4 in regulating the expression of viral genes regulated by RTA binding to sequences that share similarity to the ISRE enhancer element. Using luciferase reporter assays and qRT-PCR analysis, we show that IRF4 expression results in the inhibition of RTA protein and mRNA synthesis as well as an inhibition in RTA-mediated promoter transactivation. We also show that IRF4 binds to the promoter of RTA-target gene, ORF57, and thus likely preventing binding of RTA to its target promoters. Finally, we have confirmed the transcriptional inhibitory role of IRF4 on RREs by using a reverse genetic approach. Knockdown of IRF4 in PEL cells resulted in the spontaneous induction of RTA transcription, as well as an induction of lytic genes. Taken together our results uncover a mechanism in which the host response limits viral gene expression and lytic replication that provides an advantage to KSHV by allowing the virus to escape immune clearance and promote oncogenesis.

4.2 MATERIALS AND METHODS

4.2.1 Cell Lines and Reagents

293FT, BCBL-1, and BCBL-1-derived cells were cultured as previously described in Chapter 2. FLYRD18 cells were cultures in DMEM supplemented with 10% FBS, 100 I.U./ml penicillin, and 100 mg/ml streptomycin. Doxycycline (Clonetech) stocks were made with a 1 mg/ml concentration in H_2O and used at the indicated doses. 12-*O*-Tetradecanoylphorbol-13-acetate (TPA) was purchased from Sigma-Aldrich and used at the indicated concentrations. Dimethyl sulfoxide (DMSO) (Fisher Scientific) was used as vehicle control.

Table 6. Chapter 4 - Cell Lines.

Cell Line	Description	Source	Reference
FLYRD18	HT1080-derived packaging cell line producing Moloney murine leukemia virus expressing feline virus RD-114 envelope glycoprotein.	Staudt Lab (NIH)	[216]
BCBL-1/mCAT	BCBL-1-derived cells stably transduced with feline ecotropic receptor.	Sarkar Lab	
BCBL-1/mCAT/TetR	BCBL-1/mCAT-derived cells stably transduced with bacterial tetracycline receptor.	Sarkar Lab	
BCBL-1/shCTRL	BCL-1/mCAT/TetR -derived cells stably transduced with feline ecotropic receptor, TetR, and non-targeting shRNA.	Sarkar Lab	
BCBL-1/shIRF4	BCL-1/mCAT/TetR -derived cells stably transduced with feline ecotropic receptor, TetR, and IRF4 targeting shRNA.	Sarkar Lab	
BCBL-1/shIRF4b	BCL-1/mCAT/TetR-derived cells stably transduced with feline ecotropic receptor, TetR, and IRF4 targeting shRNA.	Sarkar Lab	
BCBL-1*i*4	BCBL-1 –derived doxycycline-inducible IRF4 expressing cell line generated by lentiviral tranduction with pInducer20/IRF4-V5.	Sarkar Lab	[169]

4.2.2 Plasmids and Retroviral vectors

Retroviral packaging plasmids pHIT60 expressing MoMuLV Gag and Pol and the ecotropic envelope-expressing plasmid pHIT/EA6X3*, along with the doxycycline-inducible non-targeting shRNA (shCTRL), IRF4 targeting shRNA (shIRF4 and shIRF4b) retroviral vectors were obtained from Dr. Louis Staudt (NIH) and have been previously described [18]. pcDNA-ORF50 and pNut-1-Luc were provided by Dr. David Lukac (Rutgers) and have been previously described [149,217]. Lentivirus packaging and the generation of stable cell lines was described in Chapter 2 – Materials and Methods. pcDNA/LANA, pcDNA/LANA2, pcDNA/ORF50 have been previously described [116,202,217]. pRL-Null vector expressing renilla luciferase was obtained from Promega.

4.2.3 RNA Isolation and qRT-PCR Analysis

BCBL-1*i*IRF4 cells were stimulated with Dox for 48 h, followed by stimulation with 15 ng/ml TPA for 2, 4, and 8 h prior to harvest. To evaluate efficient IRF4 knockdown in BCBL-1/shCTRL, BCBL-1/shIRF4, and BCBL-1/shIRF4b cells were treated with 100 ng/ml Dox for 72 hrs prior to harvest. The evaluation of lytic gene transcription was done after stimulation of BCBL-1-derived cell lines with Dox and/or TPA at the indicated doses. RNA isolation and cDNA synthesis was performed as previously described. Fold induction of target gene mRNA levels were normalized to RPL32 and non–TPA-stimulated cells (value 1).

Table 7. KSHV Lytic Gene Primer Sets

Gene	Orientation	Sequence
RPL32	Forward	5' - CAACATTGGTTATGGAAGCAACA - 3'
	Reverse	5' - TGACGTTGTGGACCAGGAACT - 3'
RTA (ORF50)	Forward	5’-GAACTACTCGAGCTGTGCCCTCCAGCTCTCAC-3’
	Reverse	5’-GGACGTAAGCTTACAGTATTCTCACAACAGAC-3’
v-IL6	Forward	5’-TGGATGCTATGGGTGATCGA-3’
	Reverse	5’-GGCTCTAGAATACCCTTGCAG-3’
PAN	Forward	5’-GTTTTCTTATGGATTATTAAGGGTC-3’
	Reverse	5’-AGGTGAAGCGGCAGCCAAGGTGAC-3’
ORF57	Forward	5’-GGGTGGTTTGATGAGAAGGA-3’
	Reverse	5’-CGCTACCAAATATGCCACCT-3’
ORF57 ISRE	Forward	5’-ACACTTATGAGTCAGTGTTTTGCCAG-3’
	Reverse	5’-GGCAGCCAGGTTATATAGTGGGATTA-3’
K8.1	Forward	5’-AAAGCGTCCAGGCCACCACAGA-3’
	Reverse	5’-GGCAGAAAATGGCACACGGTTAC-3’
ORF17	Forward	5’-GAGCGACTGCTGGCTTCAAC-3’
	Reverse	5’-CGGTGGAGAAGACTCC-3’
ORF67	Forward	5’-CCCAATATACCGCTGTGAGT-3’
	Reverse	5’-TTTCCCACCAACGGCC-3’
LANA (ORF73)	Forward	5’-ATACTCATTCTCCATCTCCTGCATTGC-3’
	Reverse	5’-TTCCTGTAGGACTTGAAAGCGGT-3’

4.2.4 Nuclear Fractionations

Nuclear lysates were prepared as described on Chapter 2 Materials and Methods.

4.2.5 Luciferase Assays

293T (1.5×10^5 cells/well) in 24-well plate were co-transfected with 100 or 500 ng of IRF4 expression plasmid, 0.4□g Nut-1 luciferase reporter construct, 24ng pRL-Null and either 75 ng of RTA cDNA or empty vector using Fugene 6 as previously indicated. Total transfected DNA

levels were kept equal with empty vector (575ng). Forty-eight hours post transfection, luciferase activity was measured using the Dual-Glo luciferase assay system (Promega). Firefly luciferase activity was normalized to renilla luciferase activity and expressed as fold induction relative to empty vector transfected cells.

4.2.6 Ectopic IRF4 Expression in BCBL-1 cells

A total of 2×10^5 BCBL-1*i*4 cells per milliliter were treated with 1 μg/ml Dox or left untreated for 48 h, followed by stimulation with 15 ng/ml TPA or DMSO for 12 h. Cells were harvested and whole cell lysates were prepared using RIPA buffer (50mM Tris-HCl [pH7.4], 150mM NaCl, 1% NP-40, 0.25% sodium deoxycholate, 1mM EDTA, 1mM PMSF, 1x Protease inhibitor cocktail) and incubated in ice for 30 minutes prior to SDS-PAGE. Equal protein concentration was resolved and immunoblotted with anti-IRF4 (Cell Signaling), DRBP76 [176], and Tubulin antibodies (Santa Cruz). Density analysis was done using ImageJ.

4.2.7 Immunoflourescent Microscopy

BCBL-1/shIRF4 cells were treated with 100 ng/ml Dox for 96hrs. Cells were fixed with 4% PFA and permeabilized with 0.1% Triton-X in PBS. Cells were seeded onto poly-Lysine coated slides (Fisher Scientific) and left to air dry. After blocking with 10% goat serum for 1 hr at 37^{o}C, cells were incubated with KSHV positive human sera for 1hr at 37^{o}C, washed and incubated with antibodies against human IgA (Sigma) 1hr at 37^{o}C. Finally, cells were incubated with mouse anti-FITC-conjugated secondary antibody (Santa Cruz) for 1hr at 37^{o}C. Slides were fixed and mounted with Vectashield containing DAPI. Images were captured with a FV1000 Olympus

confocal laser scanning microscope. A total of 36 images per condition taken from triplicate experiments were analyzed for quantification of reactivating cells.

4.2.8 Statistical Analysis

Data were analyzed using two-tailed paired Student's t-test in GraphPad Prism. Values were considered significant at $p < 0.05$.

4.3 RESULTS

Given the previously described similarities between ISRE sequences and ISRE-like RRE sequences and the demonstrated inhibition of RTA-mediated transcription by IRF7 binding to these motifs, we aimed to establish whether IRF4 could act as a negative regulator of RTA-mediated gene expression. Previously we have shown that besides being a positive regulator of ISG60 and Cig5 gene expression, IRF4 can also negatively regulate ISRE-driven host gene transcription (Figure 2-5). To determine whether IRF4 inhibits RTA-mediated transcription we co-transfected IRF4 and RTA, along with a Nut-1 (PAN) promoter luciferase reporter construct. Ectopic expression of IRF4 inhibited RTA-mediated luciferase activity in a dose-dependent manner relative to the activation of the Nut-1 promoter by RTA in cell transfected with empty vector control (Figure 4-1A).

To examine the effect of IRF4 on endogenous RTA and RTA-mediated gene expression we generated a stable cell line, BCBL-1*i*4, was generated, which expressed the Dox-inducible V5-tagged IRF4 from pInducer20/IRF4-V5. Treatment with 1 mg/ml of Dox results in the

expression of V5 tagged of IRF4 and a 60% increase in the amount of IRF4 protein localized to the nucleus (Figure 4-1B). Furthermore, the stimulation of these cells with TPA after treatment with Dox and induction of ectopic IRF4 expression resulted in a <20% reduction in RTA protein synthesis (Figure 4-1C). We determined that the inhibition in RTA protein synthesis due to reduced transcriptional induction of RTA by qRT-PCR analysis. The kinetics of RTA mRNA and ORF57, an RTA-responsive gene known to be negatively regulated by IRF7 [163], mRNA following TPA treatment was examined in cells stimulated with Dox. As observed in the immunoblot analysis, ectopic IRF4 expression resulted in 2-fold inhibition of RTA mRNA after TPA treatment (Figure 4-1D, left). Furthermore, the expression of ORF57 mRNA was also decreased by the ectopic expression of IRF4 (Figure 4-1D, right). These data suggest that IRF4 inhibits the expression of RTA-mediated viral gene expression required for the entrance of KSHV into the lytic replication cycle.

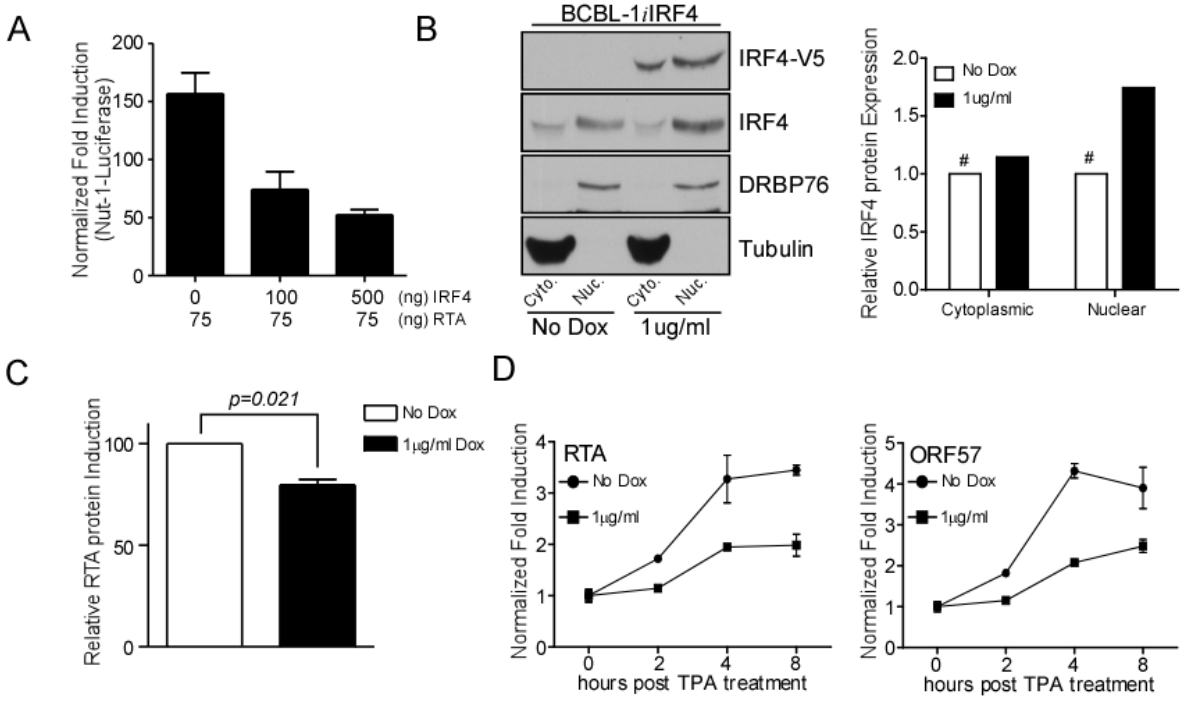

Figure 4-1. IRF4 Inhibits RTA Expression

(A) Effect of IRF4 on Nut-1 luciferase in 293T cells. 293T cells were co-transfected with 100 or 500 ng of IRF4 expression plasmid, 0.4μg Nut-1 luciferase reporter construct, 24 ng pRL-Null and either 75 ng of RTA cDNA or empty vector. Total transfected DNA levels were kept equal with empty vector. 48 h after transfection, luciferase activity was measured. Fold induction was normalized to both renilla luciferase activity and non-RTA transfected cells.
(B) Analysis of IRF4 protein expression levels in BCBL-1*i*IRF4 cells. 2×10^5 cells/ml BCBL-1*i*4 cells were treated with 1μg/ml Dox or left untreated for 48 hrs. Subcellular fractions were harvested as previously described and subjected to immunoblot with anti-RTA antibody (left). Densitometric analysis of IRF4 expression using ImageJ (right).
(C) Ectopic IRF4 expression leads to reduced RTA protein expression. 2×10^5 cells/ml BCBL-1*i*IRF4 cells were treated with 1μg/ml Dox or left untreated for 48 h, followed by stimulation with 15ng/ml TPA or DMSO for 12 h prior to harvesting. Cell lysates were subject to immunoblot with anti-RTA antibody. RTA expression levels were quantified for three independent experiments and induction was calculated relative to cells without Dox stimulation.
(D) Inhibition of RTA and ORF57 mRNA induction in BCBL-1 cells by IRF4. BCBL-1*i*IRF4 cells were stimulated with doxycycline for 48 h followed by stimulation with 15ng/ml TPA for 2, 4, and 8 h. Fold induction of RTA mRNA levels were normalized to RPL32 and non-TPA stimulated cells.

Previously we have demonstrated that IRF4 can bind to ISRE sequences, which are similar to RRE sites contained in the promoter regulatory region of some KSHV early genes. Thus we asked whether the inhibition in RTA and RTA-mediated gene expression following ectopic expression of IRF4 and stimulation with TPA could be due to the binding of IRF4 to ISRE-like elements in the promoter of the ORF57 promoter. To address this, we performed ChIP assays using antibodies targeting IRF4 followed by qPCR analysis to determine whether the ISRE-like RRE motif of ORF57 (Figure 4-2A) is bound by IRF4. Our results indicate that IRF4 indeed binds to the ORF57 ISRE-like RRE motif (Figure 4-2B) providing a potential mechanism by which IRF4 is inhibiting the expression of RTA and RTA-target genes.

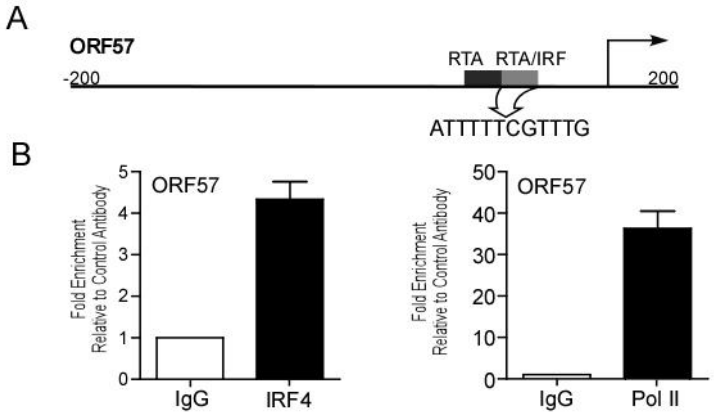

Figure 4-2. IRF4 Binds to the ORF57 Promoter in BCBL-1 Cells.

(A) Schematic representation of the ORF57 promoter-regulatory region depicting position of RTA binding sites (black) and the RTA/IRF binding (gray). The RTA/IRF target sequence has been highlighted.
(B) Chromatin-immunoprecipitation of endogenous IRF4 bound to ORF57 promoter in BCBL-1 cells. IRF4 (left) and Pol II (right) binding to the ORF57 promoter was analyzed by ChIP assay as previously described. Relative promoter occupancy was determined relative to isotype control antibody (value 1).

To investigate whether the ISG upregulation observed in PEL cells is solely mediated through constitutively high IRF4 expression, we attempted to a reverse genetics approach in PEL by short-hairpin RNA knockdown of IRF4 expression. Since we were unable to obtain stable

PEL cell lines constitutively expressing shRNA targeted against IRF4, we engineered BCBL-1 cells with doxycycline (Dox) inducible expression of either scramble control or two separate IRF4-targeting shRNAs (shIRF4, and shIRF4b). Briefly, BCBL-1 cells were engineered to stably express the ecotropic retroviral receptor by infection with an endogenous feline virus expressing mCAT, followed by infection with an ecotropic retrovirus expressing the bacterial tetracycline repressor (TETR). Cells were then transduced with retroviruses expressing inducible shRNA targeting IRF4 and a scramble control. Treatment of cells with Dox (100 ng/ml) resulted in about 50% reduction in IRF4 protein synthesis (Figure 4-3A) and mRNA expression (Figure 4-3B) in shIRF4 expressing cells, but not in scramble control (shCTRL) or shIRF4b expressing cells. Thus we used the shIRF4 expressing cells and shCTRL cells for further analysis of IRF4 function. We verified the specificity for IRF4 by immunoblot analysis of IRF proteins, IRF3 and IRF9. Although the loss of IRF4 expression was evident at 24 hrs post Dox treatment, the decrease in expression was more marked after 96 hrs. However, treatment with Dox resulted in equivalent expression of either IRF3 or IRF9 after 24 and 96hrs confirming that the shRNA targets IRF4 while not affecting expression of constitutively expressed IRF proteins. IRF expression of was not affected by Dox stimulus in the scramble control cells (Figure 4-3C). To determine if depletion of IRF4 affects RTA expression in PEL cells, we examined RTA protein synthesis in Dox (100ng/ml) treated BCBL-1 shIRF4. As expected from the observations in Figure 4-1, we observed an accumulation of RTA protein expression following the loss of IRF4 protein (Figure 4-3D). Taken together, these results suggest that IRF4 blocks the transcription of RTA as well as that of RTA-target genes.

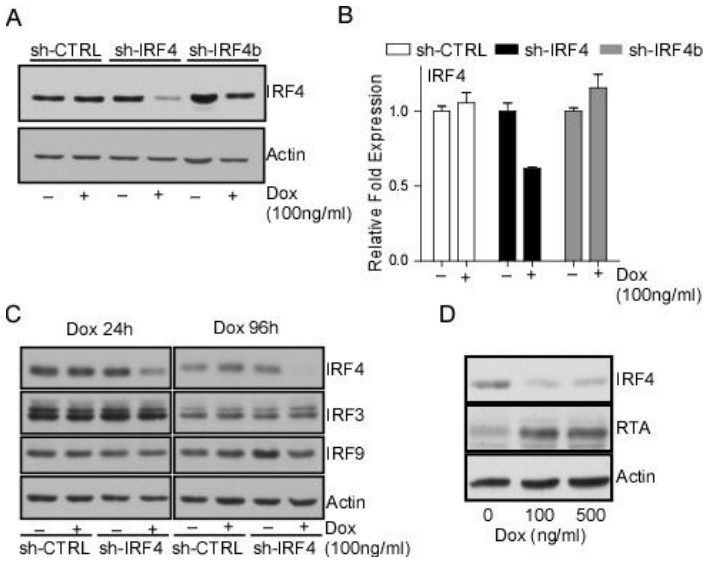

Figure 4-3. Downregulation of IRF4 Induces RTA expression

(A) Loss of IRF4 protein expression in cells expressing an IRF4 targeting short-hairpin. Whole cell lysates prepared from shRNA expressing BCBL-1 cells after 72 h treatment with 100 ng/ml Dox were immunoblotted with antibodies against IRF4 and actin.
(B) Quantitative RT-PCR analysis of IRF4 mRNA levels in short-hairpin expressing BCBL-1 cells after 72 h treatment with 100 ng/ml dox. Samples were normalized to RPL32 and expressed as fold change with respect to untreated cells (value 1).
(C) Specificity of IRF4 targeting by the short-hairpin 24 h (left) and 96 h (right) after stimulation with Dox. Whole cell lysates prepared from shRNA expressing BCBL-1 cells after 72 h Dox treatment were immunoblotted with antibodies against IRF4, IRF3, IRF9 and Actin.
(D)Nuclear accumulation of RTA expression follows loss of IRF4. Nuclear fractions were prepared from cell treated with Dox for 72 hrs. Fractions were resolved by SDS-PAGE and immunoblotted with antibodies against IRF4, RTA, DRBP76, and Tubulin.

Several physiological stress stimuli results in the reactivation of KSHV latently infected cells due to the transcriptional activation of RTA. Furthermore, chemical treatment of PEL cell lines with phorbol esters (TPA) and HDAC inhibitors also results in the induction of RTA expression, which is sufficient to initiate the lytic replication cascade. Given that loss of IRF4 resulted in an increase in RTA protein synthesis, we asked if the knockdown of IRF4 would synergize with the chemical TPA, which would confirm the role of IRF4 as a negative inhibitor of RTA transcription. Thus, we treated BCBL-1 shCTRL and shIRF4 cells with Dox for 72 hrs followed

by stimulation with 5 and 15 ng/ml TPA for 12 hrs. Stimulation with either 5 ng/ml or 15ng/ml TPA resulted in similar induction of RTA protein synthesis in both shCTRL and shIRF4 cells without Dox treatment and neither concentration affected IRF4 protein levels (Figure 4-4A, lanes 2,3,8,9). Stimulation with Dox alone, resulted in a significant decreased IRF4 protein levels was accompanied with an induction in RTA protein synthesis (lanes 10-12) as expected. The induction of RTA was in response to the loss of IRF4, as Dox treatment of shCTRL cells did not affect either IRF4 or RTA levels (lane 4). Interestingly, the induction of RTA protein sythesis was comparable in shIRF4 cells treated with Dox alone or treated with TPA-alone. In shCTRL cells Dox treatment alone had no effect in either IRF4 or RTA protein expression (lanes 4 and 1). Furthermore, co-stimulation with TPA resulted in enhanced RTA expression in sh-IRF4 cells (lanes 11 and 12) relative to Dox untreated cells (lanes 8, 9 and 5, 6) and shCTRL cells.

The observed increase in protein expression was due to the transcriptional activation of RTA as determined by qRT-PCR. Dox (100 ng/ml) treatment of shIRF4 cells led to an observed 3.4-fold increase in RTA mRNA compared to a 10.5-fold increase in mRNA transcription when cells were co-stimulated with Dox and TPA (15 ng/ml) (Figure 4-4B). These results were concordant with our previous studies demonstrating that IRF4 acts as a repressor of RTA transcription. As seen for RTA protein synthesis, both shCTRL and shIRF4 cell lines responded equally to stimulation with TPA (Figure 4-4A lanes 2,3 and 8,9), suggesting that there were no inherent differences in the ability to respond to phorbol ester treatment.

RTA plays a critical role in initiating the switch from latency to the lytic reactivation of KSHV by [218] specifically regulating the transcription of eight viral lytic genes containing RRE sequences and inducing the downstream lytic gene cascade. To examine the consequence of IRF4 downregulation on direct targets of RTA, we measured the induction of RTA-responsive

genes ORF57, vIL-6, and PAN mRNA [219] following treatment of cells with Dox and TPA. Similar to the observed RTA transcript induction, loss of IRF4 resulted in a 2 to 4-fold increase in basal early gene transcription of the three targets examined relative to untreated cells. Furthermore, co-stimulation with Dox and TPA, resulted in a significant enhancement in ORF57, PAN, and vIL-6 transcription in shIRF4 expressing cells compared to that observed in co-stimulated shCTRL cells (Figure 4-4C). To address the possibility that treatment with Dox leads to an overall increase in gene transcription, we measured the mRNA levels of the latency-associated nuclear antigen, LANA, following Dox and/or TPA stimulation. While treatment with TPA resulted in a comparable decrease in LANA mRNA in both shCTRL and shIRF4 cells, treatment with Dox led to lower LANA mRNA levels in shIRF4 cells, but not in shCTRL cells relative to non-stimulated cells. As expected, dual stimulation with Dox and TPA resulted in a decrease in LANA mRNA in both cell lines (Figure 4-4D). These results are in accordance with previous studies showing that chemical stimulation of lytic reactivation results in the decrease in LANA transcription accompanied with an induction of IE gene expression [220]. Taken together, our results indicate that IRF4 downregulation in PEL cells is likely sufficient to allow entry into the viral lytic reactivation program, rather than resulting in a non-specific activation of viral gene expression.

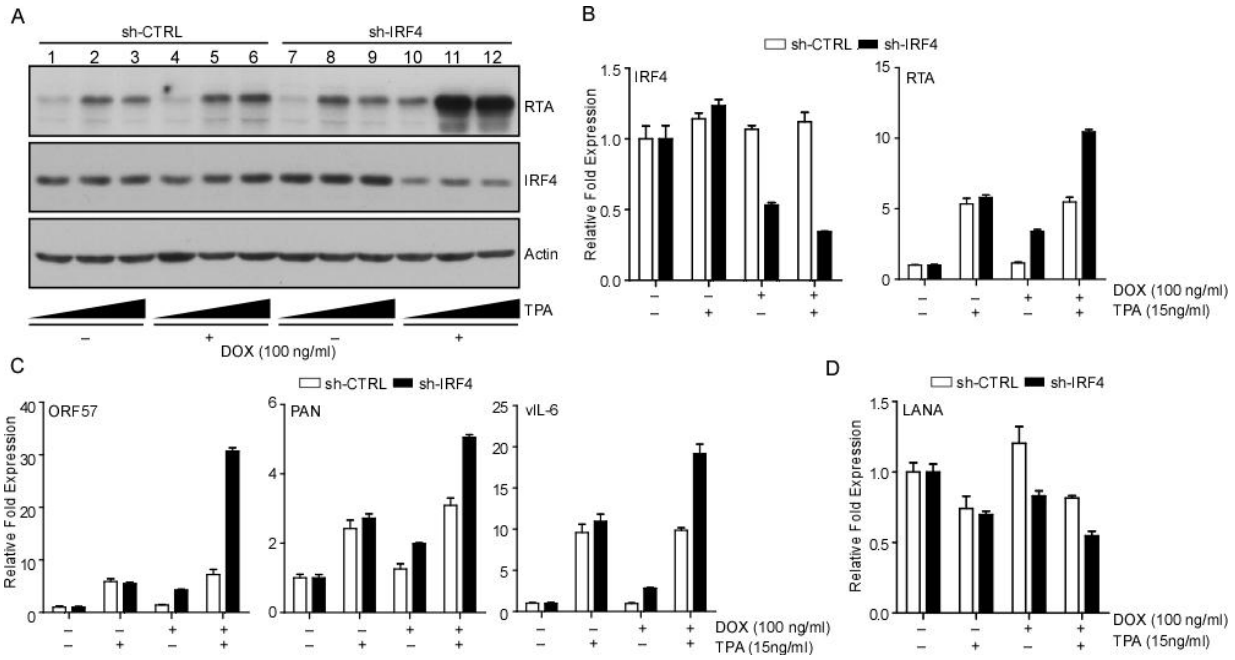

Figure 4-4. Downregulation of IRF4 Sensitizes PEL cells to TPA treatment.

(A) Analysis of RTA protein induction following Dox treatment and TPA stimulation in BCBL-1 sh-CTRL and sh-IRF4 cells. Cells were stimulated with Dox for 48 h followed by an additional treatment for 24 h with 5 or 15 ng/ml TPA. Lysates were prepared after stimulation and immunoblotted with anti-RTA, IRF4, and Actin antibodies.
(B-D) qRT-PCR analysis of IRF4 and RTA mRNA levels; (C) RTA target genes, ORF57, PAN, vIL-6 (D) LANA in Dox treated BCBL-1 sh-CTRL and sh-IRF4 cells. Cells were stimulated as previously described, total RNA was harvested and subjected to qRT-PCR. Samples were normalized to RPL32 and expressed as fold change with respect their respective untreated cells (value 1).

Bonafide lytic reactivation and viral replication is accompanied by an increase in virion structure and assembly associated gene expression. To determine whether this occurred in BCBL-1 shIRF4 cells after treatment with Dox, we measured the transcriptional induction of the genes encoding for the viral glycoprotein K8.1, ORF17, and ORF67 by qRT-PCR, we observed higher mRNA expression of all three genes in cells treated with Dox for 72 hrs, relative to non-treated cells (Figure 4-5A). Additional treatment of Dox stimulated cells with TPA, resulted in enhanced mRNA expression of the late genes, K8.1 and ORF17. Interestingly, while the expression of ORF67 mRNA was higher in cells treated with Dox relative to untreated or TPA-alone treated cells, co-stimulation of cells with Dox and TPA did not result in increased mRNA

levels compared to cells treated with Dox alone. We then examined the induction of KSHV viral protein expression in BCBL-1 shIRF4 cells stimulated with 100ng/ml Dox for 96 hrs. Cells were fixed and stained using anti-KSHV sera. We observed a significant two fold increase in cytoplasmic staining in cells in Dox treated cells (Figure 4-5B), indicating that loss of IRF4 is sufficient for the induction of lytic reactivation of a portion of BCBL-1 shIRF4 cells.

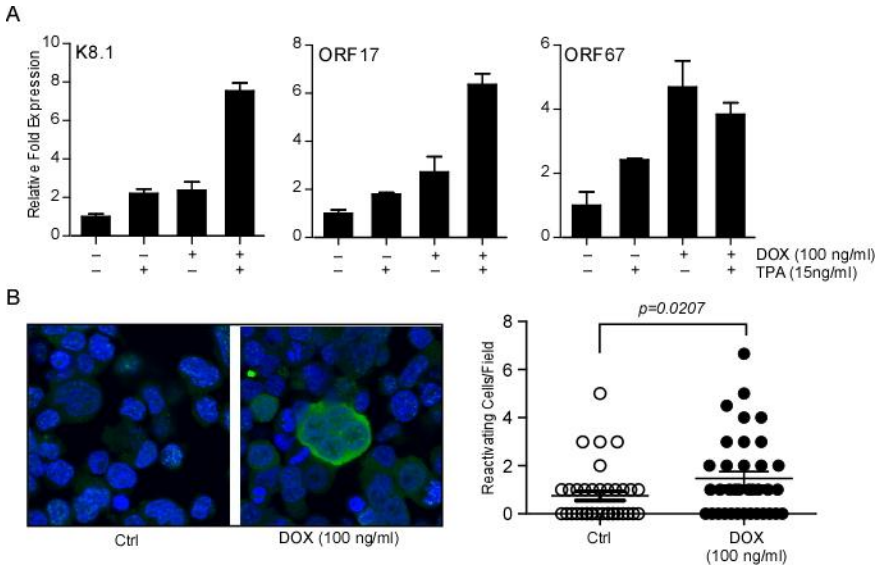

Figure 4-5. The Loss of IRF4 Upregulates Structural and DNA Replication Genes.

(A) qRT-PCR analysis of late genes K8.1, ORF17, and ORF67 in Dox treated BCBL-1 sh-CTRL and sh-IRF4 cells. Cells were stimulated as previously described, total RNA was harvested and subjected to qRT-PCR. Samples were normalized to RPL32 and expressed as fold change with respect their respective untreated cells (value 1).
(B) BCBL-1 shIRF4 cells stimulated with Dox for 96 hrs. Following stimulation, cells were fixed, stained with KSHV positive human sera (green), nuclei were stained with DAPI (blue), and samples imaged by confocal microscopy (left). Quantification of KSHV reactivation (left).

As we have previously shown that IRF4 acts as a positive regulator of ISRE-mediated expression of ISG60 and Cig5, we evaluated the effect of IRF4 knockdown on the expression of these genes. Unexpectedly, transcription of ISG60 and Cig5 was increased after IRF4 depletion, 4-fold and 6-fold respectively (Figure 4-6A). This was accompanied by an increase in ISG60

protein synthesis after Dox treatment of BCBL-1 cells (Figure 4-6B). RTA is a sequence-specific DNA binding protein that recognizes and binds to ISRE and ISRE-like sequences found in the promoter regulatory regions of cellular ISGs as well viral genes [163]. Thus, we evaluated the possibility that ISG induction observed by IRF4 silencing was due to the observed RTA induction. Ectopic expression of RTA resulted in an almost 5-fold increase in the activity of the ISRE-regulated IFNβ reporter construct relative to vector transfected cells (Figure 4-6C). Furthermore, RTA expression resulted in a 5-fold increase in the induction of ISG60 mRNA transcription (Figure 4-6D) accompanied by an increase in ISG60 protein synthesis (Figure 4-6E). Taken together, these results indicate that the loss of IRF4 induces the expression of RTA, which itself can target genes in an ISRE dependent manner. Thus, we establish a critical counterbalance between IRF4 and RTA; while the former negatively regulates viral gene expression, the latter targets similar sequences in cellular gene promoters strongly activating their expression.

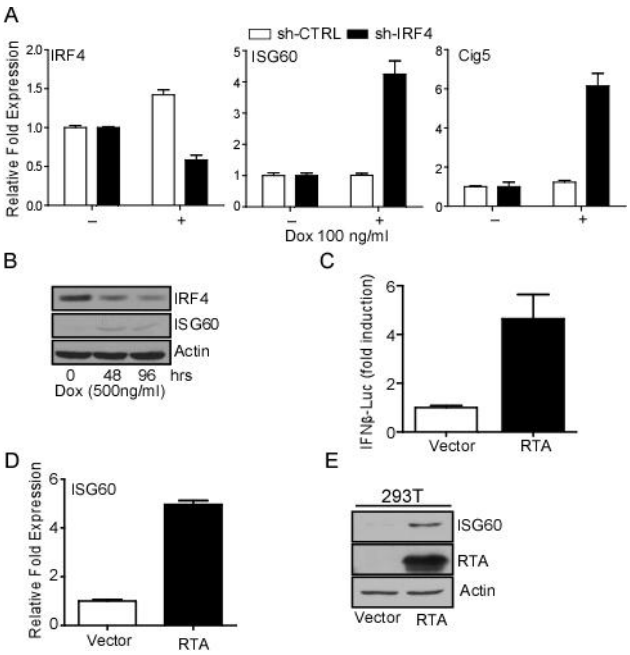

Figure 4-6. Expression of RTA Induces ISG60 Expression.

(A) Quantitative RT-PCR analysis of ISG60 and Cig5 mRNA expression in shRNA expressing BCBL-1 cells after 72 h Dox treatment. Samples were normalized to RPL32 and expressed as fold change with respect to untreated cells (value 1).
(B) Analysis of ISG60 protein induction levels in whole cell lysates prepared from sh-IRF4 expressing BCBL-1 cells after 72h treatment with Dox.
(C) Effect of RTA expression on IFNβ-promoter activity. HEK293 cells were transfected with RTA or vector control along with $IFN\beta_{125}$-luc and pRL-Null. Luciferase activity was measured as previously described. Samples were normalized to renilla luciferase control and expressed as fold change with respect to empty vector transfected cells (value 1).
(D) Quantitative RT-PCR analysis of ISG60 following ectopic expression of RTA in 293T cells. Samples were normalized to RPL32 and expressed as fold change with respect to empty vector transfected cells (value 1).
(E) Analysis of ISG60 protein induction following ectopic expression of RTA in 293T cells. Lysates were prepared 48 hrs after transfection and probed with antibodies against RTA, ISG60, and Actin.

4.4 DISCUSSION

One important feature in the life cycle of herpesviruses is their ability to establish life-long latent infections, which acts as a mechanism for immune evasion and contributes to the pathogenesis viral related malignancies. On the other hand, viral spread necessitates that viral genes be expressed, genomes replicated, and new infectious virions be assembled. The role of virally encoded genes in both the establishment of latent infection or the switch to lytic reactivation has been extensively studied. However, a better understanding of the events that determine whether the virus will establish latency or undergo lytic replication requires an understanding of both the viral and cellular signals that shape these outcomes. Given the lack of infectious models to study the biology of KSHV, most studies to date have focused in understanding latency in PEL cells as well as the extrinsic signals that result in the induction of lytic replication.

These studies have been useful in identifying various stimuli, like hypoxia, oxidative stress, UV irradiation, and chemical treatment with phorbol esters and chemical inhibitors, that result in the induction of lytic reactivation by inducing the expression of the replication and transcription activator protein (RTA), encoded by ORF50. RTA, the major immediate early (IE) protein required for the induction of early (E) gene expression, is a sequence specific DNA-binding protein, which is necessary and sufficient for lytic reactivation of KSHV in both B-cell and endothelial cells.

However, the intrinsic cellular signaling pathways that counter viral gene expression during primary infection of cells and that act during latent infection still remain to be understood. It has become increasingly evident that the innate immune response to viral infection could be a major player in the restriction of viral replication and maintaining viral latency. Studies have

shown that the importance of type I IFN signaling in this process. Infection of IFNAR−/− mice with murine gammaherpesvirus closely related to KSHV, MHV68, resulted in comparable latent infection in peritoneal cells and splenocytes as wt mice [184]. However, IFNAR deficiency led to higher rates of viral reactivation. These alterations in reactivation efficiency were found to be dependent on the inhibition of a latency-associated gene, M2, required for efficient viral reactivation. Follow-up studies showed that the expression of M2 is regulated by IRF2 binding to an ISRE in the M2 promoter during latency. IFNAR deficient mice fail to upregulate IRF2 expression thus displaying increased rates of reactivation [184-186,221]. Thus, these studies highlight an important role for the host effector proteins and transcription factors that regulate their expression in controlling viral latency.

To better understand involvement of IRF4 in regulating KSHV viral latency. We looked at the transcriptional inhibition of RTA and ISRE-like driven viral gene expression. Our reporter assay and qRT-PCR analysis show that ectopic expression of IRF4 results in the inhibition of viral gene expression concomitant with a two-fold decrease in RTA and ORF57 mRNA following chemical treatment to induce reactivation. Ye et al. [84] showed that a two-fold decrease in RTA mRNA expression after reactivation by sodium butyrate treatment in PEL cells, led to a 14-fold reduction in virus production. Thus, ectopic expression of IRF4 might results in significantly lower viral yields upon reactivation. On the other hand, we used a reverse genetics approach in which we downregulated IRF4 expression in BCBL-1 cells. This resulted in the spontaneous induction of RTA protein synthesis and downstream expression of early genes and late structural and DNA replication genes. Furthermore, we saw the accumulation of cytoplasmic lytic proteins in the absence of exogenous stimuli like TPA, UV treatment, or viral infection. Given that the loss of IRF4 sensitizes PEL cells to TPA stimulus, it would be interesting to

address whether IRF4 downregulation also confers sensitivity to reactivation following viral infection, TLR ligation, and other chemical treatment. This study shows that the expression of IRF4 leads to the inhibition of lytic reactivation. Further examination of the cellular cues that control IRF4 function in PEL and the viral mechanisms that counter its inhibitory activities during reactivation still remain to be addressed.

5.0 CONCLUSIONS AND FUTURE PERSPECTIVES

The interferon regulatory factor (IRF) 4, a hematopoietic cell-specific transcription factor that regulates the maturation and differentiation of immune cells, is found to be expressed in PEL cells. However, there is little information regarding the role of IRF4 in regulating gene expression in this malignancy. In this study, we focus on the transcriptional regulatory potential of IRF4 in the regulation of interferon-stimulated genes (ISGs), effector genes stimulated upon the detection of virus infection and IFN sensing. First, using promoter reporter assays and mRNA expression profiling in 293 cells devoid of IRF4 expression, we have established IRF4 as a direct regulator of a subset of interferon-stimulated genes (ISG). Then, we showed that IRF4 targets a subset of genes and promotes ISG transcription through direct chromatin binding at regions containing the interferon-stimulated response elements (ISRE) motifs. While the IRF proteins share redundant targets, they also possess distinct transcriptional profiles. Independent of the association of transcription factors that specify the motifs recognized by IRF proteins, the nucleotides flanking the core ISRE sequence also dictate target specificity [5]. Mapping of IRF4 targeted motifs through careful sequence analysis of putative binding sites identified by ChIP-seq would allow us to predict and identify effector genes involved in the pathogenesis of PEL and other IRF4-associated diseases. Moreover, it would allow us to better understand how the concomitant activation of IRF4 with various transcriptions factors, like NF-κB, serves to broaden and magnify the transcriptional profile of IRF4.

In the past, our group has employed cell-based assays to carry out efficient screens of small molecule inhibitors to identify modifiers of TLR signaling pathways [170,222]. These same strategies can be employed to identify both chemical and genetic modulators of IRF4 function with therapeutic potential against IRF4-associated autoimmune diseases, cancers, and the modulation of host responses to infection. Here, we have generated cell-based systems (293*i*4 and RL24*i*4) that allowed us to identify targets of IRF4 and viral encoded modulators of IRF4 activity. Using 293*i*4 cells, we explored the IRF4-specific immunomodulatory functions of three KSHV latency associated proteins: LANA, LANA2, and vFLIP. We have identified the Kaposi sarcoma-associated herpesvirus (KSHV)-encoded viral FLICE inhibitory protein (vFLIP) as a novel enhancer of IRF4-mediated gene expression, and through mechanistic studies we have shown that this function is NF-κB dependent. Based on studies that show enhanced PRDII activation by vFLIP [141] and studies showing the recruitment of c-REL to the ISG60 promoter after IFN treatment [223], is due to binding of NF-κB to -κB responsive elements in the promoter of ISG60. An understanding of the relationship between the cellular response to viral infection and the mechanisms by which the virus counteracts these responses is crucial for a better understanding of KSHV pathogenesis and the molecular differences between endothelial and B-cell malignancies.

Genome-wide gene expression profiling in HUVEC cells has been carried out to understand the cellular response to KSHV infection of endothelial cells. A comparative analysis of these studies has shown that KSHV induces the differential expression of innate immune genes including transcription factors, effector genes, and proinflammatory cytokines [224]. Interestingly, vFLIP has been shown to be required for the sustained induction of STAT1 activation and ISG expression during after infection of HUVEC cells [140]. These studies, along

with ours, strengthen the function of vFLIP as an enhancer of IRF regulated genes. Further investigation will establish the significance of immune gene activation in the context of KSHV latency. RNAi screens could provide useful information with regard to the specific role of ISGs and IFN response in both the establishment of latency during primary infection and the maintenance of latency in PEL and KS cells.

Chronic viral infection triggers intrinsic cellular responses that are aimed to inhibit viral replication, protein expression, and spread. The innate immune response to viral infection is initiated by the recognition of pathogen associated molecules that trigger signaling cascades resulting in the carefully orchestrated activation of transcription factors that stimulate the production of antiviral cytokines and chemokines. Cytokine secretion is necessary to alert non-infected cells and promote the expression of cellular effectors that promote the clearance of viral infections. The secretion of chemokines is paramount to elicit a proper adaptive immune response to the invading pathogen. To better understand the significance and consequences of these intrinsic responses it is important to fully understand how they function in regulating the replication of viruses and how the invading pathogen circumvents these responses.

Thus, to prevent immune recognition and clearance, KSHV has developed strategies that allows it to persist in the infected cell. A great deal of effort has been placed on understanding the mechanisms by which KSHV evades the host response. To achieve this, KSHV encodes molecular decoys that resemble immune components and act to negatively regulate the response of their cellular counterparts. Moreover, the role of the latency-associated proteins in promoting immune evasion and establishment of viral latency has also been extensively described. To fully understand the viral strategies for evasion one must also understand how the pressure exerted by the host response and how it carefully balances the outcomes of KSHV infections.

Various cellular proteins that participate in KSHV reactivation have been identified. These include both kinases (PI3K[147], Pim-1 and Pim-3 [225], ERK1/2 [226], and PKC [227]) and transcription factors (like Sp1 [228], C/EBP [229], CBF1/CSL [230,231], Oct-1 [232], HMGB-1 [233], and XBP-1 [147,234] that promote RTA induction and RTA-mediated viral gene expression. On the other hand, antagonists of RTA induction and RTA-mediated gene expression have also been identified. These proteins also include signaling molecules like Tousled-like kinases (TLKs) [220] and the transcriptional regulators, K-RBP [235], IRF7 [160], and Hey1 [236]. However, it should also be noted that the regulation of signaling events downstream of RTA induction and transcriptional activation are also important in guaranteeing successful viral replication. Thus, differentiating those molecules and modifications that initiate RTA transcription and synthesis, the transcriptional function of RTA, and the effect of modulation of downstream lytic replication is imperative for a better understanding of KSHV biology and the development of effective treatment therapies.

In conclusion, we postulate that IRF4 is one of the molecules that shape the outcomes of KSHV infections. IRF4 exerts KSHV antiviral activity in B-cells by binding of DNA elements in cellular and viral genes promoting both indirect (ISGs) and direct (RRE inhibition) silencing of lytic gene expression following primary infection (Figure 5-1). This in turn, aids the virus in maintaining latency and avoiding immune clearance, establishing lifelong infections in the host. While not an oncogene per se, IRF4 promotes the cellular addiction to the oncogenes expressed by KSHV. Thus, IRF4 targeted therapies in combination with anti-herpetic treatments, could prove useful in the treatment of KSHV associated malignancies, PEL and multicentric Castleman's disease.

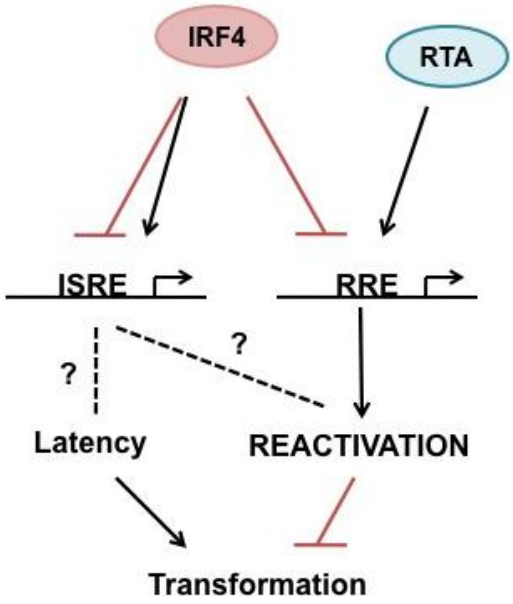

Figure 5-1. Proposed Model of IRF4 Function in PEL Cells.

IRF4 and RTA balance the KSHV life cycle. ISRE and ISRE-like RRE motifs located in cellular and viral gene promoters direct IRF4 to these promoters, regulating target gene expression. This results in the inhibition of viral lytic reactivation induced by RTA; thus, promoting KSHV latency. On the other hand, induction of cellular ISG expression potentially contributes to inhibiting viral reactivation and promoting cellular transformation.

APPENDIX A

MECHANISM OF INTERFERON STIMULATED GENE INDUCTION BY SV40 LARGE T ANTIGEN

Work described in this section was completed by authors Adriana Forero, Ole V. Gjoerup, Christopher Bakkenist, James M. Pipas, and Saumendra N. Sarkar.

A.1 INTRODUCTION

The polyomavirus family consists of small double–stranded DNA viruses that infect a wide variety of hosts. Infection with polyomaviruses is ubiquitous amongst the human population and generally results in subclinical infections in healthy hosts. However, upon the onset of AIDS-related, age related, and iatrogenic immune suppression, manifestations of clinical disease associated with viral infection become apparent. In humans, infection with JC polyoma virus (JCV) is linked to the induction of progressive multifocal leukoencephalopathy (PML) [237,238]. Meanwhile, infection with BK polyoma virus (BKV) results in the induction of polyomavirus-associated nephropathy or hemorrhagic cystitis after immunosuppression [239]. To date, there are few successful therapies for the treatment of polyomavirus related diseases. Thus, an understanding the interactions between the virus and the host response to viral infection is crucial for the development of new effective therapies.

The wealth of knowledge of polyomavirus biology has stemmed from studies utilizing the prototypic polyoma virus, Simian Virus 40 (SV40). SV40 encodes early proteins (large T antigen, small t antigen and 17K t) encoded by the T antigen locus and late proteins with structural and auxiliary functions in regulating the host cellular responses. The SV40 large T antigen (LT) is a well characterized multi-functional protein, which controls the replication of viral DNA, regulates host cellular proliferation and gene expression, and can promote cellular transformation. These functions are largely mediated by the interaction of LT with numerous

cellular proteins [240]. Understanding the processes deregulated by the interaction of LT and cellular proteins is crucial for understanding the pathogenesis of polyomaviruses and their transformative phenotype.

The induction of both intrinsic and extrinsic genotoxic stress damages DNA and triggers the DNA-damage response DDR signaling cascade, mediated by the kinases ataxia-telangiectesia mutated (ATM) and ATM and Rad3-related (ATR). Activation of these kinases by double-strand DNA breaks and single strand DNA gaps, respectively, results in the induction of the DNA repair proteins and cell cycle arrest in order to maintain genome integrity [241]. Multiple studies have provided evidence that infection with mouse polyoma virus (MPyV) [242], JCV [243], BKV [244], and SV40 [245-247] leads to the activation of both ATM and ATR kinase activity. Induction of DDR is required for the induction and hijacking of the DNA-repair machinery to mediate the replication of viral genomes. Moreover, it has been shown that expression of SV40 LT protein alone is sufficient for the activation of the ATM/ATR [247]. However, the cellular consequences of compromising the DDR are still not clearly understood.

Detection of viral infection in epithelial cells and fibroblasts triggers cytoplasmic and nuclear sensors that initiate a signaling cascade that results in the activation of type I IFN, IFNβ, and the expression of virus-induced interferon-stimulated genes (ISG). Secretion of IFNβ then triggers the interferon response signaling pathway characterized by the induction of IFNα and the further induction of ISGs. The ISG have antiviral effector functions that limit the replication of viral genomes, inhibit both cellular and viral protein synthesis, and promote the death of the infected cell [2]. Previous studies have shown that infection of glial cells with JCV results in a strong induction of ISGs likely accounting for the lack of disease progression in immunocompetent individuals [248]. Using mouse while genome arrays, we have shown that

SV40 LT expression results in a tissue specific altered gene expression [249]. Stable expression of LT in mouse embryonic fibroblasts or immortalized human fibroblasts led to the induction of genes involved in the IFN response. However, in the absence of an active virus infection, the signaling pathways involved in the ISG induction remain elusive.

In this study, we examine the mechanisms by which ectopic expression of SV40 LT antigen results in the induction of interferon stimulated genes in human fibroblasts. Our results show that the induction of ISGs is a conserved function amongst the polyomaviruses. We show LT expression results in the upregulation of IRF1 protein, which in turn, results in enhanced transcription and secretion of IFNβ and its downstream genes. Furthermore, we show that the induction of a DNA damage response is sufficient to induce the expression of IRF1, in an ATR kinase activity dependent manner. Our data links mediators of the DNA damage response with the regulation of type I IFN responses and the induction of innate immune gene expression in the absence of viral infection.

A.2 MATERIALS AND METHODS

A.2.1 Cell lines and Reagents

The cell lines used in this study have been described on Table 8. 293-Ampho (Phoenix amphotropic) cell line and 293FT cells were cultured in Dulbecco's Modified Eagle Medium (Lonza) supplemented with 10% fetal bovine serum (Atlanta Biologicals) and 100 I.U./ml penicillin and 100 mg/ml streptomycin (Lonza). HCT116 cells were cultured in McCoy's 5A medium (Lonza) containing 10% fetal bovine serum (Atlanta Biologicals) and 100 I.U./ml

penicillin and 100 mg/ml streptomycin (Lonza). BJ/TERT and BJ/TERT derived cell lines were cultured in Dulbecco's Modified Eagle Medium (Lonza) supplemented with 20% Medium 199 (Invitrogen), 10% fetal bovine serum (Atlanta Biologicals) and 100 I.U./ml penicillin and 100 mg/ml streptomycin (Lonza). Hexydimethrine bromide (Polybrene) was used for viral infections at a final concentration of 8 μg/ml (Sigma-Aldrich). The selection antibiotics Blasticidin (5 μg/ml) and Puromycin (1 μg/ml) were obtained from InvivoGen. Cyclohexamide was used at a final concentration of 50 ng/ml (Sigma-Aldrich). ATM kinase inhibitor, KU60019, was obtained from Astra Zeneca and used at a final concentration of 2 μM. ATR kinase inhibitor ETP-46464 was previously described [250] and used at various concentrations as indicated. UCN-01 inhibitor was DMSO (Fisher Scientific) was used as vehicle control for kinase inhibitor experiments.

Table 8. Appendix C - Cell Lines.

Cell Line	Description	Source	Reference
293-Ampho	HEK293 cells stably expressing amphotropic receptor for retroviral packaging.	Nolan Lab (Stanford University)	[251]
293FT	HEK293 cells transfromend with SV40 Large T antigen.	Invitrogen (Cat no. R700-07)	
HCT116	Colorectal carcinoma cell line derived from p53 wt male patient.	ATCC® CCL-247 Lotze Lab (University of Pittsburgh)	
BJ/TERT	BJ human foreskin fibroblast derived from a male patient. Immortalized by stable expression of human TERT gene.	Gjoerup Lab (University of Pittsburgh)	[252]
BJ/TERT LBNCX	BJ/TERT derived cell lines stably transduced with the retroviral vector pLBNCX.	Gjoerup Lab	[247]
BJ/TERT LT	BJ/TERT derived cell lines stably transduced with retroviral vector pLBNCX encoding the SV40 LT cDNA.	Gjoerup Lab	[247]
BJ/TERT LBNCX shCTRL	BJ/TERT derived cell lines stably transduced with the retroviral vector pLBNCX and pLKO.1 vector expressing a non-targeting shRNA.	Sarkar Lab	
BJ/TERT LT shIFNAR	BJ/TERT derived cell lines stably transduced with the retroviral vector pLBNCX encoding SV40 LT cDNA and a pLKO.1 vector expressing an IFNAR1 targeting shRNA.	Sarkar Lab	
BJ/TERT shCTRL	BJ/TERT derived cell lines stably transduced pLKO.1 vector expressing a non-targeting shRNA.	Sarkar Lab	
BJ/TERT shIFNAR	BJ/TERT derived cell lines stably transduced with a pLKO.1 vector expressing an IFNAR1 targeting shRNA.	Sarkar Lab	
BJ/TERT LBNCX shIRF1	BJ/TERT derived cell lines stably transduced with the retroviral vector pLBNCX and a pLKO.1 vector expressing an IRF1 targeting shRNA.	Sarkar Lab	
BJ/TERT LT shIRF1	BJ/TERT derived cell lines stably transduced with the retroviral vector pLBNCX encoding SV40 LT cDNA and a pLKO.1 vector expressing an IRF1 targeting shRNA.	Sarkar Lab	
BJ/TERT shIRF1	BJ/TERT derived cell lines stably transduced with a pLKO.1 vector expressing an IRF1 targeting shRNA.	Sarkar Lab	

A.2.2 Plasmids and Viruses

Plasmids encoding the polyoma virus LT antigen were obtained form Dr. Ole Gjoerup. Retroviral plasmids pLBNCX and pLBNCX-LT encoding the SV40 LT cDNA have been previously described [247]. pCMV-LT plasmid encoding SV40 LT cDNA was previously described [253]. Plasmids encoding JCV and BKV LT cDNA have been described in [254]. Plasmids encoding IRF1 (pcDNA3.1/HisA/huIRF1) and IRF7 (pCMV/FLAG-IRF7, and IRF9 (pCMV/p48) have been previously described [208,255]. pLKO.1 based lentiviral vectors expressing short hairpin RNA targeting IRF1 (TRCN0000014669) and IFNAR1 (TRCN0000059017) were purchased from Sigma-Aldrich. Vesicular stomatitis virus expressing GFP (VSV-GFP) [177] was grown in BHK21 cells. Encephalomyocarditis virus (EMCV), obtained from ATCC (VR-1479), and HSV-1 (K26) [256] were grown in Vero cells. Sendai virus (Cantell strain) was purchased from Charles River Laboratories. Multiplicity of infection (m.o.i) and virus titers were determined by growth in their respective producer cell lines.

A.2.3 Retroviral and lentiviral infection and stable cell line generation

Retroviral vectors pLBNCX and pLBNCX-LT were transfected into ($1x10^7$) Phoenix amphotropic packaging cell line (293-Ampho) using Fugene 6 (Roche) following manufacturer's guidelines. Supernatants (~7 mL) were harvested 48 h post-transfection and filtered through a 0.45-μm membrane (Millipore) and stored at -80°C. BJ/TERT cells were infected with 1 ml of virus supernatant in the presence of 8 μg/ml polybrene and placed under antibiotic selection with

Blasticidin (5 μg/ml) 48 hrs after transfection. Antibiotic resistant cells were used for further studies.

pLKO.1 shRNA delivery lentiviral vectors were packaged in 293FT cells by transient transfection with Fugene 6 (Roche). BJ/TERT-derived pLKO.1 transduced cells were generated by overnight lentiviral infection with virus packaged from pLKO.1 shCTRL or pLKO.1 shIFNAR in the presence of 8 μg/ml polybrene (Sigma-Aldrich). 48 hrs post-infection, cells were selected with 1μg/ml Puromycin (InvivoGen) for 7 days. Puromycin-resistant cells were pooled and used for further studies.

A.2.4 Luciferase Assays

HEK293T (1.5×10^5 cells/well) in 24-well plate were co-transfected with 250 ng empty vector, IRF1, IRF7, and IRF9 cDNA, 400ng luciferase reporter construct, and 50ng pRL-null using Fugene 6 at a 1: 3 DNA to transfection reagent ratio. Twenty-four hours later, the cells from each well were collected by trypsin-EDTA digestion and seeded into 6 wells in 96-well plate. Forty-eight hours post transfection we measured luciferase activity using the Dual-Glo luciferase assay system (Promega,). Firefly luciferase activity was normalized to renilla luciferase activity and expressed as fold changes as indicated. BJ/TERT cells were transfected with 1 μg pGL3 Basic or pIFNβ_{125}-luc plasmid using Lipofectamine 2000.

A.2.5 Immunoblotting

Whole cell lysates were prepared as previously described in Chapter 2. Primary antibody incubation with antibodies against SV LT (pAb 416 and 419) [247], ISG56 and ISG60 [176],

OASL (Abgent), IRF1 (Santa Cruz), IRF7 (Santa Cruz), IRF9 (Santa Cruz), GFP (Santa Cruz), Sendai virus C-protein [257], phospho-p53 (Ser15) or total p53 (DO1) (Santa Cruz), Actin (Santa Cruz), and Tubulin (SantaCruz) was done overnight in 10% nonfat dry milk. Membranes were then washed twice with TBS-T and incubated with horseradish peroxidase-conjugated anti-mouse or anti-rabbit immunoglobulin G (IgG) diluted at 1:10000 in TBS-T plus 10% nonfat dry milk. Blots were revealed by enhanced chemiluminescence using Hy-Glo reagent (Denville) according to manufacturer's protocol.

A.2.6 RNA Isolation and qRT-PCR Analysis.

Total RNA was harvested from $1x10^6$ BJ/TERT LBNCX or LT cells as previously described in Chapter 2 Materials and methods. cDNA synthesis and qRT-PCR analysis was done as previously described using primers sets from Table 4. Target gene expression was normalized to RPL32 and vector expressing cells (value 1).

A.2.7 IRF3 Dimerization Assays.

BJ/TERT, BJ/TERT LBNCX, and BJ/TERT LT cells (1×10^6) were plated in 10 cm plates. BJ/TERT cells were infected with 300 HAU/ml of SeV for 8 hrs. Were washed with PBS and lysed in 70 μl of lysis buffer (50mM Tris-HCl, pH7.5; 150 mM NaCl; 1mM EDTA; 1% NP-40; 2 mM Na_3VO_4; 10 mM NaF; 12 mM β-glycerophosphate). Lysates were then diluted in equal volumes of PAGE loading buffer (2X) (0.125M Tris-HCl, pH6.8; 20% glycerol; 0.1 mg/ml BPB dye.) Samples were resolved in an 8% polyacrylamide gel by Native PAGE using PAGE running buffer (3 g/L Tris; 144 g/L; 1% deoxycholic acid). Protein was transferred to PVDF membranes

and probed with anti-IRF3 antibody [176] overnight in 10% nonfat dry milk. Membranes were then washed twice with TBS-T and incubated with horseradish peroxidase-conjugated anti-rabbit immunoglobulin G (IgG) diluted at 1:10000 in TBS-T plus 10% nonfat dry milk. Blots were revealed by enhanced chemiluminescence using Hy-Glo reagent (Denville) according to manufacturer's protocol.

A.2.8 UV Irradiation of BJ/TERT Cells.

BJ/TERT were plated at 70% confluency in 10cm dishes and left to attach overnight. Cells were then treated 2uM of ATM kinase inhibitor (KU60019) or 5uM of ATR kinase inhibitor (ETP-46464) for two hours prior to UV-irradiation. Medium was removed and cells were washed twice with PBS and irradiated with $20J/m^2$ UV. Fresh medium containing the ATM/ATR kinase inhibitors was added on to the cells and cells were incubated for 22 hrs post irradiation. Lysates were prepared as described above and protein expression was determined by immunoblot analysis.

A.2.9 Viral replication assays

BJ/TERT LBNCX or BJ/TERT LT cells were infected with VSV-GFP (m.o.i = 10), HSV-1 (K26) at an m.o.i = 5, or EMCV (m.o.i = 5). Infected cell supernatants were harvested at the indicated timepoints and kept at -80 ^{o}C until further use. Infectious virus production measured by plaque assay on Vero (HSV-1 and EMCV) or BHK-21 (VSV) cells. 48 hours post infection, plaques were counted and virus production was quantified as plaque forming units (PFU)/ml.

Alternatively, BJ/TERT LT cells were plated at 80% confluency and treated with 50 ng/ml Cyclohexamide (CHX) for 17 hrs prior to treatment with specific ATR kinase inhibitor ETP-46464. Cells were washed twice with PBS and incubated with 4 μm ETP-46464 or DMSO. Cells were washed once again, followed by infection with EMCV (m.o.i. = 50) for 30hrs. Virus growth was quantified by plaque assay on BHK21 cells and expressed as plaque forming units (PFU)/ml.

A.2.10 Cellular viability determination by crystal violet staining.

BJ/TERT LT cells were plated in 12-well plated and treated as described above. Thirty hours post-infection supernatants were harvested for plaque assay. Cells were stained with crystal violet (0.01%) overnight. Plates were washed with distilled water and left to dry. The retained crystal violet was solubilized by resuspension with 600 μl 2% SDS solution in PBS for 30 minutes at room temperature and constant shaking. Absorbance at 600 nm was then used to determine crystal violet. Cellular viability was expressed as change relative to mock-infected cells (value 1).

A.3 RESULTS

Previous studies on the global changes in gene expression induced by SV40 Large T antigen (LT) expression identified a significant number of interferon stimulated genes (ISG) upregulated in mouse embryo fibroblasts [258]. The induction of ISG protein expression appears to be common to other human polyomavirus LT expression, as infection with JC virus has also been

shown to induce the expression of an IFN response transcriptional signature. In order to confirm whether LT antigens encoded by human polyomavirus induce the expression of ISGs, we transiently transfected SV40, BKV, and JCV LT cDNA in HCT116 cells. Expression of SV40 LT led to a robust induction of ISG60 (IFIT3) protein synthesis, similar to the induction observed in JCV LT transduced cells BKV LT, which has a reduced stability and is generally detected at lower levels, could marginally induce the expression of ISGs relative to SV40 or LT, although they overall ISG expression was increased (Figure 5-2A). We then utilized SV40 LT to further characterize the induction of these subsets of genes in human fibroblasts. Stable expression of LT, in BJ/TERT cells resulted in an increase in the protein levels of ISG60 and the related protein ISG56 (IFIT1). Furthermore, the synthesis of OASL protein was also upregulated in LT expressing cells relative to vector control cells (Figure 5-2B). The increase in protein synthesis was accompanied by an increase in ISG56, ISG60, and OASL mRNA transcription, suggesting that LT stimulates the transcription of these genes, which results in increased protein expression (Figure 5-2C, Top). Other human ISGs also identified in the mouse genome arrays, Cig5 and ISG15, were also detected in human fibroblasts (Figure 5-2C, Bottom).

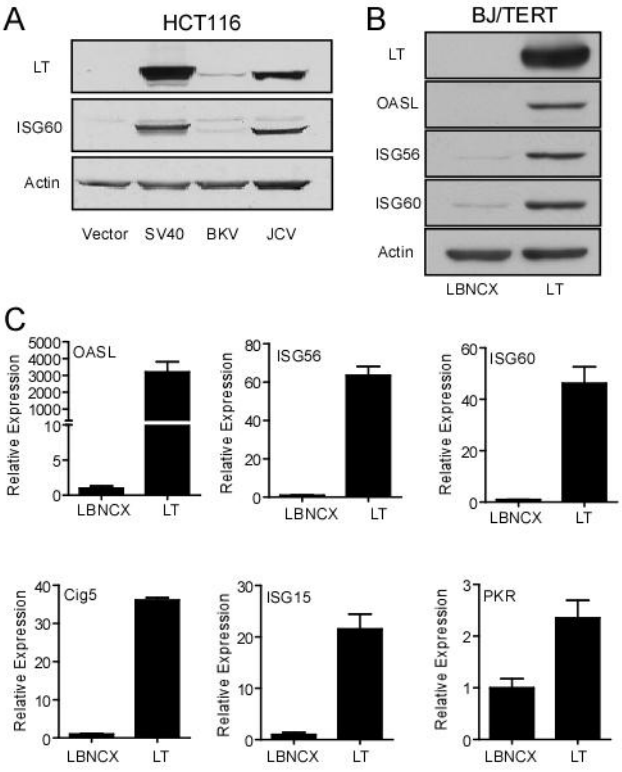

Figure 5-2. Polyoma Virus T Antigen Induces ISG Expression.

(A) Induction of ISG60 by Polyoma virus LT antigen. HCT116 cells ($1x10^6$) were transiently transfected with (1 μg) SV40, (5 μg) BKV, and (1 μg) JCV LT expression vectors or equal mass of empty vector control. 72 hrs post transfection, lysates were prepared and probed with antibodies against LT, IS60, and Actin.
(B) Induction of ISG protein expression in human fibroblasts. Lysates were prepared from BJ/TERT cells stably expressing SV40 LT antigen or empty vector and probed with antibodies against LT, OASL, ISG56, IS60, and Actin.
(C) Induction of ISG transcripts in human fibroblasts. Lysates were prepared from BJ/TERT cells stably expressing SV40 LT antigen or empty vector and probed with antibodies against LT, OASL, ISG56, IS60, and Actin.

Given the strong upregulation of ISGs, we investigated whether the expression of these genes resulted in the protection of LT expressing fibroblasts from infection with different viruses. BJ/TERT cells were infected with vesicular stomatitis virus (VSV), a (-) single-stranded RNA (ssRNA) virus expressing green fluorescent protein (VSV-GFP) at an m.o.i of 10, and incubated for 24 hrs following infection. BJ/TERT cells either expressing LBNCX or LT were resistant to the cytopathic effects of VSV infection. However, analysis by fluorescent microscopy showed readily detectable GFP expression in empty vector (LBNCX) expressing cells, while there was little to no detectable GFP expression in cells stably expressing LT (Figure 5-3A). Similarly, immunoblot analysis of GFP expression in VSV-GFP infected cells, showed decrease GFP protein in cells expressing LT, relative to cells expressing empty vector. The decrease in viral protein synthesis was also observed after infection with Sendai virus (SeV), also a (-) ssRNA. BJ/TERT LT cells infected with SeV for 24 hrs, failed to synthesize the major capsid protein (C-protein) confirming that LT expression restricts viral protein sysnthesis upon superinfection with RNA viruses (Figure 5-3B). To examine the overall effect on virus replication, BJ /TERT expressing LT and vector control cells were infected with VSV and EMCV, a (+) ss-RNA virus, and growth was assessed 1-48 hrs post infection. The growth of VSV (Figure 5-3C) and EMCV (Figure 5-3D) was severely impaired by the expression of LT. We then tested whether LT expression could inhibit the growth of a dsDNA virus, HSV-1. Growth of HSV-1 in BJ/TERT cells expressing LT was decreased by 2-log relative to the growth in empty vector expressing cells (Figure 5-3D). Taken together, these results suggest that the increase in ISG expression induced LT protects cells from viral infection.

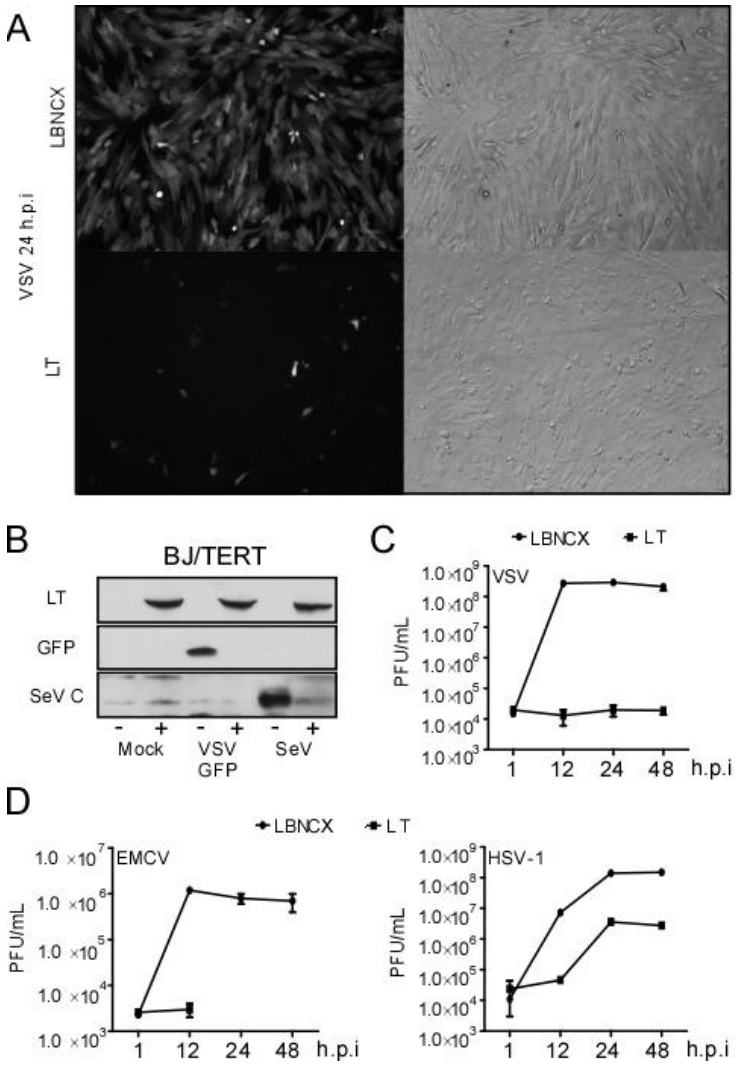

Figure 5-3. SV40 LT Expression Protects Cells from Viral Infection.

(A) GFP expression in VSV-GFP infected BJ/TERT cells. BJ/TERT cells expressing SV40 LT or vector control were infected with VSV-GFP (m.o.i 10) for 24 hrs. GFP expression was detected by fluorescence microscopy.
(B) Analysis of viral protein expression in infected BJ/TERT cells. BJ/TERT cells expressing SV40 LT or vector control were infected with VSV-GFP (m.o.i 5) or SeV (200 HAU/ml) for 24 hrs. Lysates were prepared and probed with antibodies against LT, GFP, and SeV C-protein.
(C) Analysis of VSV growth in BJ/TERT cells. BJ/TERT cells expressing SV40 LT or vector control were infected with VSV-GFP (m.o.i 5). Supernatants were harvested at the indicated time-points and virus replication was measured by plaque assay on BHK21 cells.
(D) Analysis of EMCV growth in BJ/TERT cells. BJ/TERT cells expressing SV40 LT or vector control were infected with EMCV (m.o.i 5). Supernatants were harvested at the indicated time-points and virus replication was measured by plaque assay on Vero cells.
(E) Analysis of HSV-1 growth in BJ/TERT cells. BJ/TERT cells expressing SV40 LT or vector control were infected with HSV-1 (K26-GFP) (m.o.i 5). Supernatants were harvested at the indicated time-points and virus replication was measured by plaque assay on Vero cells.

In the context of a viral infection, the expression of ISGs generally follows nucleic acid sensing by cytoplasmic and nuclear receptors, which activates IRF3 and its downstream induction of IFNβ and ISGs. Type I IFNs then bind to the type I IFN receptor, IFNAR1, activating of the JAK/STAT signaling pathway. This results in the tyrosine (Tyr) phosphorylation of STAT1 and formation of the STAT1/STAT2/IRF9 (ISGF3) signaling complex that further regulates the expression of ISGs. Previously, we showed that LT expression in MEF fibroblasts resulted in the direct phosphorylation of STAT1 at Tyr701 in the absence of type I IFN induction. Moreover, we showed that STAT1 Tyr701 was also phosphorylated in LT expressing human cells [258]. Thus, to confirm that the induction of ISGs in human fibroblasts is due to the independent from type I IFN, we examined the effect of IFNAR knockdown in BJ/TERT cells. As expected, expression of LT antigen resulted in the increased ISG mRNA expression in cells expressing a non-targeting shRNA. Surprisingly, downregulation of IFNAR1 resulted in a decrease in ISG60, OASL, and the interferon responsive gene, MxA mRNA (Figure 5-4A), suggesting that a type I IFN protein is involved in the induction of ISGs in human cells.

Indeed, the ectopic expression of LT resulted in the stimulation of IFNβ transcription in shCTRL cells. Downregulation of IFNAR1 resulted in further enhancement of IFNβ, likely due to the lack of a negative feedback loop required to dampen the induction of type I IFN (Figure 5-4B, left). Interestingly, the transcription of ISG15 followed the same pattern of expression as seen for IFNβ transcription (Figure 5-4B, right), suggesting that transcriptional activation of both genes is controlled by the same factor involved in the early phase of the interferon synthesis pathway, while the upregulation of ISG60, OASL, and MxA is largely dependent on the activation of the JAK/STAT signaling pathway following IFNβ detection. Additionally, we

measured the levels of IFNAR1 expression in shCTRL and shIFNAR cells expressing either the empty vector or LT. While the expression of LT led to a slight increase in IFNAR1 mRNA expression, targeting of IFNAR1 with shRNA led to nearly 90% decrease in mRNA expression in both LBNCX and LT expressing cells lines (Figure 5-4C). Together, the data suggest that in human fibroblasts the activation of cellular factors involved in the transcriptional upregulation of IFNβ are likely being targeted by LT, consequently lead to the induction of ISGs.

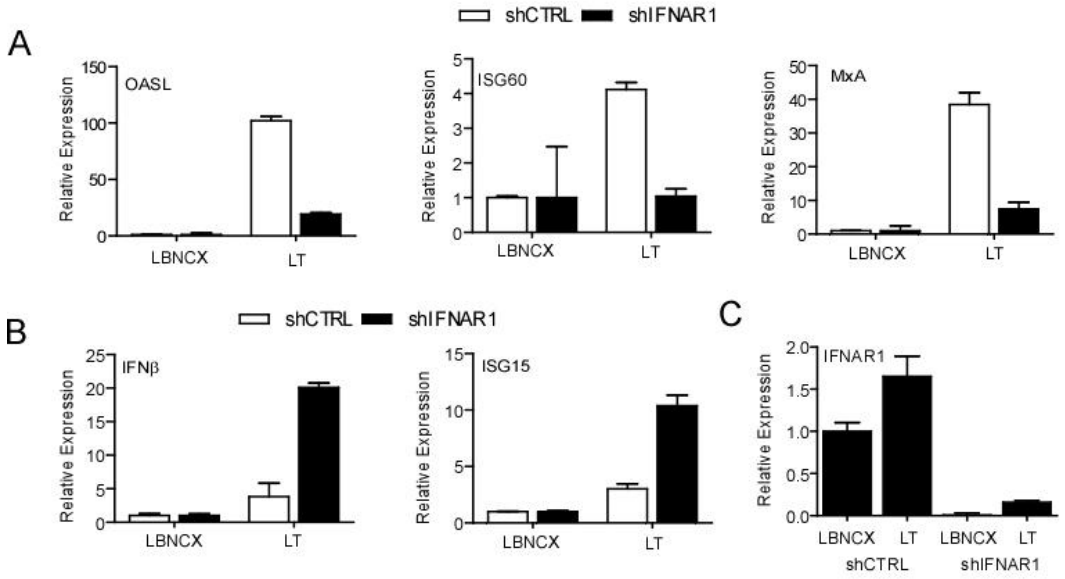

Figure 5-4. Type I IFN Receptor is Necessary for ISG Amplification.

(A) Analysis of ISG induction in IFNAR1 knockdown cells. RNA was harvested from BJ/TERT cells expressing either empty vector or SV40 LT cDNA as well as a short hairpin targeting IFNAR1. Expression of OASL, ISG60, and MxA was analyzed by qRT-PCR. Samples were normalized to RPL32 and expressed as fold change with respect to LBNCX vector control cells (value 1).
(B) Analysis of IFNβ and ISG15 induction in IFNAR1 knockdown cells. RNA was harvested from BJ/TERT cells expressing either empty vector or SV40 LT cDNA as well as a short hairpin targeting IFNAR1. Expression of IFNβ and ISG15 mRNA was analyzed by qRT-PCR. Samples were normalized to RPL32 and expressed as fold change with respect to LBNCX vector control cells (value 1).
(C) Validation of IFNAR knockdown in BJ/TERT cells. RNA was harvested from BJ/TERT cells expressing either empty vector or SV40 LT cDNA as well as a short hairpin targeting IFNAR1. Expression of IFNAR1 mRNA was analyzed by qRT-PCR. Samples were normalized to RPL32 and expressed as fold change with respect to LBNCX vector control cells expressing the non-targeting shRNA (value 1).

Given that IFNβ gene expression was detected in LT expressing cells, we postulate that the mechanism of ISG induction in human fibroblast relies on factors involved in the regulation of type I IFN induction. As observed in shCTRL and shIFNAR expressing cells, IFNβ mRNA was readily detectable in BJ/TERT cells stably expressing LT or BJ/TERT cells treated p(I):(C) overnight. However, the induction of IFNβ mRNA following p(I):(C) treatment was 20 times greater than that observed by LT expression (Figure 5-5A). To our surprise, the induction of type I IFN by LT was restricted to the stimulation of IFNβ transcription as no transcription of IFNα genes was detected in BJ/TERT LT cells by qRT-PCR analysis using Pan-IFNα targeting primers. We examined the response of BJ/TERT cells to p(I):(C) and were able to measure a readily detectable induction of IFNα transcription (Figure 5-5B). These results suggest that LT activates factors that lead to a low induction of IFNβ in the absence of IFNα induction; however, dsRNA stimulation results in the activation of a second set of transcriptional activators, which can effectively induce high levels of IFNβ expression resulting in the downstream induction of IFNα.

The major regulators of transcription in the IFN response pathways are the IRF family of proteins. Five of these proteins, IRF1, IRF3, IRF5, IRF7, and IRF9 are ubiquitously expressed amongst different tissues where they positively regulate the expression of ISGs. . The activation of IRF3 leads to its dimerization and translocation into the nucleus, leading to the induction of IFNβ transcription. To determine if the expression of LT induces the activation of IRF3 we examined the presence of IRF3 dimers in LT and SeV infected cells. IRF3 dimers were readily detected in BJ/TERT cells 8 hrs after viral infection. However, the expression of LT or vector control failed to stimulate IRF3 activation (Figure 5-5C). With the exception of IRF3, the induction of protein synthesis acts as a regulatory step in the transcriptional activation of these

factors. Thus, we explored whether LT altered their level of expression. Comparison of IRF protein expression in BJ/TERT LT cells and empty vector expressing cells showed a significant increase in IRF1, IRF7, and IRF9 (Figure 5-5D, left). On the other hand, the transcription of IRF5, which is involved in both the induction of IFN and the inhibition cellular replication, was drastically downregulated by LT (Figure 5-5D, right). Expression of IRF3, the primary mediator of the dsRNA sensing and IFNβ secretion and we observed a slight decrease in mRNA expression in LT expressing cells. These results suggested then that the induction of IFNβ was likely mediated by IRF1, IRF7, or IRF9. To examine the effect of these proteins on IFNβ promoter activation, we co-transfected 293 cells with IRF1, IRF7, or IRF9 cDNA and IFNβ_{125}-luc and pRL-null as a transfection control. Expression of IRF1 resulted in over 10-fold increase in promoter activity while IRF7 transduction resulted in a 5-fold induction in promoter activity relative to vector control transfected cells (Figure 5-5E). Given that IRF9 resulted in a weak induction in our reporter assay and that IFNβ mRNA levels were enhanced after the downregulation of IFNAR1 rather than being reduced, we excluded the possibility that IRF9 is involved in the direct activation of IFNβ transcription in BJ/TERT LT cells. We verified the activity of the IFNβ_{125}-luc in BJ/TERT cells by transient transfection of BJ/TERT LT with 1 μg IFNβ_{125}-luc and recorded a 10-fold increase in luciferase activity relative to the luciferase activity observed in pGL3-basic transfected cells (Figure 5-5F).

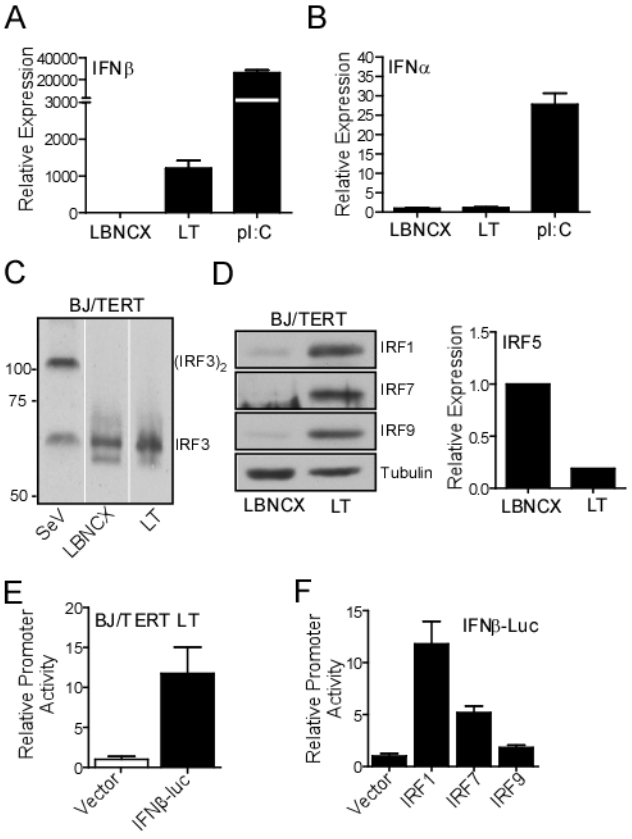

Figure 5-5. SV40 LT Promotes the Induction IFNβ Expression.

(A and B) SV40LT induction of type I IFN. BJ/TERT cells were stimulated with poly(I):poly(C) 100 μg/ml or stably transduced with LBNCX or SV40 LT. Total RNA was extracted from $1x10^7$ cells and IFNβ (A) and Pan-IFNα (B) mRNA levels were analysed by qRT-PCR. mRNA expression was normalized to RPL32 and expressed relative to vector control expressing cells (value 1).
(C) IRF3 dimerization assay. Lysates were prepared from BJ/TERT cells stably expressing vector control, SV40 LT, or cells infected with 300 HAU/ml for 8 hrs. Protein was resolved by Native PAGE and probed with anti-IRF3 antibodies.
(D) Modulation of IRF gene expression by SV40 LT. Lysates were prepared from BJ/TERT cells stably expressing vector control or SV40 LT and probed with antibodies against the antiviral mediators IRF1, IRF7, and IRF9 as well as Tubulin (D). Total RNA was extracted from $1x10^7$ BJ/TERT cells stably expressing vector control or SV40 LT and IRF5 and IRF3 mRNA levels were analysed by qRT-PCR (E). Target gene mRNA expression was normalized to RPL32 and expressed relative to vector control expressing cells (value 1).
(E) Induction of IFNβ promoter activity by IRF proteins. IRF1, IRF7, or IRF9 cDNA was co-transfected with IFNβ□□5-luc and pRL-null in 293 cells. Firefly luciferase activity was normalized to renilla luciferase activity and promoter activity was expressed as change relative to vector control transfected cells (value 1).
(F) SV40 LT expression induces the IFNβ promoter. 1 μg of IFNβ luciferase reporter construct or pGL3 basic vecor control was transiently transfected in BJ/TERT LT cells. Firefly luciferase was normalized to empty vector expressing cells (value 1).

In order to define whether either IRF1 or IRF7 is required for the induction of IFNβ promoted by LT, we used knocked down the expression of these genes by transiently transfecting siRNA targeting IRF1 or IRF7 in BJ/TERT LT cells. The downregulation of IRF1, specifically, was accompanied by a decrease in the expression of ISGs, previously determined to be induced in an IFNAR1-dependent manner as determined by the loss of OASL and ISG60 protein expression. Furthermore, loss of IRF1 expression led to a decrease of IRF7, which not only regulates ISG expression, but is also an IFNβ responsive ISG. However, knockdown of IRF7 did not affect the expression of either ISGs or IRF1 (Figure 5-6A). The loss of ISG expression was due to a decrease in transcriptional activation of these genes as determined by the decrease in mRNA levels following the knockdown of IRF1. Downregulation of IRF1 in BJ/TERT LT cells also led to the inhibition of IFNβ mRNA, explaining the concomitant loss of ISG expression. Again, the knockdown IRF7 had no effect in the transcription of ISGs and resulted in a slight increase in IFNβ transcription (Figure 5-6B). Knockdown of either IRF1 or IRF7 had a similar effect on the transcription of OASL, likely due to the loss of IFNβ synthesis. We then examined the effect of knocking down IRF1 and IRF7 on the expression of these genes. Transient targeting of IRF1 resulted in a 50% loss in IRF1 mRNA expression, while targeting IRF7 had no effect on the transcription of IRF1 (Figure 5-6C). However, silencing of IRF1 led to a 50% decrease in IRF7 transcription, which was lower than the almost 90% loss in IRF7 mRNA observed when IRF7 was silenced specifically (Figure 5-6D). The modulation of gene expression that followed the downregulation of IRF1 was not due to changes in LT, as equivalent protein and mRNA expression was detected after downregulation of either gene (Figure 5-6E and A).

We further supported our siRNA studies by measuring the induction of IFNβ mRNA in cell stably expressing an IRF1-targeting shRNA. As previously observed, IRF1 knockdown cells

resulted in a 40% loss of IFNβ transfection and a 50% decrease in IRF1 without any effect on the expression of SV40 LT (Figure 5-6F). These results suggest IRF1 controls IFNβ transcription and that response to IFNβ secretion leads to the IFNAR1 dependent activation of IRF7 and IRF9, which then can participate in the enhanced expression of ISGs like OASL, ISG60, and MxA.

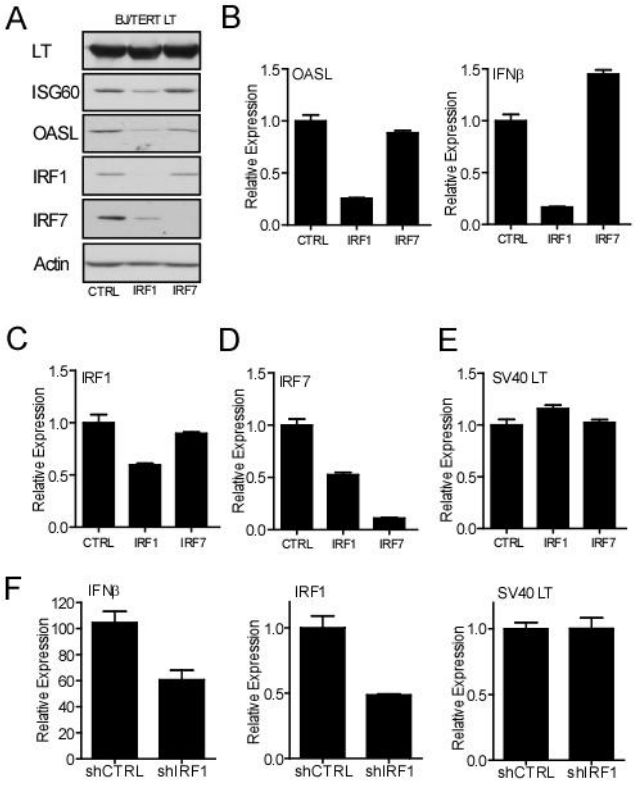

Figure 5-6. Induction of IRF1 Results in IFNβ Transactivation.

(A) Requirement for IRF1 in the induction of ISG protein synthesis. Briefly, BJ/TERT cells were transfected with 160 pmoles of siRNA against IRF1 and IRF7 and incubated for 48 hrs. Lysates were prepared and probed with antibodies against OASL, ISG60, SV40 LT, IRF1, IRF7, and Actin.

(B-E) IRF1 and IRF7 requirement for the transcriptional induction of IFNβ and OASL. IFNβ and OASL (B), IRF1 (C), IRF7 (D), and SV40 LT (E) mRNA levels were assessed by qRT-PCR. Briefly, BJ/TERT cells were transfected with 160 pmoles of siRNA against IRF1 and IRF7. Total RNA was harvested and cDNA was synthezised. Expression of target genes was determined by qRT-PCR analysis and normalized to RPL32 and control siRNA transfected cells (value 1).

(E) Analysis of ISG protein expression in IRF1 and IRF7 knockdown cells. BJ/TERT LT cells were transfected with siRNA gainst IRF1 and IRF7 as described above. Lysates were prepared and probed with antibodies against SV40 LT, ISG60, OASL, IRF1, IRF7, and Actin.

(F) Analysis of IFNβ mRNA expression in IRF1 knockdown cells. BJ/TERT cells were stably transduced with an shRNA targeting IRF1 or a non-targeting shRNA. Cells were then stably transduced with pLBNCX or pLBNCX-LT. Total RNA was harvested and mRNA expression was determined by qRT-PCR. Expression of target genes was normalized to RPL32 and reported relative to the enhancement observed over empty vector expressing cells (value 1).

Expression of LT has been shown to induce DNA damage in human fibroblasts and the activation of an ATM/ATR kinase mediated DNA damage response (DDR) [243,244,247]. Moreover, the induction DDR has previously been associated with the induction of IRF1 protein expression [259]. We confirmed that the induction of DNA damage by UV irradiation in fibroblast resulted in the induction of both IRF1 and IRF7. Following genotoxic insult, ATM/ATR activation results in the phosphorylation of p53 at Ser15, which leads to the stabilization of p53. We inquired whether either ATM or ATR kinase activity is involved in the in the stabilization of both IRF1 and p53 by pre-treating cells with ATM and ATR specific inhibitors prior to UV irradiation (Figure 5-7A). The induction of IRF1 and IRF7 was comparable in BJ/TERT cells treated with ATM inhibitor (KU60019) was comparable to the induction observed in DMSO treated cells. However, ATR kinase inhibitor (ETP-46464) treatment resulted in a marked decrease in the induction of IRF1 protein synthesis concomitant with a loss of IRF7 expression (Figure 5-7B).

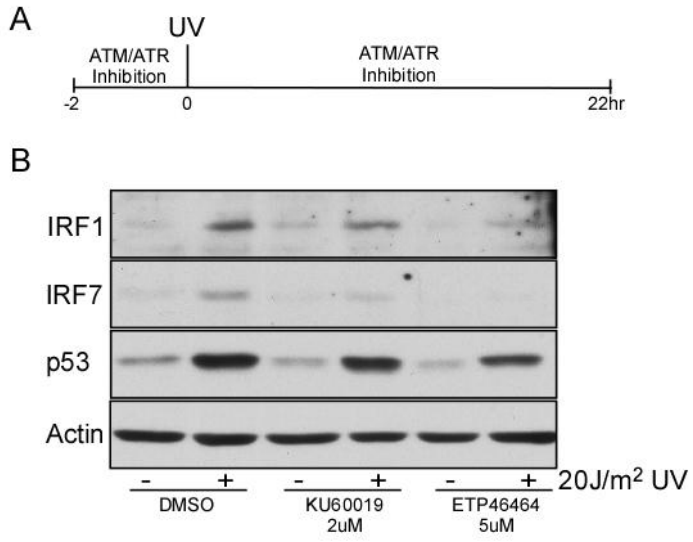

Figure 5-7. DNA Damage Induces IRF1 and IRF7 in an ATR Kinase dependent manner.

(A) Schematic representation of experimental design. Briefly, BJ/TERT were plated at 70% confluency in 10cm dishes and treated with 2uM or 5uM of ATM (KU60019) or ATR (ETP-46464) kinase inhibitor respectively. Cells were then irradiated with 20J/m^2 UV and further incubated for 22 hrs post irradiation in the presence of kinase inhibitors.
(B) Analysis of IRF1 and IRF7 induction in UV-irradiated BJ/TERT cells. Lysates were prepared from cells stimulated as described above and probed with antibodies against IRF1, IRF7, p53, and Actin.

We then asked if the inhibition of ATR kinase activity in cells stably expressing LT could also result in a decrease in ISG expression and IRF1 stabilization. As observed in UV irradiated cells, 24 hr treatment of BJ/TERT LT cells with ATM kinase inhibitor (KU60019) did not affect the expression IRF1 or OASL, and the levels of protein expression were comparable to those detected in cells treated with DMSO. On the other hand, ATR kinase inhibition led to a decrease in OASL protein synthesis following a reduction in the expression of IRF1. Given that LT antigen is modified by ATM, we tested whether inhibitor treatment affected the LT protein stability. Treatment with either inhibitor did not affect the level of LT protein expression (Figure 5-8A). We confirmed that ATM and ATR kinase activity was inhibited by measuring whether inhibitor treatment decrease the phosphorylation p53 at Ser15. Indeed, both ATM and ATR

specific kinase inhibitors led to a decrease in Ser15 phosphorylation without affecting the stability of p53 in BJ/TERT LT cells (Figure 5-8B).

Expression of IRF1 can be regulated by either the transcriptional activation of IRF1 mRNA or by post-translational modifications that stabilize IRF1 protein expression. In order to determine whether ATR kinase activity is involved in either of these two regulatory responses, me quantified the levels of IRF1 mRNA after treatment of BJ/TERT LT cells with ATM or ATR kinase inhibitors. ATR kinase inhibition led to a decrease in the transcription of IRF1 mRNA, while ATM inhibition had no effect on IRF1 mRNA expression. Likewise, ATR kinase inhibition led to a decrease in IFNβ mRNA levels, accounting for both the decrease in OASL mRNA and protein expression (Figure 5-8C).

Finally, we addressed whether the inhibition of IFNβ, due to the loss of ATR kinase activity, reverses the protection of fibroblast from viral infection afforded by LT expression. First, we treated BJ/TERT LT cells with 50 ng/ml cyclohexamide (CHX) for 17 hrs to inhibit the LT-mediated transcription of IFNβ. Thus, we pre-incubated cells with ATR kinase inhibitor followed by 2 hr adsorption of VSV-GFP onto the cells. Finally, we incubated both mock infected and infected cell with either ETP-46464 or DMSO for an additional 30 hrs. ATR kinase inhibition decreased the LT protection of cells from virus mediated cells death as we observed a significant decrease (~25%) in cell survival relative to the induction of cell death in DMSO treated cells (Figure 5-8C, left). The loss in viability was accompanied by a 25% increase in viral growth in BJ/TERT LT cells devoid of ATR kinase activity (Figure 5-8D, right). Taken together, our results suggest that LT triggers the DNA damage response and relies on ATR to enhanced expression of IRF1. This results in the induction of low levels IFNβ that generate an antiviral

state and protects cells from viral infection through the induction of effectors that negatively regulate viral replication and gene expression.

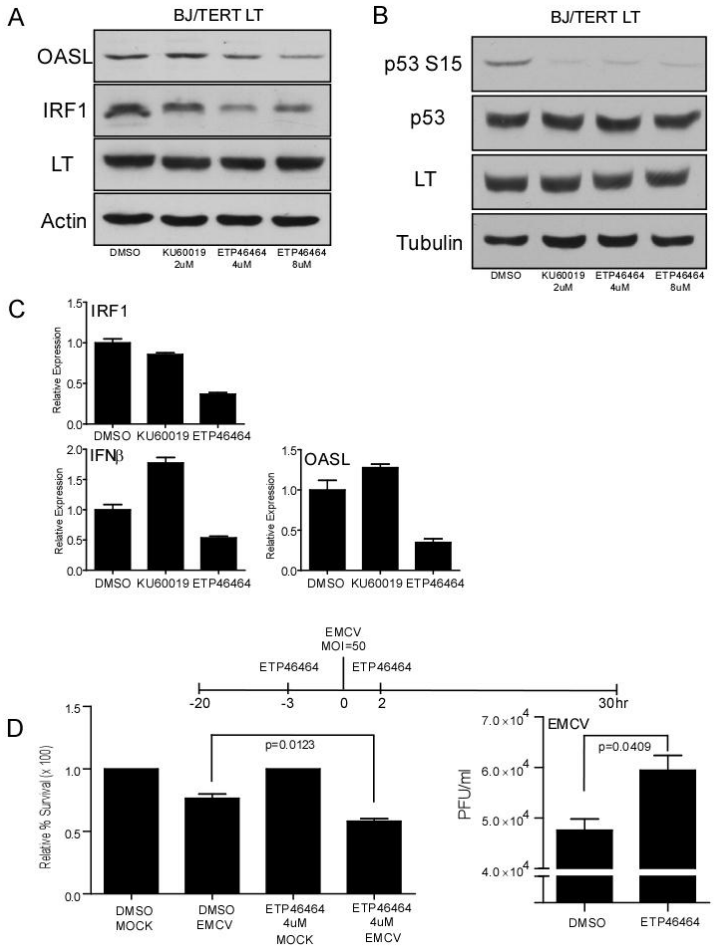

Figure 5-8. Induction of ISGs by LT dependent on ATR Kinase activity.

(A) Analysis of ISG induction in ATM/ATR kinase inhibitor treated BJ/TERT LT cells. Lysates were prepared from BJ/TERT cells stimulated for 24 hrs with the indicated doses of KU60019 or ETP46464. Levels of OASL, IRF1, LT, and Actin were detected by immunoblot.
(B) Analysis of p53 phosphorylation in ATM/ATR kinase inhibitor treated BJ/TERT LT cells. Cells were treated as described above. Lysates were prepared, and probed with antibodies against phosphorylated p53 (Serine 15), total p53, and Actin.
(C) Analysis of IFNβ mRNA in ATM/ATR kinase inhibitor treated BJ/TERT LT cells. Total RNA was prepared from BJ/TERT cells stimulated for 24 hrs with 2 μM KU60019 or 4 μM ETP-46464. Expression of IFNβ, IRF1, and OASL were determined by qRT-PCR. Samples were normalized to RPL32 and vehicle treated cells (value 1).
(D) EMCV growth in BJ/ETRT LT cells treated with ETP-46464. In brief, BJ/TERT LT cells were plated in 12-well plates at an 80% confluency. Cells were treated with CHX (50 ng/ml) for 17hrs prior to viral infection. Three hours prior to EMCV infection, cells were stimulated with 5 μM of ETP-46464. Cells were then infected with EMCV (m.o.i 50). Infected cells were stained with crystal violet to determine cell survival relative to mock-infected cells (left). Supernatants were harvested 30hrs post infection and viral growth in DMSO or ATR kinase inhibitor treated infected cells was determined by plaque assay on Vero cells (right).

A.4 DISCUSSION

In this study we have defined the mechanism by which stable expression of SV40 LT induces the expression of IFN-stimulated genes. Our results indicate that the induction of ISGs occurred in both an IFNAR1-dependent and IFNAR1-independent manner. Thus, this suggested that LT expression results in the induction of factors that control the expression of type I IFNs. Indeed, we observed a strong upregulation of IFNβ mRNA by LT accompanied by increases in the expression of regulators of IFN responses: IRF1, IRF7, and IRF9. Furthermore, we show both LT expression and UV irradiation result in the stabilization of IRF1 expression through the induction of ATR kinase activation, specifically, which leads to the upregulation of IFNβ expression. Thus, our study emphasizes the interface between the DNA-damage response (DDR) and the IFNβ antiviral response, which is largely mediated by ATR kinase.

The DDR is a complex cellular network involved in the detection of genotoxic stress, which triggers cell-cycle arrest and DNA repair or triggers apoptosis if the insult fails to be repaired. The major sensors of DDR are the phosphoinositide 3-kinase related kinases (PIKK), ATM and ATR, that act on substrates that include check-point kinases that magnify the signaling cascade. Early studies have connected DDR to the induction of IRF1 expression [259-262]. IRF1 is an important mediator of IFN responses [263-265], although its role in the regulation of other stress responses is still not clearly understood. Studies have implicated IRF1in the induction, along with p53, of genes involved in the regulation of cell growth, susceptibility to transformation by oncogenes, induction of apoptosis [259,260]. Mechanistic studies examining the regulation of IRF-1 expression, have linked ATM with the induction of IRF-1 in epithelial cells [259]. Other studies have also identified NF-κB as a crucial factor involved in the induction

of IRF1 and IRF7 expression in human epithelial cells [266]. Thus, it is likely that the triggering of DDR is a mechanism to protect genome integrity and to some extent, act as an antiviral response against virus infection.

The relationship between viruses and DDR has become an interesting subject of investigation. Much attention has been placed on understanding the complex molecular interactions between DNA viruses and the DDR (Reviewed in [267,268]). Detection of viral genomes as damaged DNA, the expression of viral oncogenes which deregulate cell-cycle checkpoints and promote replicative stress, and the induction of reactive oxygen species are all triggers for a response that can have potentially deleterious consequences for both the virus and the infected cell. On the other hand, other studies have elucidated ways in which invading pathogens hijack these pathways during the course of infection to promote efficient replication of their genomes [268]. Using a virally encoded oncogene and employing chemical inhibitors of the master regulatory kinases of the DDR, ATM and ATR, we were able to distinguish the signaling pathways and shed light on the connection between DDR and antiviral IFN responses. Although we have not shown how ATR is able to induce IRF1 and which ATR substrate is necessary, our future studies will be directed towards this.

Classic IFN induction has been viewed mostly as being caused by virus infection and sensing of viral nucleic acid. Here, we show a unique mechanism for LT mediated induction of IFN that is distinct from previous mechanisms and provide a mechanistic connection between DDR and IFN induction. The DDR is a complex cellular network involved in the detection of genotoxic stress, which triggers cell-cycle arrest and DNA repair or triggers apoptosis if the insult fails to be repaired. The major sensors of DDR are the phosphoinositide 3-kinase related kinases (PIKK), ATM and ATR that act on substrates that include check-point kinases that

magnify the signaling cascade. Early studies have connected DDR to IRF1 on a different context [259-262]. Discovered as an important mediator of IFN responses [263-265], the role of IRF1 in the regulation of other stress responses is still not clearly understood. Studies have implicated IRF1in the induction, along with p53, of genes involved in the regulation of cell growth, susceptibility to transformation by oncogenes, induction of apoptosis [260]. Mechanistic studies examining the regulation of IRF-1 expression, have linked ATM with the induction of IRF-1 in epithelial cells [259]. Other studies have also identified NF-κB as a crucial factor involved in the induction of IRF1 and IRF7 expression in human epithelial cells [266]. Thus, it is likely that the triggering of DDR is a mechanism to protect genome integrity and to some extent, act as an antiviral response against virus infection.

In the context of virus infection much attention has been on understanding the complex molecular interactions between DNA viruses and the DDR (Reviewed in [267,268]). Detection of viral genomes as damaged DNA, the expression of viral oncogenes which deregulate cell-cycle checkpoints and promote replicative stress, and the induction of reactive oxygen species are all triggers for a response that can have potentially deleterious consequences for both the virus and the infected cell. On the other hand, other studies have elucidated ways in which invading pathogens hijack these pathways during the course of infection to promote efficient replication of their genomes [268]. Using a virally encoded oncogene and investigating the master regulatory kinases of the DDR, ATM and ATR, we were able to distinguish the signaling pathways and shed light on the connection between DDR and antiviral IFN responses.

We have shown that while the induction of ATM and ATR-triggered signaling cascades lead to the activation of proteins of benefit for viral replication and immune evasion, the ATR-signaling arm specifically acts as a sensor of virus induced replicative stress and potentially

promotes viral elimination through the induction of IFN responses in human fibroblasts. This notion is further supported by previous observations of specific targeting of ATR-mediated signaling during the course of viral infections. HSV-1 relies on the induction of both ATM and ATR activity early in infection to stimulate the replication of viral genomes, while effectively degrading ATR at later time points to successfully complete the infectious cycle [269,270]. Similarly, the polyomavirus [242-245,247,271] and human papillomaviruses [272] also induce the DDR machinery for viral replication while countering these responses during the late phases of viral replication for the completion of the infectious cycle.

Interestingly, RNA viruses, like HIV-1 [273], avian infectious bronchitis virus [274], Hepatitis C virus [275], and Rift Valley Fever [276], have also been shown to trigger DNA-damage responses. Thus, it is likely that these viruses have developed strategies to overcome the blockade imposed by the induction of DDR-mediated IFN induction. Indeed, studies provide evidence that Rift Valley Fever Virus non-structural (NS) proteins induce replicative stress that triggers the ATM signaling pathway and enhances viral replication. On the other hand, NSs target ATR-signaling, specifically, to further promote viral growth [276]. Thus, while we and others have provided evidence that the ATR signaling pathway is involved in the regulation of immune responses, the overall role of ATR in mediating antiviral responses still remains to be clarified.

DNA tumor viruses not only benefit from the induction of effector genes that can promote genome replication, but also have developed strategies to prevent the arrest in cellular replication, cellular death, and other potential antiviral effects mediated by DDR [267]. In particular, SV40 LT can efficiently abrogate the transcriptional functions of p53, preventing the induction of apoptosis [240]. This in turn can result in the abrogation of a negative inhibition of

DDR and thus contribute to the constitutive secretion of low levels of IFNβ in human fibroblasts stably transduced with LT. Elevated levels of IFNβ induce the expression of genes involved in the IFN responsive pathway, which have been previously shown to be upregulated in certain types of cancer and promote poor prognosis and response to therapy [5,188-194]. Furthermore, some of the effector genes of the IFN response are epigenetic modifiers that promote nuclear programming and modify cellular gene expression [277]. Thus, we propose that the induction of DNA damage and IFN responses by LT, in the absence of viral infection and intact apoptotic responses, contributes to the global changes in gene expression observed in LT transformed cells and adds to the transformative capacity of LT.

APPENDIX B

ENHANCED APOPTOSIC RESPONSES TO DOUBLE-STRANDED RNA IN METASTATIC HNSCC IS INDEPENDENT FROM IFNAR-MEDIATED SIGNALING

Work described in this section was partly published in Cancer Research (Cancer Res. 2012 Jan 1;72(1):45-55) by authors Naoki Umemura, Jianzhong Zhu, Yvonne K. Mburu, Adriana Forero, Paishiun N. Hsieh, Ravikumar Muthuswamy, Pawel Kalinski, Robert L. Ferris, and Saumendra N. Sarkar.

B.1 INTRODUCTION

Head and neck squamous cell carcinomas (HNSCC) are the sixth most common cancer worldwide [278]. Lymph node metastasis is associated with poor prognosis of HNSCC and metastatic disease accounts for most cancer mortality [24]. Thus, it is important to elucidate the intrinsic differences between primary tumors and their metastatic lesions to better understand the disease and to develop effective therapies. Synthetic double-stranded RNAs that are cognate ligands of TLR3 have been used as adjuvants to cancer immunotherapies to further enhance their proapoptotic activity in cancer cells. Using paired autologous primary and metastatic head and neck squamous cell carcinoma cell lines and tumor specimens, the potential therapeutic application of TLR3 ligands in metastatic progression was explored. Metastatic tumor cell lines showed enhanced apoptosis relative to primary cells in response to TLR stimulation by p(I):(C) treatment. Primary and metastatic cells did not display any differences in TLR3 expression and sensing of synthetic dsRNA.

In this study, we examine the role of type I IFN signaling on the enhanced apoptosis observed in metastatic cells. Using shRNA lentiviral expression vectors, we were able to knokdown IFNAR1 expression and show that while ISG expression is enhanced by IFNAR1 activation, the enhanced apoptotic effect of p(I):(C) treatment in metastatic cells is does not require IFN signaling. Rather the enhanced apoptosis was found to be due to defective p(I):(C)–mediated NF-κB activation in metastatic cells (Figure 5-9).

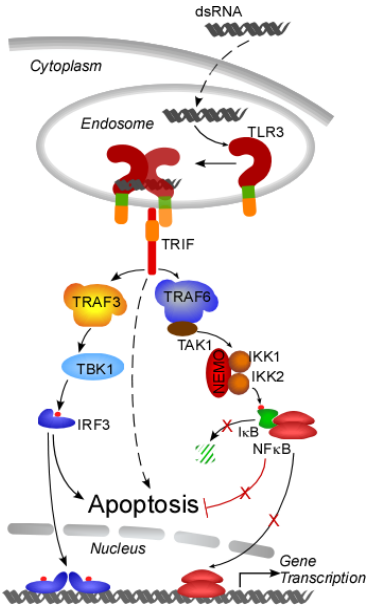

Figure 5-9. Proposed Model for Enhanced Apoptosis in Metastatic HNSCC Cells.

Schematic representation of TLR3 signaling pathway. Sensing of dsRNA results in the dimerization of TLR3 and signaling through TRIF. Engagement of the TRAF3 complex results in the activation of IRF3 and the transcription of effector genes that result in cell apoptosis. TRAF6-mediated signaling results in the activation of NF-κB in primary tumor cells, which promotes the expression of proinflammatory genes and negatively regulates cellular apoptosis. Defective NF-κB signaling in metastatic cells results in enhanced IRf3-mediated apoptosis.

B.2 MATERIALS AND METHODS

Cell lines

The cell lines used in this study have been described on Table 9. HNSCC cell lines, PCI15A and PCI15B, PCI15B-derived cells, and 293FT were cultured in DMEM (Lonza) containing 10% FBS (Atlanta Biologicals) and 100 I.U./ml penicillin and 100 mg/ml streptomycin (Lonza). BJ/TERT cells were cultured in 80% DMEM, 20% Medium 199 (Invitrogen), 10% FBS, and 100 I.U./ml penicillin and 100 mg/ml streptomycin.

Table 9. Appendix A - Cell Lines

Cell Line	Description	Source	Reference
BJ/TERT	hTERT immortalized BJ Fibroblasts	Gjoerup Lab (Tufts University)	[252]
BJ/TERT shCTRL	hTERT immortalized BJ Fibroblasts expressing scrambled shRNA. Generated by lentiviral tranduction with pLKO.1 - shCTRL	Sarkar Lab (University of Pittsburgh)	
BJ/TERT shIFNAR	hTERT immortalized BJ Fibroblast expressing scrambled shRNA. Generated by lentiviral tranduction with pLKO.1 – shIFNAR1	Sarkar Lab	
PCI-15A	Human epithelial cells derived from primary HNSCC tumor lesions.	Whiteside Lab (University of Pittsburgh)	[279]
PCI-15A shCTRL	PCI-15A-derived cell line expressing scrambled shRNA. Generated by lentiviral tranduction with pLKO.1 - shCTRL	Sarkar Lab	[280]
PCI-15B shIFNAR	PCI-15B-derived cell line expressing shRNA targeting IFNAR1. Generated by lentiviral tranduction with pLKO.1 – shIFNAR1	Sarkar Lab	[280]
PCI-15B	Human epithelial cells derived from recurrent metastatic HNSCC lesions from the same donor as PCI15A.	Whiteside Lab (University of Pittsburgh)	[279]
PCI-15B shCTRL	PCI-15B-derived cell line expressing scrambled shRNA. Generated by lentiviral tranduction with pLKO.1 - shCTRL	Sarkar Lab	[280]
PCI-15B shIFNAR	PCI-15B-derived cell line expressing shRNA targeting IFNAR1. Generated by lentiviral tranduction with pLKO.1 – shIFNAR1	Sarkar Lab	[280]

B.2.1 Lentivirus packaging and generation of stable cell lines

Lentiviral vectors (pLKO.1) for the delivery of constitutively expressed shRNA were used in this study. Specifically, the vectors targeting IFNAR1 (shIFNAR) were purchased from Sigma-Aldrich and scramble control hairpin (shCTRL) was obtained from Addgene (plasmid 10879). The specific targeting sequences are described in Table 10 below.

Table 10. pLKO.1 Based shRNA Delivery Vectors.

Clone	TRC Number	Target Sequence
shCTRL		CCGCAGGTATGCACGCGT
shIFNAR Clone 1	TRCN0000059017	GTTGACTCATTTACACCATTT
shIFNAR Clone 3	TRCN0000059015	CGACATCATAGATGACAACTT
shIFNAR Clone 4	TRCN0000059014	CCTTAGTGATTCATTCCATAT
shIFNAR Clone 5	TRCN0000059013	GCCAAGATTCAGGAAATTATT

Lentiviruses were packaged in 293FT cells using the methodology described in Chapter 2 materials and methods. PCI15B-derived pLKO.1 cells were generated by overnight lentiviral infection with virus packaged from pLKO.1 shCTRL or pLKO.1 shIFNAR in the presence of 5 μg/ml polybrene (Sigma-Aldrich). 48 hrs post-infection, cells were selected with 1 μg/ml Puromycin (InvivoGen) for 7 days. Puromycin-resistant cells were pooled and used for further studies.

B.2.2 RNA Isolation and Quantitative Reverse Transcriptase Polymerase Chain Reaction Analysis qRT-PCR.

RNA isolations and cDNA synthesis was performed as described in Chapter 2 materials and methods. Samples were subjected to SYBR green real-time PCR using a CFX96 real time system

(Bio-Rad). IFNAR1 cDNA was specifically amplified using primers: (Forward) 5' – GAAACCACTGACTGTATATTGTGTGAAA – 3'and (Reverse) 5' - CAGCGTCACTAAAAACACTGCTTT – 3'. RPL32 primer set sequences have been previously described in Table 4. Each sample was normalized to RPL32 and expressed as fold change with respect to vector expressing cells (value 1).

B.2.3 Immunoblotting

Cells were treated with 25 or 50 μg/ml p(I):(C) (GE) for 24 hrs and lysed as described in Chapter 2 Materials and Methods. Lysates were resolved in 8% SDS–polyacrylamide gels. Proteins were transferred to PVDF membranes, washed twice in Tris-buffered saline with Tween 20 (TBS-T; 20 mM Tris, 0.5 M NaCl [pH 7.5] plus 0.5% Tween 20) and blocked for 1hr in 10% nonfat dry milk TBS-T. Primary antibody incubation with anti-ISG56 antibody[176], anti-Cleaved PARP (Asp214, Cell Signaling), or anti-Actin (Santa Cruz) was done overnight in 10% nonfat dry milk. Membranes were then washed twice with TBS-T and incubated with horseradish peroxidase-conjugated anti-mouse or anti-rabbit immunoglobulin G (IgG) diluted at 1:10,000 in TBS-T plus 10% nonfat dry milk. Blots were revealed by enhanced chemiluminescence using Hy-Glo reagent (Denville) according to manufacturer's protocol.

B.2.4 Caspase 3 and Caspase 7 activity

PCI15B shCTRL or PCI15B shIFNAR cell ($2x10^4$) were seeded on 96-well plates. Cells were treated with 12, 25, 50 μg/ml p(I):(C) of for 24 hrs. Plates were then allowed to equilibrate to room temperature and 20 μl of Caspase-Glo® 3/7 Assay (Promega) were added to each well.

Plates were then incubated 30 minutes to 3 hrs at room temperature on a plate shaker. Luminescence emitted was measured using luminescence plate reader. Results were expressed as relative light units (x1000).

B.3 RESULTS AND DISCUSSION

To evaluate the efficiency of IFNAR1 silencing by lentiviral shRNA vectors, we infected immortalized human fibroblasts, BJ/TERT, with one of four different lentivirus clones expressing IFNAR1 targeting sequences (shIFNAR1) or scramble control (shCTRL) and stable cell lines were generated by selection with puromycin. The levels of IFNAR1 mRNA expression relative to scramble control were measured by qRT-PCR. Three of the lentiviral constructs showed 50-60% silencing (clones 3-5) while transduction of cells with lentiviral clone 1 resulted in a 90% reduction in IFNAR1 mRNA (Figure 5-10A).

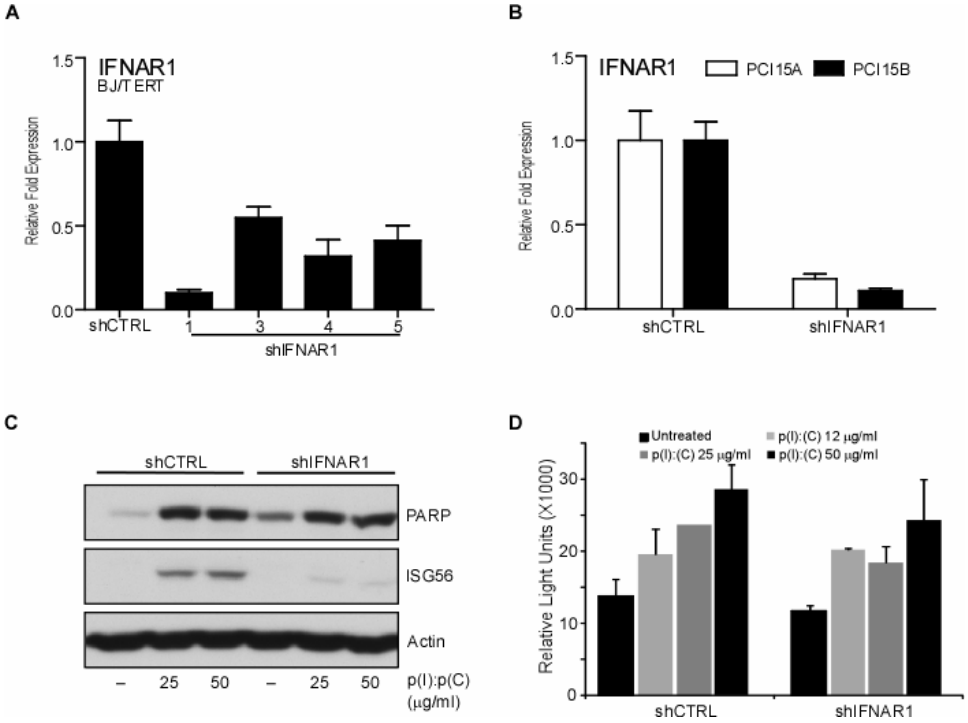

Figure 5-10. Enhanced Apoptosis in Metastatic Cells is Independent of IFNAR Signaling.

(A) Analysis of IFNAR1 knockdown efficiency. Total RNA was harvested from BJ/TERT cells stably expressing shRNA targeting IFNAR1 or non-targeting shRNA (shCTRL) and subjected to qRT-PCR. Samples were normalized to RPL32 and expressed as fold change respective to shCTRL cells (value 1).
(B) IFNAR1 expression in PCI15A and PCI15B cells stably expressing IFNAR1 targeting shRNA. Total RNA was extracted from PCI15A and PCI15B cells stably expressing shRNA targeting IFNAR1 or non-targeting shRNA (shCTRL) and subjected to qRT-PCR. Samples were normalized to RPL32 and expressed as fold change respective to shCTRL cells (value 1).
(C) PARP induction in IFNAR knockdown cells. PCI15B shCTRL and shIFNAR cells were stimulated with increasing doses of p(I):p(C) as indicated. Lysates were prepared and probed with antibodies against cleaved PARP (Asp 214), ISG56, and Actin.
(D) Requirement of IFNAR1 in mediating the apoptotic response to dsRNA stimulus. PCI15B shCTRL and shIFNAR cells were stimulated with increasing doses of p(I):p(C) as indicated. Caspase 3/7 activity was measured using a Caspase-Glo® 3/7 Assay.

Lentiviral clone 1 was chosen for its maximal knockdown efficiency and in conjunction with the scramble control was used to stably transduce primary and metastatic HNSCC cells (PCI15A and B respectively). We observed an 80-90% reduction in IFNAR1 mRNA levels in these cell lines (Figure 5-10B). The effect of IFNAR downregulation response to p(I):(C) treatment in PCI15B cells was examined by measuring the levels of ISG56 induction following stimulation. Treatment with poly(I):poly(C) resulted in the induction of ISG56 protein synthesis

in both shCTRL and shIFNAR1 cells. Since type I IFN secretion results in an autocrine and paracrine enhancement of ISG56 protein synthesis, ISG56 expression was dramatically decreased in shIFNAR1 relative to shCTRL cells as expected following TLR3 ligation (Figure 5-10C). To determine whether response to IFN was involved in the enhanced apoptotic after p(I):(C) treatment, we measured the levels of cleaved PARP protein. No differences were observed in the induction of ISG56 protein after stimulation with either 25 or 50 ng/ml as compared to the induction of ISG56 observed in shCTRL cells. To further confirm the independence of enhanced apoptosis on IFNAR1, we determined the activity of pro-apoptotic caspases by measuring the cleavage of the luminogenic Caspase3/7 DEVD substrate in PCI15B shCTRL and shIFNAR cells treated for 24 hrs with increasing p(I):(C) doses. The response to p(I):(C) treatment was comparable between both cells lines for all doses tested (Figure 5-10D). Taken together, these results in suggest that the differential apoptotic response to p(I):(C) is not due to defects in type I IFN responses. Using type I IFN neutralizing antibodies we have shown that the this phenomenon occurs independent of IFN signaling [280]. Thus, we determined that the enhanced apoptotic effect of dsRNA treatment is due to defects in the signaling pathway regulating the activation of transcription factors that control the secretion of IFNβ rather than on the secondary IFN responsive signaling cascade. Ultimately, a defect in the activation of NF-κB following TLR3 ligation in metastatic cells was identified as being important for enhanced apoptosis.

APPENDIX C

ANTIVIRAL ACTIVITY OF HUMAN OASL IS MEDIATED BY MIMICKING UBIQUITIN CHAINS TO ACTIVATE RIG-I PATHWAY

Work described in this section was completed by authors Jianzhong Zhu, Yugen Zhang, Rolando A. Cuevas, Adriana Forero, Jayeeta Dhar, Mikkel Søes Ibsen, Jonathan Leo Schmid-Burgk, Madhavi K. Ganapathiraju, Takashi Fujita, Rune Hartmann, Zhijian J. Chen, Sailen Barik, Veit Hornung, Carolyn B. Coyne,

and Saumendra N. Sarkar

C.1 INTRODUCTION

Recognition of viral RNA by the cytoplasmic receptors retinoic acid inducible gene I (RIG-I) or melanoma differentiation-associated gene 5 (MDA5) [281,282] engages the adaptor mitochondrial antiviral-signaling protein (MAVS) [283-286] and initiates a signaling cascade that leads to the transcriptional activation of antiviral genes and type I interferons (IFN) [287,288]. This pathway is also important in the detection viral DNA as it is transcribed into RNA by RNA polymerase III (RNA PolIII) [289,290]. RLR function is mediated by the controlled expression of protein expression, the detection of dsRNA, and post-translational modifications that induce conformational changes and activate signaling cascades. Furthermore, ubiquitin conjugation plays an important role in the activation of RLR signaling pathways [291].

The oligoadenylate synthtases (OAS) are a family of proteins characterized by their ability to synthesize the 2'-5' oligoadenylates required for RNaseL activation and downstream RNA degradation [292]. Human oligoadenylate synthtase-like (OASL), is related to the OAS family given that it possesses an N-terminal OAS-like domain, which harbors critical mutations in the catalytic site rendering it null of 2'-5' OAS activity. Two unique tandem ubiquitin-like domains (UBL) are found in the C-terminus of OASL although the importance of these domains in regulating OASL function has yet to be defined [293,294].

We have previously established that that OASL expression results in higher IFN and ISG induction and protein expression following viral infection. Here we characterize the antiviral

function of OASL in enhancing RIG-I-mediated signaling, showing that ectopic OASL expression confers protection against RNA and DNA viruses, without affecting signaling through the adaptor protein, STING. Furthermore, we explored the ability of OASL to reconstitute RIG-I mediated signaling in the absence of ubiquitin. Finally, we have generated a series of eukaryotic expression vectors and baculovirus expressing OASL and RIG-I mutants to study the mechanism of OASL and RIG-I interactions.

C.2 MATERIALS AND METHODS

C.2.1 Cell lines and viruses

The cell lines used in this study have been described on Table 11. HEK293 cells, HEK293-derived cell lines, U20S, HT1080, Vero, and BHK21 cells were cultured in Dulbecco's Modified Eagle Medium (Lonza) containing 10% fetal bovine serum (Atlanta Biologicals) and 100 I.U./ml penicillin and 100 mg/ml streptomycin (Lonza). SF9 cells were cultured in Grace's insect medium (Invitrogen) supplemented with 10% FBS and 10 μg/ml gentamicin (Invitrogen). Cells were cultured at 27^{o}C. Sendai virus (SeV, Cantell strain) was purchased from Charles River Laboratories (Wilmington, MA); Encephalomyocarditis virus (EMCV) was purchased from ATCC **(**CR-1479) and the EGFP-tagged Vesicular stomatitis virus (VSV) and GFP-tagged HSV-1 (K26) [256] viruses have been previously described. p(I):(C) was purchased from GE and resuspended in nuclease free dH_20.

Table 11. Appendix B - Cell Lines

Cell Line	Description	Source
HEK293/pLenti	HEK293-derived cells stably transduced with pLenti-CMV-Puro vector.	Sarkar Lab
HEK293/OASL-V5	HEK293-derived cells stably transduced with C-terminal V5-tagged OASL.	Sarkar Lab
HT1080	Fibrosarcoma epithelial cell derived from a male patient.	Sarkar Lab ATCC® CLL-121
HT1080/pLenti	HT1080 derived cells stably transduced with pLenti-CMV-Puro vector.	Sarkar Lab
HT1080/OASL-V5	HT1080- derived cells stably transduced with C-terminal V5-tagged OASL.	Sarkar Lab
U2OS/shUb	U2OS-derived cells stably expressing shRNA against Ubiquitin.	Cheng Lab (UT Southwestern) [295,296]
U2OS/ shUb/pLenti	U2OS/shUb-derived cells stably transduced with pLenti-CMV-Hygro vector.	Sarkar Lab
U2OS/shUB/OASL-V5	U2OS/shUb-derived cells stably transduced with C-terminal V5-tagged OASL.	Sarkar Lab
Vero	African green monkey kidney epithelial cells	ATCC® CLL-81
BHK-21	Baby hamster kidney fibroblast cells	ATCC® CLL-10
Sf9	*Spodoptera frugiperda* epithelial cells	ATCC® CRL-1711

C.2.2 Lentivirus packaging and generation of stable cell lines

Lentiviral OASL expression was generated by LR recombination of pENTR/D-TOPO OASL-V5 plasmid or empty pENTR vector with pLenti/CMV/Hygro (Addgene). Lentiviruses were packaged as previously described in Chapter 2 – Materials and Methods. U2OS/shUb cells were

infected with concentrated lentivirus preparations in the presence of 5 μg/ml polybrene. Cells were placed under selection with 800 μg/ml hygromycin 48 hrs post transfection. Pooled cells displaying hygromycin resistance were used for further studies.

C.2.3 STING stimulations

293 cells ($3x10^5$) were plated in 24-well plates. Cells were then transfected with 5uM of oligonucleotides, AT2 with a phosphorothioate backbone (PTO) or AT5 with a phosphodiester backbone (PDE) (Kindly provided by Dr. Kate Fitzgerald at U Mass, and described in [297]) or 1 μg p(I):(C). Briefly, oligos or p(I):(C) were dissolved in OptiMEM (Invitrogen) in a final volume of 25 μl (Mix A). In a second tube, 10 μl of Lipofectamine 2000 were dissolved in 15 μl OptiMEM (Mix B). Both mixes were incubated for 5 mins at room temperature. Mixes A and B were then mixed together and incubated for 15 mins to promote Lipofectamine:DNA complex formation prior to the addition to cells. At 9 hours post transfection, total RNA was harvested and samples were subjected to qRT-PCR analysis to measure mRNA expression of IFNβ.

C.2.4 Plasmids and Baculoviral vectors

RIG-I and MDA5 deletion mutants, tagged with FLAG, were cloned by PCR amplification using the primers described on Table 12. PCR products were ligated into the pENTR-D/TOPO construct following manufacturer's guidelines. Eukaryotic expression vectors were generated by LR recombination of pENTR/D-TOPO/RIG-I 1-186, pENTR/D-TOPO/RIG-I 1-240, pENTR/D-TOPO/RIG-I 232-797, or pENTR/D-TOPO/RIG-I 1-797-925 into pcDNA/DEST47 using Gateway® LR clonase® II kit (Invitrogen) following manufacturer's guidelines. OASL-V5 CDS

was cloned into pENTR-D/TOPO as previously described (cloning performed by YZ). In order to generate recombinant baculovirus vectors, pENTR/D-TOPO/RIG-I 1797-925 plasmid was LR recombined with pDEST20 (Invitrogen), Gateway® LR Clonase® II kit using following manufacturer's guidelines. LR recombination into pDEST20 introduced an N-terminal Glutathione S-transferase (GST)-tag to be used for recombinant protein purification. OASL was subcloned, using a similar strategy, into pDEST10. This recombination introduced an N-terminal 6xHis tag to the OASL vector to be used for affinity purification of recombinant OASL protein. Both pDEST20/RIG-I vectors and pDEST10/OASL vectors were used to transform DH10BAC cells to generate recombinant baculovirus DNA. Transformed bacteria was grown in Luria agar plates containing 150 μg/ml kanamycin, 7 μg/ml gentamicin, 10 μg/ml tetracycline, 100 μg/ml Bluo-gal , and 40 μg/ml IPTG. Single white colonies were picked after growth for 24-48 hrs at 37^{o}C and phenotypes were verified by colony PCR. Positive colonies were expanded in medium with selection antibiotics and plasmids were prepared using the (Invitrogen) following manufacturer's guidelines.

Table 12. Appendix C - Cloning Primers

Primer Name	Sequence
RIG-I_F1	5’ -CACCATGGACTACAAGGACGACGATGACAAGACCACCGAGCAGCGA-3’
RIG-I_R186	5’-TCACCACAGTTCACTGAA-3’
RIG-I_R240	5’-TCATGGGCTGTACAAGTT-3’
RIG-I_F232	5’-CACCATG GACTTACAAGGACGACGATGACAAG GTGTCTGATACAAAC-3’
RIG-I_F797	5’-CACCATG GACTTACAAGGACGACGATGACAAG CCAAAACCTGTACCT-3’
RIG-I_R797	5’- TCATGGTTTTTCTTGACTATC-3’
RIG-I_925	5’ - TCATTTGGACATTTCTGCTGGATCAA -3’
RIG-I_F1 Long	5’-CACCATGGATTATAAAGATGACGATGATAAAACCACCGAGCAGCGACGCAGCCTGCAAGC - 3’
RIG-I_R925 Long	5’ - TCATTTGGACATTTCTGCTGGATCAAATGGTATCTTCTCAAAATGAAAGTCC - 3’

C.2.5 Baculovirus production

Baculovirus DNA (GST-RIG-I 797-925 Bacmid or His-OASL FL Bacmid) was transfected with Cellfectin® II (Invitrogen) into Sf9 cells in antibiotic free medium using manufacturer’s guidelines. Briefly, $8x10^5$ cells/ml were plated in antibiotic and serum-free medium and left attach for 15 minutes. Meanwhile, we diluted 8 µl in 100 µl in unsupplemented Grace’s Medium and in a separate tube we diluted 1 µl baculovirus DNA in 100 µl Grace’s Medium. The DNA and transfection reagent mixture were combined and incubated15–30 minutes at room temperature, before adding to cells. Transfected Sf9 cells were incubate cells at 27°C for 5 hours. The transfection medium was removed and replaced with 2 ml of complete growth medium. Cells were then incubated for 72 hrs and supernatant containing recombinant

baculovirus was harvested. Supernatants were clarified by centrifugation at 500 x g for 5 minutes to remove cells and large debris. The viral yield from the OASL expressing baculovirus was assessed by qPCR using OASL primers described in Chapter 2.

C.2.6 Protein purification

Sf9 cells in T-75 flasks were inoculated with baculovirus at an m.o.i of 1 (as determined by qPCR) and incubated for 48-72 hrs until cytopathic effect (CPE) was detectable. Cells were harvested by centrifugation at 500 x g for 5 minutes. Pellets were washed with PBS, aliquoted into 4 equal fractions, and frozen at -80^{o}C. OASL protein was purified using the Ni-NTA agarose from (Qiagen). Recombinant RIG-I CTD (797-925) protein was purified by using the GST-spin purification kit (Pierce) following manufacturer's guidelines. Full length RIG-I recombinant protein was a kind gift of Dr. James Chen (UT Southwestern). Purified proteins were resolved by SDS-PAGE and stained with Coomassie Brilliant Blue R-250 stain (0.1% Coomassie Blue, 50% methanol, 10% glacial acetic acid) to check purity and concentration. Gels were destained by thorough washing in destaining solution (50% methanol, 10% glacial acetic acid) and air-dried using DryEase® Mini-Gel Drying System (Invitrogen) following manufacturer's guidelines.

C.2.7 RNA Isolation and qRT-PCR

RNA isolations and qRT-PCR analysis was performed as described in Chapter 2 - materials and methods. Primers sets used for RPL32, OASL, ISG56 and ISG60 induction have also been

previously described in Chapter 2. Each sample was normalized to RPL32 and expressed as fold change with respect to vector expressing cells (value 1).

C.2.8 Immunoblotting

Whole cell lysates were prepared as previously described. Primary antibody incubation with anti-V5 antibody (Invitrogen), anti- FLAG (Sigma-Aldrich), and anti-Tubulin (Santa Cruz) was done overnight in 10% nonfat dry milk. Membranes were then washed twice with TBS-T and incubated with horseradish peroxidase-conjugated anti-mouse or anti-rabbit immunoglobulin G (IgG) diluted at 1:10000 in TBS-T plus 10% nonfat dry milk. Blots were revealed by enhanced chemiluminescence using Hy-Glo reagent (Denville) according to manufacturer's protocol.

C.2.9 Determination of viral growth

HEK293/pcDNA or HEK293/OASL were infected with VSV-GFP (m.o.i = 0.01), HSV-1 (K26) (m.o.i = 5), or EMCV (m.o.i = 5). Infected cell supernatants were harvested at the indicated timepoints and kept at -80 ^{o}C until further use. Infectious virus production measured by plaque assay on Vero (HSV-1 and EMCV) or BHK-21 (VSV) cells. 48 hours post infection, plaques were counted and virus production was quantified as plaque forming units (PFU)/ml.

C.2.10 Statistical Analysis

Statistical Analysis was done using a two-tailed Student *t* test analysis using GraphPad Prism.

C.3 RESULTS AND DISCUSSION

C.3.1 Antiviral activity of OASL

Stimulation of the RIG-I signaling pathway results in the activation of IRF3 and induction of IFN-stimulated gene expression. One of the effector genes induced OASL, which others in the laboratory have shown to interact with RIG-I enhancing the induction of type I IFN and ISGs after viral infection (unpublished data). To examine whether the enhanced expression of these confers increase antiviral immunity, we examined the growth of two RNA viruses, VSV and EMCV, and a DNA virus, HSV-1. While both VSV and MDA are detected by cytosolic ds RAN sensors, VSV triggers the activation of the RIG-I signaling pathways, while EMCV is detected by MDA5. Infection of 293 cells ectopically expressing OASL or empty vector control with VSV resulted in an almost 50% reduction of VSV growth 8 hrs post infection (Figure 5-11A). Interestingly, the growth of EMCV was comparable between the empty vector and OASL expressing cells (Figure 5-11B). We tested a third virus, HSV-1, a DNA virus that has been shown to induce RIG-I activation through the generation of RNA PolIII transcripts [290]. Ectopic expression of OASL led to a 50% decrease in viral growth 24 hrs post infection as determined by plaque assay (Figure 5-11C).

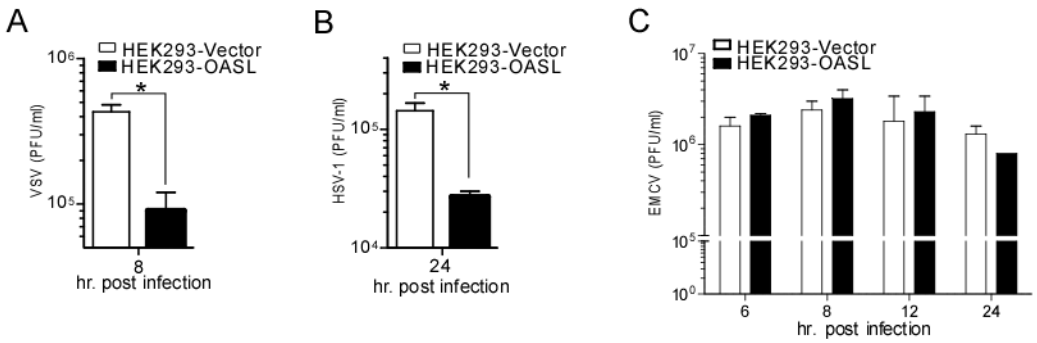

Figure 5-11. OASL Protects Cells From Viral Infections That Activate RIG-I

A) Reduction of VSV replication by OASL. HEK293-OASL stable cells and HEK293-vector stable cells were infected with VSV- GFP at 5 m.o.i. Eight hours post-infection supernatants were harvested and virus titers were determined by plaque assay on BHK21 cells.
B) OASL expression inhibits HSV-1 replication. HEK293-OASL stable cells and HEK293-vector stable cells were infected with HSV-1 at 5 m.o.i. Cell-free supernatants were collected at 24 h post infection and subjected to virus titration by plaque assay on Vero cells. * $P < 0.05$ by two-tailed Student *t* test analysis using GraphPad Prism.
C) OASL expression has no effect in EMCV replication. HEK293-OASL stable cells and HEK293-vector stable cells were infected with EMCV at 5 m.o.i. Supernatants were harvested at the indicated time points and virus titers were determined by plaque assay on Vero cells. * $P < 0.05$ by two-tailed Student t test.

The *Plasmodium falciparum* (Pf) genome contains AT-rich tracks that have been shown to induce type I IFNs through pathways not involving known DNA sensors TLR9, DAI, RNA polymerase-III or IFI16/p204. However, IFNβ secretion and ISG induction follows the activation of a signaling cascade mediated by the activator STING, TBK1, and IRF3-IRF7 activation [297]. Since the expression of OASL is also upregulated through STING activation, we examined whether ectopic OASL activation could enhance the response to AT-Rich DNA. We transfected HEK293 cells stably expressing OASL or vector control with oligonucleotides (ODNs) that were designed based on a portion of the Pf genome on chromosome 9 that contains three AT rich-repeats, or p(I):(C). The oligonucleotides were designed in either a phosphorothiorate backbone (PTO; AT2) or a phosphodiester backbone (PDE; AT5). Following 9 hrs after transfection, we harvested total RNA and measured the induction of ISG56 and IFNβ transcripts. As expected, the transfection of p(I):(C) led to an induced the expression of ISG56, which was higher in cells

expressing OASL. Transfection with either AT2 or AT5 failed to induce the expression of ISG56 9 hrs after transfection (Figure 5-12A). Again, transfection of pI:C led to the activation of RIG-I and an almost 2-fold enhancement of IFNβ induction over vector control cells. The expression of IFNβ was readily detectable in cells transfected with AT2 expressed, although similar levels were detected whether OASL was ectopically expressed or not. The transfection of AT5 did not stimulate the induction of IFNβ in either cell tested (Figure 5-12B). Taken together, these results suggest that the enhanced IFN response mediated by OASL exerts antimicrobial activity specifically against pathogens that trigger RIG-I activation.

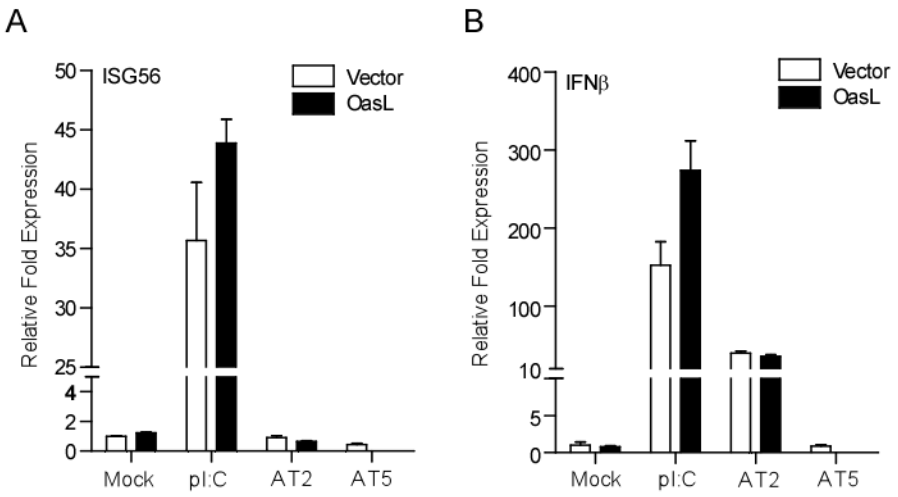

Figure 5-12. OASL Fails to Enhance the Response to AT-Rich DNA.

Effect of OASL expression on the response to AT-Rich DNA stimulation. HEK293-OASL stable cells and HEK293-vector stable cells were transfected with 5 μM AT-rich oligonucleotides or 1 μg p(I):(C). Nine hours post-transfection, total RNA was harvested and the induction of ISG56 (A) or IFNβ was measured.

C.3.2 Structural interactions between OASL and RIG-I

The activation of RIG-I requires a two-step mechanism in which binding of 5'-triphosphate RNA (5' ppp-RNA) precedes the binding of K63-linked poly-ubiquitin chains

[298,299]. Ubiquitin, a 76-amino acid polypeptide, plays critical roles in the regulation of signaling pathways including trafficking, cell cycle regulation, DNA repair, protein stabilization, and the activation of innate immune responses and inflammation [300]. In the absence of the catalytic activity, characteristic of the OAS proteins, the antiviral mechanism of human OASL has remained elusive. Structurally, OASL contains two tandem ubiquitin-like domains (UBL) in the C-terminus, which distinguish the protein from other members of the OAS family [293,301]. The UBL domains are necessary for the antiviral effects mediated by OASL [302-304]. Studies in our laboratory have shown an interaction between OASL and RIG-I (unpublished data from JZ and YZ). To examine whether expression of OASL enhanced RIG-I activation, we employed U2OS cells stably expressing a tetracycline-inducible shRNA against ubiquitin [296]. Treatment of U2OS/shUB cells for 72 with tetracycline (TET) (1 μg/ml resulted in the loss of UBC expression (Figure 5-13A). We then stably transduced U2OS-shUB with a lentivirus expressing OASL-V5 or empty vector and cells were placed under antibiotic selection with Hygromycin B. The expression of OASL was examined in our stable cell lines (U2OS/shUb/OASL and U2OS/shUB/pLenti) using antibodies against the V5 epitope (Figure 5-13B). U2OS/shUb/OASL and U2OS/shUB/pLenti cells were treated with TET for 72 hrs followed by infection with 2 and 5 HAU/ml SeV for 12 hrs. As expected, infected cells ectopically expressing OASL expressed 2-3 times higher levels of ISG60 mRNA than vector expressing cells at the doses tested. Cells stimulated with TET prior to infection showed drastically reduced ISG60 expression with similar levels of induction regardless of OASL expression (Figure 5-13C). Ubiquitin has been shown to be an important peptide in the regulation of innate immune signaling responses [300], it is expected that ablation of protein expression results in diminished responses to viral infection.

Thus, indicating that the UBL-domain interactions of OASL and RIG-I should be further studied in an *in vitro* cell-free based system.

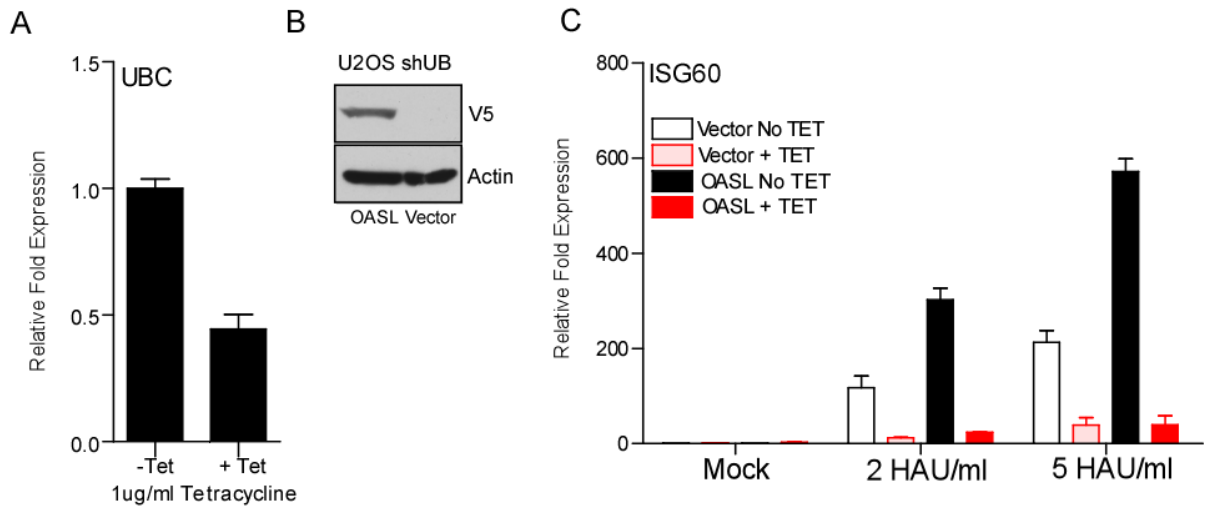

Figure 5-13. Ubiquitin is Required for ISG induction.

A) Downregulation of ubiquitin in USOS/shUb cells. U2OS/shUb cells ($1x10^6$) were stimulated with 1 μg/ml tetracycline. After 72 hrs stimulation, with medium changes every 24 hrs, total RNA was harvested and UBC mRNA was measured. Samples were normalized to RPL32 control and expression was reported relative to non-stimulated cells (Value 1).
B) Ectopic expression of OASL in U2OS/shUb. U2OS/shUB cells were infected with pLenti or pLenti/Hygro/OASL and selected with hygromycin. Lysates were prepared from stable pools and probed with antibodies against V5 and Actin.
C) SeV induction of ISG60 mRNA in the absence of ubiquitin. U2OS/shUB/OASL-V5 stable cells and vector stable cells were treated with 1 μg/ml tetracycline for 72 hrs. Cells were then infected with 2 or 5 HAU/ml SeV for 12 hrs. Total RNA was harvested and ISG60 mRNA expression was measured by qRT-PCR. Samples were normalized to RPL32 control and expression was reported relative to non-stimulated, mock-infected cells (Value 1).

First, we have generated eukaryotic expression vectors coding for FL-RIG-I as well as truncation mutants of RIG-I (Figure 5-14A). RIG-I truncation mutants (1-186), (1-240), (232-797), and (797-925) were generated by PCR amplification with the primers described in Table 12. PCR fragments were cloned into pENTR/D-TOPO, sequence verified, and further recombined with pcDNA47/DEST using the Gateway® LR clonase® II enzyme kit to generate eukaryotic expression vectors. We assessed the expression of our recombinant proteins by transfecting the pcDNA47-based vectors in 293T cells. After 48 hrs, we examined protein expression by

immunoblot using antibodies against the FLAG epitope. FL-RIG-I protein was detected around 100 kDa, as expected from the predicted molecular weight (102 kDa). The expression of the N-terminal CARD domain mutants 1-186 and 1-240 was also readily detected at the corresponding sizes (~21 kDa and 27 kDa respectively). The proteins corresponding to the N-terminal constructs 232-797 and 797-925 was detected at ~75 kDa and 15 kDa, respectively (Figure 5-14B, right). Thus, we have generated a recombinant protein expression system to ectopically express the RIG-I truncated proteins in eukaryotic allowing us to perform immunoprecipitation (IP) assays to identify the minimal domains required for the interactions between OASL and RIG-I. Furthermore, our pcDNA47 vector contains a T7 RNA polymerase promoter making these suitable plasmids for the *in vitro* cell-free based synthesis of recombinant proteins. Finally, we generated recombinant baculoviruses expressing $(His)_6$-OASL (FL) and GST-RIG-I 797-925. We purified recombinant proteins from 48-72 hr infected Sf9 cells by affinity purification. Purified proteins were resolved by SDS-PAGE and stained with Coomassie Brilliant Blue. Purified $(His)_6$-OASL (predicted 65 kDa) was detected at a molecular weight of around 55 kDa and GST-tagged RIG-I 797-925 ran between 15-20 kDa as expected. GST-RIG-I (FL) was kindly provided by ZJ Chen and was detected at about 100 kDa as expected (Figure 5-14B, left). Future experiments employing our recombinant proteins will be used to study cell free *in vitro* protein-protein interactions, as well as doing in vitro reconstitution of the RIG-I signaling pathways. Taken together, we have generated reagents to study RIG-I-OASL interactions in in vitro systems or using cell-based functional assays.

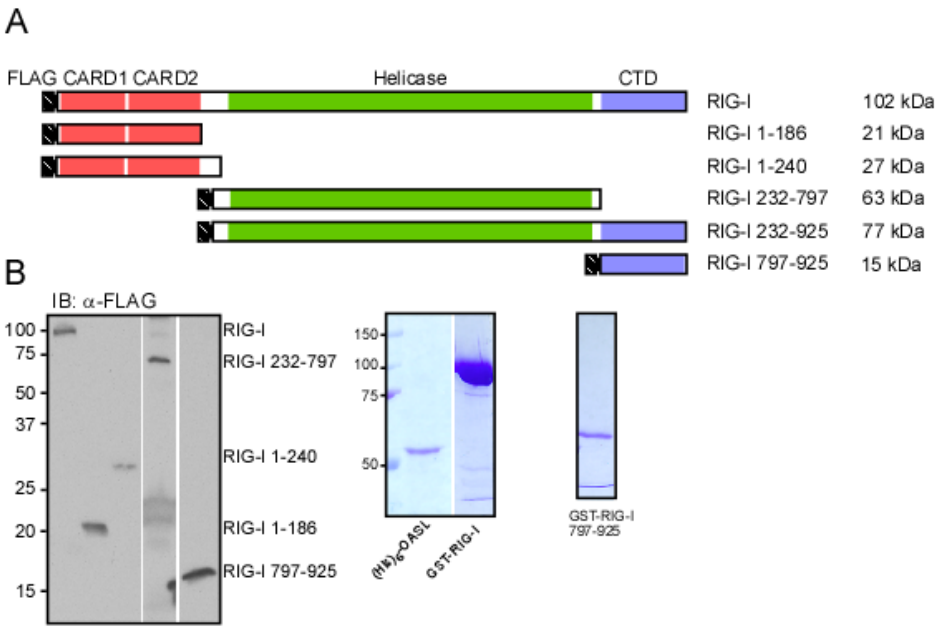

Figure 5-14. Cloning of RIG-I Truncation Mutants.

A) Schematic representation of the RIG-I truncation mutants, their corresponding amino acids, and predicted molecular weights. N-terminal CARD domains (red), linker regions (white), helicase domain (green), and C-terminal domain (CTD) (lilac) are depicted.
B) Expression of RIG-I truncation mutants. (Left) 293T cells were transfected with FL-RIG-I, N-terminal FLAG-tagged RIG-I constructs (1-186) and (1-240), RIG-I helicase domain (232-797), and the CTD truncation construct (797-925). Lysates were prepared and probed with antibodies against FLAG epitope (Sigma-Aldrich). Recombinant protein isolated from Sf9 cells were purified using Ni-NTA agarose (OASL) or GST-conjugated resin (GST-RIG-I 797-925). Proteins were resolved by SDS-PAGE and gels were stained with Coomassie Blue.

BIBLIOGRAPHY

1. Honda K, Taniguchi T (2006) IRFs: master regulators of signalling by Toll-like receptors and cytosolic pattern-recognition receptors. Nat Rev Immunol 6: 644-658.

2. Ikushima H, Negishi H, Taniguchi T (2013) The IRF Family Transcription Factors at the Interface of Innate and Adaptive Immune Responses. Cold Spring Harb Symp Quant Biol.

3. Savitsky D, Tamura T, Yanai H, Taniguchi T (2010) Regulation of immunity and oncogenesis by the IRF transcription factor family. Cancer Immunol Immunother 59: 489-510.

4. Tamura T, Yanai H, Savitsky D, Taniguchi T (2008) The IRF family transcription factors in immunity and oncogenesis. Annual review of immunology 26: 535-584.

5. Cheon H, Holvey-Bates EG, Schoggins JW, Forster S, Hertzog P, et al. (2013) IFNbeta-dependent increases in STAT1, STAT2, and IRF9 mediate resistance to viruses and DNA damage. EMBO J.

6. Grandvaux N, Servant MJ, tenOever B, Sen GC, Balachandran S, et al. (2002) Transcriptional profiling of interferon regulatory factor 3 target genes: direct involvement in the regulation of interferon-stimulated genes. J Virol 76: 5532-5539.

7. Eisenbeis CF, Singh H, Storb U (1995) Pip, a novel IRF family member, is a lymphoid-specific, PU.1-dependent transcriptional activator. Genes Dev 9: 1377-1387.

8. Eguchi J, Kong X, Tenta M, Wang X, Kang S, et al. (2013) Interferon regulatory factor 4 regulates obesity-induced inflammation through regulation of adipose tissue macrophage polarization. Diabetes.

9. Eguchi J, Wang X, Yu S, Kershaw EE, Chiu PC, et al. (2011) Transcriptional control of adipose lipid handling by IRF4. Cell Metab 13: 249-259.

10. Lu R, Medina KL, Lancki DW, Singh H (2003) IRF-4,8 orchestrate the pre-B-to-B transition in lymphocyte development. Genes Dev 17: 1703-1708.

11. Ma S, Pathak S, Trinh L, Lu R (2008) Interferon regulatory factors 4 and 8 induce the expression of Ikaros and Aiolos to down-regulate pre-B-cell receptor and promote cell-cycle withdrawal in pre-B-cell development. Blood 111: 1396-1403.

12. Ma S, Pathak S, Mandal M, Trinh L, Clark MR, et al. (2010) Ikaros and Aiolos inhibit pre-B-cell proliferation by directly suppressing c-Myc expression. Mol Cell Biol 30: 4149-4158.

13. Pongubala JM, Nagulapalli S, Klemsz MJ, McKercher SR, Maki RA, et al. (1992) PU.1 recruits a second nuclear factor to a site important for immunoglobulin kappa 3' enhancer activity. Mol Cell Biol 12: 368-378.

14. Mittrucker HW, Matsuyama T, Grossman A, Kundig TM, Potter J, et al. (1997) Requirement for the transcription factor LSIRF/IRF4 for mature B and T lymphocyte function. Science 275: 540-543.

15. Cattoretti G, Shaknovich R, Smith PM, Jack HM, Murty VV, et al. (2006) Stages of germinal center transit are defined by B cell transcription factor coexpression and relative abundance. J Immunol 177: 6930-6939.

16. Grumont RJ, Gerondakis S (2000) Rel induces interferon regulatory factor 4 (IRF-4) expression in lymphocytes: modulation of interferon-regulated gene expression by rel/nuclear factor kappaB. J Exp Med 191: 1281-1292.

17. Gupta S, Jiang M, Anthony A, Pernis AB (1999) Lineage-specific modulation of interleukin 4 signaling by interferon regulatory factor 4. J Exp Med 190: 1837-1848.

18. Shaffer AL, Emre NCT, Lamy L, Ngo VN, Wright G, et al. (2008) IRF4 addiction in multiple myeloma. Nature 454: 226-231.

19. Mamane Y, Sharma S, Petropoulos L, Lin R, Hiscott J (2000) Posttranslational regulation of IRF-4 activity by the immunophilin FKBP52. Immunity 12: 129-140.

20. Biswas PS, Gupta S, Chang E, Song L, Stirzaker RA, et al. (2010) Phosphorylation of IRF4 by ROCK2 regulates IL-17 and IL-21 production and the development of autoimmunity in mice. J Clin Invest 120: 3280-3295.

21. Wang L, Ning S (2013) Interferon Regulatory Factor 4 Is Activated through c-Src-Mediated Tyrosine Phosphorylation in Virus-Transformed Cells. J Virol 87: 9672-9679.

22. Shaffer AL, Emre NC, Romesser PB, Staudt LM (2009) IRF4: Immunity. Malignancy! Therapy? Clin Cancer Res 15: 2954-2961.

23. Meraro D, Gleit-Kielmanowicz M, Hauser H, Levi BZ (2002) IFN-stimulated gene 15 is synergistically activated through interactions between the myelocyte/lymphocyte-specific transcription factors, PU.1, IFN regulatory factor-8/IFN consensus sequence binding protein, and IFN regulatory factor-4: characterization of a new subtype of IFN-stimulated response element. J Immunol 168: 6224-6231.

24. Pathak S, Ma S, Trinh L, Lu R (2008) A role for interferon regulatory factor 4 in receptor editing. Mol Cell Biol 28: 2815-2824.

25. Rosenbauer F, Waring JF, Foerster J, Wietstruk M, Philipp D, et al. (1999) Interferon consensus sequence binding protein and interferon regulatory factor-4/Pip form a complex that represses the expression of the interferon-stimulated gene-15 in macrophages. Blood 94: 4274-4281.

26. Xu WD, Pan HF, Ye DQ, Xu Y (2012) Targeting IRF4 in autoimmune diseases. Autoimmun Rev 11: 918-924.

27. Teng Y, Takahashi Y, Yamada M, Kurosu T, Koyama T, et al. (2007) IRF4 negatively regulates proliferation of germinal center B cell-derived Burkitt's lymphoma cell lines and induces differentiation toward plasma cells. Eur J Cell Biol 86: 581-589.

28. Acquaviva J, Chen X, Ren R (2008) IRF-4 functions as a tumor suppressor in early B-cell development. Blood 112: 3798-3806.

29. Carbone A, Gloghini A, Cozzi MR, Capello D, Steffan A, et al. (2000) Expression of MUM1/IRF4 selectively clusters with primary effusion lymphoma among lymphomatous effusions: implications for disease histogenesis and pathogenesis. Br J Haematol 111: 247-257.

30. Carbone A, Gloghini A, Larocca LM, Capello D, Pierconti F, et al. (2001) Expression profile of MUM1/IRF4, BCL-6, and CD138/syndecan-1 defines novel histogenetic subsets of human immunodeficiency virus-related lymphomas. Blood 97: 744-751.

31. Iida S, Rao PH, Butler M, Corradini P, Boccadoro M, et al. (1997) Deregulation of MUM1/IRF4 by chromosomal translocation in multiple myeloma. Nat Genet 17: 226-230.

32. Mamane Y, Grandvaux N, Hernandez E, Sharma S, Innocente SA, et al. (2002) Repression of IRF-4 target genes in human T cell leukemia virus-1 infection. Oncogene 21: 6751-6765.

33. Sharma S, Grandvaux N, Mamane Y, Genin P, Azimi N, et al. (2002) Regulation of IFN regulatory factor 4 expression in human T cell leukemia virus-I-transformed T cells. J Immunol 169: 3120-3130.

34. Imaizumi Y, Kohno T, Yamada Y, Ikeda S, Tanaka Y, et al. (2001) Possible involvement of interferon regulatory factor 4 (IRF4) in a clinical subtype of adult T-cell leukemia. Jpn J Cancer Res 92: 1284-1292.

35. Sharma S, Mamane Y, Grandvaux N, Bartlett J, Petropoulos L, et al. (2000) Activation and regulation of interferon regulatory factor 4 in HTLV type 1-infected T lymphocytes. AIDS Res Hum Retroviruses 16: 1613-1622.

36. Mamane Y, Sharma S, Grandvaux N, Hernandez E, Hiscott J (2002) IRF-4 activities in HTLV-I-induced T cell leukemogenesis. J Interferon Cytokine Res 22: 135-143.

37. Xu D, Zhao L, Del Valle L, Miklossy J, Zhang L (2008) Interferon regulatory factor 4 is involved in Epstein-Barr virus-mediated transformation of human B lymphocytes. J Virol 82: 6251-6258.

38. Izumiya Y, Izumiya C, Hsia D, Ellison TJ, Luciw PA, et al. (2009) NF-kappaB serves as a cellular sensor of Kaposi's sarcoma-associated herpesvirus latency and negatively regulates K-Rta by antagonizing the RBP-Jkappa coactivator. J Virol 83: 4435-4446.

39. Wang L, Toomey NL, Diaz LA, Walker G, Ramos JC, et al. (2011) Oncogenic IRFs provide a survival advantage for Epstein-Barr virus- or human T-cell leukemia virus type 1-transformed cells through induction of BIC expression. J Virol 85: 8328-8337.

40. Banerjee S, Lu J, Cai Q, Saha A, Jha HC, et al. (2013) The EBV Latent Antigen 3C Inhibits Apoptosis through Targeted Regulation of Interferon Regulatory Factors 4 and 8. PLoS Pathog 9: e1003314.

41. Qu Z, Xiao G (2011) Human T-cell lymphotropic virus: a model of NF-kappaB-associated tumorigenesis. Viruses 3: 714-749.

42. Ramos JC, Ruiz P, Jr., Ratner L, Reis IM, Brites C, et al. (2007) IRF-4 and c-Rel expression in antiviral-resistant adult T-cell leukemia/lymphoma. Blood 109: 3060-3068.

43. Ellerman V, Bang, O (1908) Experimentelle leukämie bei hühnern. Centralbl f Bakteriol: 595–609.

44. Rous P (1911) A Sarcoma of the Fowl Transmissible by an Agent Separable from the Tumor Cells. J Exp Med 13: 397-411.

45. Rous P (1910) A Transmissible Avian Neoplasm. (Sarcoma of the Common Fowl.). J Exp Med 12: 696-705.

46. Gross L (1958) Viral etiology of spontaneous mouse leukemia; a review. Cancer Res 18: 371-381.

47. Gross L (1976) The fortuitous isolation and identification of the polyoma virus. Cancer Res 36: 4195-4196.

48. Rubin H, Temin HM (1958) Infection with the Rous sarcoma virus in vitro. Fed Proc 17: 994-1003.

49. Temin HM, Rubin H (1958) Characteristics of an assay for Rous sarcoma virus and Rous sarcoma cells in tissue culture. Virology 6: 669-688.

50. Stehelin D (1976) The transforming gene of avian tumor viruses. Pathol Biol (Paris) 24: 513-515.

51. Stehelin D, Guntaka RV, Varmus HE, Bishop JM (1976) Purification of DNA complementary to nucleotide sequences required for neoplastic transformation of fibroblasts by avian sarcoma viruses. J Mol Biol 101: 349-365.

52. Stehelin D, Varmus HE, Bishop JM, Vogt PK (1976) DNA related to the transforming gene(s) of avian sarcoma viruses is present in normal avian DNA. Nature 260: 170-173.

53. Vogt M, Dulbecco R (1963) Steps in the neoplastic transformation of hamster embryo cells by polyoma virus. Proc Natl Acad Sci U S A 49: 171-179.

54. Vogt M, Dulbecco R (1962) Studies on cells rendered neoplastic by polyoma virus: the problem of the presence of virus-related materials. Virology 16: 41-51.

55. Vogt M, Dulbecco R (1960) Virus-Cell Interaction with a Tumor-Producing Virus. Proc Natl Acad Sci U S A 46: 365-370.

56. Baltimore D (1970) RNA-dependent DNA polymerase in virions of RNA tumour viruses. Nature 226: 1209-1211.

57. Temin HM, Mizutani S (1970) RNA-dependent DNA polymerase in virions of Rous sarcoma virus. Nature 226: 1211-1213.

58. Parkin DM (2006) The global health burden of infection-associated cancers in the year 2002. Int J Cancer 118: 3030-3044.

59. Epstein MA, Achong BG, Barr YM (1964) Virus Particles in Cultured Lymphoblasts from Burkitt's Lymphoma. Lancet 1: 702-703.

60. Henle W, Diehl V, Kohn G, Zur Hausen H, Henle G (1967) Herpes-type virus and chromosome marker in normal leukocytes after growth with irradiated Burkitt cells. Science 157: 1064-1065.

61. Pattle SB, Farrell PJ (2006) The role of Epstein-Barr virus in cancer. Expert Opin Biol Ther 6: 1193-1205.

62. Blumberg BS, Alter HJ, Visnich S (1965) A "New" Antigen in Leukemia Sera. JAMA 191: 541-546.

63. Prince AM (1968) An antigen detected in the blood during the incubation period of serum hepatitis. Proc Natl Acad Sci U S A 60: 814-821.

64. Lupberger J, Hildt E (2007) Hepatitis B virus-induced oncogenesis. World J Gastroenterol 13: 74-81.

65. Poiesz BJ, Ruscetti FW, Gazdar AF, Bunn PA, Minna JD, et al. (1980) Detection and isolation of type C retrovirus particles from fresh and cultured lymphocytes of a patient with cutaneous T-cell lymphoma. Proc Natl Acad Sci U S A 77: 7415-7419.

66. Popovic M, Lange-Wantzin G, Sarin PS, Mann D, Gallo RC (1983) Transformation of human umbilical cord blood T cells by human T-cell leukemia/lymphoma virus. Proc Natl Acad Sci U S A 80: 5402-5406.

67. Popovic M, Sarin PS, Robert-Gurroff M, Kalyanaraman VS, Mann D, et al. (1983) Isolation and transmission of human retrovirus (human t-cell leukemia virus). Science 219: 856-859.

68. Hinuma Y, Nagata K, Hanaoka M, Nakai M, Matsumoto T, et al. (1981) Adult T-cell leukemia: antigen in an ATL cell line and detection of antibodies to the antigen in human sera. Proc Natl Acad Sci U S A 78: 6476-6480.

69. Matsuoka M, Yasunaga JI (2013) Human T-cell leukemia virus type 1: replication, proliferation and propagation by Tax and HTLV-1 bZIP factor. Curr Opin Virol.

70. zur Hausen H (1976) Condylomata acuminata and human genital cancer. Cancer Res 36: 794.

71. Boshart M, Gissmann L, Ikenberg H, Kleinheinz A, Scheurlen W, et al. (1984) A new type of papillomavirus DNA, its presence in genital cancer biopsies and in cell lines derived from cervical cancer. EMBO J 3: 1151-1157.

72. Durst M, Gissmann L, Ikenberg H, zur Hausen H (1983) A papillomavirus DNA from a cervical carcinoma and its prevalence in cancer biopsy samples from different geographic regions. Proc Natl Acad Sci U S A 80: 3812-3815.

73. zur Hausen H (2009) Papillomaviruses in the causation of human cancers - a brief historical account. Virology 384: 260-265.

74. Kuo G, Choo QL, Alter HJ, Gitnick GL, Redeker AG, et al. (1989) An assay for circulating antibodies to a major etiologic virus of human non-A, non-B hepatitis. Science 244: 362-364.

75. Choo QL, Kuo G, Weiner AJ, Overby LR, Bradley DW, et al. (1989) Isolation of a cDNA clone derived from a blood-borne non-A, non-B viral hepatitis genome. Science 244: 359-362.

76. McGivern DR, Lemon SM (2011) Virus-specific mechanisms of carcinogenesis in hepatitis C virus associated liver cancer. Oncogene 30: 1969-1983.

77. Thomas DL (2013) Global control of hepatitis C: where challenge meets opportunity. Nat Med 19: 850-858.

78. Beral V, Peterman TA, Berkelman RL, Jaffe HW (1990) Kaposi's sarcoma among persons with AIDS: a sexually transmitted infection? Lancet 335: 123-128.

79. Chang Y, Cesarman E, Pessin MS, Lee F, Culpepper J, et al. (1994) Identification of herpesvirus-like DNA sequences in AIDS-associated Kaposi's sarcoma. Science 266: 1865-1869.

80. Feng H, Taylor JL, Benos PV, Newton R, Waddell K, et al. (2007) Human transcriptome subtraction by using short sequence tags to search for tumor viruses in conjunctival carcinoma. J Virol 81: 11332-11340.

81. Feng H, Shuda M, Chang Y, Moore PS (2008) Clonal integration of a polyomavirus in human Merkel cell carcinoma. Science 319: 1096-1100.

82. Shuda M, Feng H, Kwun HJ, Rosen ST, Gjoerup O, et al. (2008) T antigen mutations are a human tumor-specific signature for Merkel cell polyomavirus. Proc Natl Acad Sci U S A 105: 16272-16277.

83. Alter HJ, Purcell RH, Shih JW, Melpolder JC, Houghton M, et al. (1989) Detection of antibody to hepatitis C virus in prospectively followed transfusion recipients with acute and chronic non-A, non-B hepatitis. N Engl J Med 321: 1494-1500.

84. Ye FC, Zhou FC, Xie JP, Kang T, Greene W, et al. (2008) Kaposi's sarcoma-associated herpesvirus latent gene vFLIP inhibits viral lytic replication through NF-kappaB-mediated suppression of the AP-1 pathway: a novel mechanism of virus control of latency. J Virol 82: 4235-4249.

85. Uldrick TS, Whitby D (2011) Update on KSHV epidemiology, Kaposi Sarcoma pathogenesis, and treatment of Kaposi Sarcoma. Cancer Lett 305: 150-162.

86. Engels EA, Atkinson JO, Graubard BI, McQuillan GM, Gamache C, et al. (2007) Risk factors for human herpesvirus 8 infection among adults in the United States and evidence for sexual transmission. J Infect Dis 196: 199-207.

87. Martro E, Esteve A, Schulz TF, Sheldon J, Gambus G, et al. (2007) Risk factors for human Herpesvirus 8 infection and AIDS-associated Kaposi's sarcoma among men who have sex with men in a European multicentre study. Int J Cancer 120: 1129-1135.

88. Dotti G, Fiocchi R, Motta T, Facchinetti B, Chiodini B, et al. (1999) Primary effusion lymphoma after heart transplantation: a new entity associated with human herpesvirus-8. Leukemia 13: 664-670.

89. Gessain A, Sudaka A, Briere J, Fouchard N, Nicola MA, et al. (1996) Kaposi sarcoma-associated herpes-like virus (human herpesvirus type 8) DNA sequences in multicentric Castleman's disease: is there any relevant association in non-human immunodeficiency virus-infected patients? Blood 87: 414-416.

90. Soulier J, Grollet L, Oksenhendler E, Cacoub P, Cazals-Hatem D, et al. (1995) Kaposi's sarcoma-associated herpesvirus-like DNA sequences in multicentric Castleman's disease. Blood 86: 1276-1280.

91. Cesarman E, Moore PS, Rao PH, Inghirami G, Knowles DM, et al. (1995) In vitro establishment and characterization of two acquired immunodeficiency syndrome-related lymphoma cell lines (BC-1 and BC-2) containing Kaposi's sarcoma-associated herpesvirus-like (KSHV) DNA sequences. Blood 86: 2708-2714.

92. Cesarman E, Chang Y, Moore PS, Said JW, Knowles DM (1995) Kaposi's sarcoma-associated herpesvirus-like DNA sequences in AIDS-related body-cavity-based lymphomas. N Engl J Med 332: 1186-1191.

93. Carbone A, Cesarman E, Spina M, Gloghini A, Schulz TF (2009) HIV-associated lymphomas and gamma-herpesviruses. Blood 113: 1213-1224.

94. Simas JP, Efstathiou S (1998) Murine gammaherpesvirus 68: a model for the study of gammaherpesvirus pathogenesis. Trends Microbiol 6: 276-282.

95. Orzechowska BU, Powers MF, Sprague J, Li H, Yen B, et al. (2008) Rhesus macaque rhadinovirus-associated non-Hodgkin lymphoma: animal model for KSHV-associated malignancies. Blood 112: 4227-4234.

96. Carbone A, Cesarman E, Gloghini A, Drexler HG (2010) Understanding pathogenetic aspects and clinical presentation of primary effusion lymphoma through its derived cell lines. AIDS 24: 479-490.

97. Jaffe ES (1996) Primary body cavity-based AIDS-related lymphomas. Evolution of a new disease entity. Am J Clin Pathol 105: 141-143.

98. Chen YB, Rahemtullah A, Hochberg E (2007) Primary effusion lymphoma. Oncologist 12: 569-576.

99. Gaidano G, Gloghini A, Gattei V, Rossi MF, Cilia AM, et al. (1997) Association of Kaposi's sarcoma-associated herpesvirus-positive primary effusion lymphoma with expression of the CD138/syndecan-1 antigen. Blood 90: 4894-4900.

100. Simonelli C, Spina M, Cinelli R, Talamini R, Tedeschi R, et al. (2003) Clinical features and outcome of primary effusion lymphoma in HIV-infected patients: a single-institution study. J Clin Oncol 21: 3948-3954.

101. Boulanger E, Gerard L, Gabarre J, Molina JM, Rapp C, et al. (2005) Prognostic factors and outcome of human herpesvirus 8-associated primary effusion lymphoma in patients with AIDS. J Clin Oncol 23: 4372-4380.

102. Russo JJ, Bohenzky RA, Chien MC, Chen J, Yan M, et al. (1996) Nucleotide sequence of the Kaposi sarcoma-associated herpesvirus (HHV8). Proc Natl Acad Sci U S A 93: 14862-14867.

103. Trus BL, Heymann JB, Nealon K, Cheng N, Newcomb WW, et al. (2001) Capsid structure of Kaposi's sarcoma-associated herpesvirus, a gammaherpesvirus, compared to those of an alphaherpesvirus, herpes simplex virus type 1, and a betaherpesvirus, cytomegalovirus. J Virol 75: 2879-2890.

104. Wen KW, Damania B (2010) Kaposi sarcoma-associated herpesvirus (KSHV): molecular biology and oncogenesis. Cancer Lett 289: 140-150.

105. Moore PS, Chang Y (1998) Antiviral activity of tumor-suppressor pathways: clues from molecular piracy by KSHV. Trends Genet 14: 144-150.

106. Sarid R, Flore O, Bohenzky RA, Chang Y, Moore PS (1998) Transcription mapping of the Kaposi's sarcoma-associated herpesvirus (human herpesvirus 8) genome in a body cavity-based lymphoma cell line (BC-1). J Virol 72: 1005-1012.

107. Dresang LR, Teuton JR, Feng H, Jacobs JM, Camp DG, 2nd, et al. (2012) Coupled transcriptome and proteome analysis of human lymphotropic tumor viruses: insights on the detection and discovery of viral genes. BMC Genomics 12: 625.

108. Mesri EA, Cesarman E, Boshoff C (2010) Kaposi's sarcoma and its associated herpesvirus. Nat Rev Cancer 10: 707-719.

109. Sathish N, Yuan Y (2011) Evasion and subversion of interferon-mediated antiviral immunity by Kaposi's sarcoma-associated herpesvirus: an overview. J Virol 85: 10934-10944.

110. Verma SC, Lan K, Robertson E (2007) Structure and function of latency-associated nuclear antigen. Curr Top Microbiol Immunol 312: 101-136.

111. Cloutier N, Flamand L (2010) Kaposi sarcoma-associated herpesvirus latency-associated nuclear antigen inhibits interferon (IFN) beta expression by competing with IFN regulatory factor-3 for binding to IFNB promoter. J Biol Chem 285: 7208-7221.

112. Lu F, Tsai K, Chen HS, Wikramasinghe P, Davuluri RV, et al. (2012) Identification of host-chromosome binding sites and candidate gene targets for Kaposi's sarcoma-associated herpesvirus LANA. J Virol 86: 5752-5762.

113. Robinson BA, O'Connor MA, Li H, Engelmann F, Poland B, et al. (2012) Viral interferon regulatory factors are critical for delay of the host immune response against rhesus macaque rhadinovirus infection. J Virol 86: 2769-2779.

114. Baresova P, Pitha PM, Lubyova B (2013) Distinct Roles of Kaposi's Sarcoma-Associated Herpesvirus-Encoded Viral Interferon Regulatory Factors in Inflammatory Response and Cancer. J Virol 87: 9398-9410.

115. Lubyova B, Pitha PM (2000) Characterization of a novel human herpesvirus 8-encoded protein, vIRF-3, that shows homology to viral and cellular interferon regulatory factors. J Virol 74: 8194-8201.

116. Rivas C, Thlick AE, Parravicini C, Moore PS, Chang Y (2001) Kaposi's sarcoma-associated herpesvirus LANA2 is a B-cell-specific latent viral protein that inhibits p53. J Virol 75: 429-438.

117. Esteban M, Garcia MA, Domingo-Gil E, Arroyo J, Nombela C, et al. (2003) The latency protein LANA2 from Kaposi's sarcoma-associated herpesvirus inhibits apoptosis induced by dsRNA-activated protein kinase but not RNase L activation. J Gen Virol 84: 1463-1470.

118. Munoz-Fontela C, Marcos-Villar L, Gallego P, Arroyo J, Da Costa M, et al. (2007) Latent protein LANA2 from Kaposi's sarcoma-associated herpesvirus interacts with 14-3-3 proteins and inhibits FOXO3a transcription factor. J Virol 81: 1511-1516.

119. Lubyova B, Kellum MJ, Frisancho JA, Pitha PM (2007) Stimulation of c-Myc transcriptional activity by vIRF-3 of Kaposi sarcoma-associated herpesvirus. J Biol Chem 282: 31944-31953.

120. Wies E, Mori Y, Hahn A, Kremmer E, Sturzl M, et al. (2008) The viral interferon-regulatory factor-3 is required for the survival of KSHV-infected primary effusion lymphoma cells. Blood 111: 320-327.

121. Lubyova B, Kellum MJ, Frisancho AJ, Pitha PM (2004) Kaposi's sarcoma-associated herpesvirus-encoded vIRF-3 stimulates the transcriptional activity of cellular IRF-3 and IRF-7. J Biol Chem 279: 7643-7654.

122. Joo CH, Shin YC, Gack M, Wu L, Levy D, et al. (2007) Inhibition of interferon regulatory factor 7 (IRF7)-mediated interferon signal transduction by the Kaposi's sarcoma-associated herpesvirus viral IRF homolog vIRF3. J Virol 81: 8282-8292.

123. Wies E, Hahn AS, Schmidt K, Viebahn C, Rohland N, et al. (2009) The Kaposi's Sarcoma-associated Herpesvirus-encoded vIRF-3 Inhibits Cellular IRF-5. J Biol Chem 284: 8525-8538.

124. Sturzl M, Hohenadl C, Zietz C, Castanos-Velez E, Wunderlich A, et al. (1999) Expression of K13/v-FLIP gene of human herpesvirus 8 and apoptosis in Kaposi's sarcoma spindle cells. J Natl Cancer Inst 91: 1725-1733.

125. Bertin J, Armstrong RC, Ottilie S, Martin DA, Wang Y, et al. (1997) Death effector domain-containing herpesvirus and poxvirus proteins inhibit both Fas- and TNFR1-induced apoptosis. Proc Natl Acad Sci U S A 94: 1172-1176.

126. Hu S, Vincenz C, Buller M, Dixit VM (1997) A novel family of viral death effector domain-containing molecules that inhibit both CD-95- and tumor necrosis factor receptor-1-induced apoptosis. J Biol Chem 272: 9621-9624.

127. Matta H, Mazzacurati L, Schamus S, Yang T, Sun Q, et al. (2007) Kaposi's sarcoma-associated herpesvirus (KSHV) oncoprotein K13 bypasses TRAFs and directly interacts with the IkappaB kinase complex to selectively activate NF-kappaB without JNK activation. J Biol Chem 282: 24858-24865.

128. Sun Q, Matta H, Chaudhary PM (2003) The human herpes virus 8-encoded viral FLICE inhibitory protein protects against growth factor withdrawal-induced apoptosis via NF-kappa B activation. Blood 101: 1956-1961.

129. Sun Q, Zachariah S, Chaudhary PM (2003) The human herpes virus 8-encoded viral FLICE-inhibitory protein induces cellular transformation via NF-kappaB activation. J Biol Chem 278: 52437-52445.

130. Matta H, Chaudhary PM (2004) Activation of alternative NF-kappa B pathway by human herpes virus 8-encoded Fas-associated death domain-like IL-1 beta-converting enzyme inhibitory protein (vFLIP). Proc Natl Acad Sci U S A 101: 9399-9404.

131. Sun Q, Matta H, Lu G, Chaudhary PM (2006) Induction of IL-8 expression by human herpesvirus 8 encoded vFLIP K13 via NF-kappaB activation. Oncogene 25: 2717-2726.

132. Chugh P, Matta H, Schamus S, Zachariah S, Kumar A, et al. (2005) Constitutive NF-kappaB activation, normal Fas-induced apoptosis, and increased incidence of lymphoma in human herpes virus 8 K13 transgenic mice. Proc Natl Acad Sci U S A 102: 12885-12890.

133. Xu Y, Ganem D (2007) Induction of chemokine production by latent Kaposi's sarcoma-associated herpesvirus infection of endothelial cells. J Gen Virol 88: 46-50.

134. Grossmann C, Ganem D (2008) Effects of NFkappaB activation on KSHV latency and lytic reactivation are complex and context-dependent. Virology 375: 94-102.

135. Guasparri I, Keller SA, Cesarman E (2004) KSHV vFLIP is essential for the survival of infected lymphoma cells. J Exp Med 199: 993-1003.

136. Guasparri I, Wu H, Cesarman E (2006) The KSHV oncoprotein vFLIP contains a TRAF-interacting motif and requires TRAF2 and TRAF3 for signalling. EMBO Rep 7: 114-119.

137. Chaudhary PM, Jasmin A, Eby MT, Hood L (1999) Modulation of the NF-kappa B pathway by virally encoded death effector domains-containing proteins. Oncogene 18: 5738-5746.

138. Liu L, Eby MT, Rathore N, Sinha SK, Kumar A, et al. (2002) The human herpes virus 8-encoded viral FLICE inhibitory protein physically associates with and persistently activates the Ikappa B kinase complex. J Biol Chem 277: 13745-13751.

139. Punj V, Matta H, Chaudhary PM (2012) A computational profiling of changes in gene expression and transcription factors induced by vFLIP K13 in primary effusion lymphoma. PLoS One 7: e37498.

140. Alkharsah KR, Singh VV, Bosco R, Santag S, Grundhoff A, et al. (2011) Deletion of Kaposi's sarcoma-associated herpesvirus FLICE inhibitory protein, vFLIP, from the viral genome compromises the activation of STAT1-responsive cellular genes and spindle cell formation in endothelial cells. J Virol 85: 10375-10388.

141. Cloutier N, Grandvaux N, Flamand L (2007) Synergistic activation of interferon-beta gene transcription by the viral FLICE inhibitory protein of Kaposi's sarcoma-associated herpesvirus and type I IFN activators. Eur J Immunol 37: 2772-2778.

142. Moore PS, Gao SJ, Dominguez G, Cesarman E, Lungu O, et al. (1996) Primary characterization of a herpesvirus agent associated with Kaposi's sarcomae. J Virol 70: 549-558.

143. Lu F, Zhou J, Wiedmer A, Madden K, Yuan Y, et al. (2003) Chromatin remodeling of the Kaposi's sarcoma-associated herpesvirus ORF50 promoter correlates with reactivation from latency. J Virol 77: 11425-11435.

144. Zoeteweij JP, Moses AV, Rinderknecht AS, Davis DA, Overwijk WW, et al. (2001) Targeted inhibition of calcineurin signaling blocks calcium-dependent reactivation of Kaposi sarcoma-associated herpesvirus. Blood 97: 2374-2380.

145. Davis DA, Rinderknecht AS, Zoeteweij JP, Aoki Y, Read-Connole EL, et al. (2001) Hypoxia induces lytic replication of Kaposi sarcoma-associated herpesvirus. Blood 97: 3244-3250.

146. Gregory SM, West JA, Dillon PJ, Hilscher C, Dittmer DP, et al. (2009) Toll-like receptor signaling controls reactivation of KSHV from latency. Proc Natl Acad Sci U S A 106: 11725-11730.

147. Kati S, Tsao EH, Gunther T, Weidner-Glunde M, Rothamel T, et al. (2013) Activation of the B cell antigen receptor triggers reactivation of latent Kaposi's sarcoma-associated herpesvirus in B cells. J Virol 87: 8004-8016.

148. Sun R, Lin SF, Staskus K, Gradoville L, Grogan E, et al. (1999) Kinetics of Kaposi's sarcoma-associated herpesvirus gene expression. J Virol 73: 2232-2242.

149. Lukac DM, Renne R, Kirshner JR, Ganem D (1998) Reactivation of Kaposi's sarcoma-associated herpesvirus infection from latency by expression of the ORF 50 transactivator, a homolog of the EBV R protein. Virology 252: 304-312.

150. Sakakibara S, Ueda K, Chen J, Okuno T, Yamanishi K (2001) Octamer-binding sequence is a key element for the autoregulation of Kaposi's sarcoma-associated herpesvirus ORF50/Lyta gene expression. J Virol 75: 6894-6900.

151. Chen J, Ueda K, Sakakibara S, Okuno T, Parravicini C, et al. (2001) Activation of latent Kaposi's sarcoma-associated herpesvirus by demethylation of the promoter of the lytic transactivator. Proc Natl Acad Sci U S A 98: 4119-4124.

152. Gradoville L, Gerlach J, Grogan E, Shedd D, Nikiforow S, et al. (2000) Kaposi's sarcoma-associated herpesvirus open reading frame 50/Rta protein activates the entire viral lytic cycle in the HH-B2 primary effusion lymphoma cell line. J Virol 74: 6207-6212.

153. Chang PJ, Miller G (2004) Autoregulation of DNA binding and protein stability of Kaposi's sarcoma-associated herpesvirus ORF50 protein. J Virol 78: 10657-10673.

154. Wang SE, Wu FY, Fujimuro M, Zong J, Hayward SD, et al. (2003) Role of CCAAT/enhancer-binding protein alpha (C/EBPalpha) in activation of the Kaposi's sarcoma-associated herpesvirus (KSHV) lytic-cycle replication-associated protein (RAP) promoter in cooperation with the KSHV replication and transcription activator (RTA) and RAP. J Virol 77: 600-623.

155. Lukac DM, Kirshner JR, Ganem D (1999) Transcriptional activation by the product of open reading frame 50 of Kaposi's sarcoma-associated herpesvirus is required for lytic viral reactivation in B cells. J Virol 73: 9348-9361.

156. Guito J, Lukac DM (2012) KSHV Rta Promoter Specification and Viral Reactivation. Front Microbiol 3: 30.

157. Staudt MR, Dittmer DP (2007) The Rta/Orf50 transactivator proteins of the gamma-herpesviridae. Curr Top Microbiol Immunol 312: 71-100.

158. Chang PJ, Shedd D, Gradoville L, Cho MS, Chen LW, et al. (2002) Open reading frame 50 protein of Kaposi's sarcoma-associated herpesvirus directly activates the viral PAN and K12 genes by binding to related response elements. J Virol 76: 3168-3178.

159. Deng H, Song MJ, Chu JT, Sun R (2002) Transcriptional regulation of the interleukin-6 gene of human herpesvirus 8 (Kaposi's sarcoma-associated herpesvirus). J Virol 76: 8252-8264.

160. Wang J, Zhang J, Zhang L, Harrington W, Jr., West JT, et al. (2005) Modulation of human herpesvirus 8/Kaposi's sarcoma-associated herpesvirus replication and transcription activator transactivation by interferon regulatory factor 7. J Virol 79: 2420-2431.

161. Yu Y, Wang SE, Hayward GS (2005) The KSHV immediate-early transcription factor RTA encodes ubiquitin E3 ligase activity that targets IRF7 for proteosome-mediated degradation. Immunity 22: 59-70.

162. Yu Y, Hayward GS (2010) The ubiquitin E3 ligase RAUL negatively regulates type i interferon through ubiquitination of the transcription factors IRF7 and IRF3. Immunity 33: 863-877.

163. Zhang J, Wang J, Wood C, Xu D, Zhang L (2005) Kaposi's sarcoma-associated herpesvirus/human herpesvirus 8 replication and transcription activator regulates viral and cellular genes via interferon-stimulated response elements. J Virol 79: 5640-5652.

164. Hrdlickova R, Nehyba J, Bose HR, Jr. (2001) Interferon regulatory factor 4 contributes to transformation of v-Rel-expressing fibroblasts. Mol Cell Biol 21: 6369-6386.

165. de Veer MJ, Sim H, Whisstock JC, Devenish RJ, Ralph SJ (1998) IFI60/ISG60/IFIT4, a new member of the human IFI54/IFIT2 family of interferon-stimulated genes. Genomics 54: 267-277.

166. Lou YJ, Pan XR, Jia PM, Li D, Xiao S, et al. (2009) IRF-9/STAT2 [corrected] functional interaction drives retinoic acid-induced gene G expression independently of STAT1. Cancer Res 69: 3673-3680.

167. Arguello M, Sgarbanti M, Hernandez E, Mamane Y, Sharma S, et al. (2003) Disruption of the B-cell specific transcriptional program in HHV-8 associated primary effusion lymphoma cell lines. Oncogene 22: 964-973.

168. Brass AL, Kehrli E, Eisenbeis CF, Storb U, Singh H (1996) Pip, a lymphoid-restricted IRF, contains a regulatory domain that is important for autoinhibition and ternary complex formation with the Ets factor PU.1. Genes Dev 10: 2335-2347.

169. Forero A, Moore PS, Sarkar SN (2013) Role of IRF4 in IFN-Stimulated Gene Induction and Maintenance of Kaposi Sarcoma-Associated Herpesvirus Latency in Primary Effusion Lymphoma Cells. J Immunol 191: 1476-1485.

170. Zhu J, Smith K, Hsieh PN, Mburu YK, Chattopadhyay S, et al. (2010) High-throughput screening for TLR3-IFN regulatory factor 3 signaling pathway modulators identifies several antipsychotic drugs as TLR inhibitors. J Immunol 184: 5768-5776.

171. Renne R, Zhong W, Herndier B, McGrath M, Abbey N, et al. (1996) Lytic growth of Kaposi's sarcoma-associated herpesvirus (human herpesvirus 8) in culture. Nat Med 2: 342-346.

172. Arvanitakis L, Mesri EA, Nador RG, Said JW, Asch AS, et al. (1996) Establishment and characterization of a primary effusion (body cavity-based) lymphoma cell line (BC-3) harboring kaposi's sarcoma-associated herpesvirus (KSHV/HHV-8) in the absence of Epstein-Barr virus. Blood 88: 2648-2654.

173. Boshoff C, Gao SJ, Healy LE, Matthews S, Thomas AJ, et al. (1998) Establishing a KSHV+ cell line (BCP-1) from peripheral blood and characterizing its growth in Nod/SCID mice. Blood 91: 1671-1679.

174. Menezes J, Leibold W, Klein G, Clements G (1975) Establishment and characterization of an Epstein-Barr virus (EBC)-negative lymphoblastoid B cell line (BJA-B) from an exceptional, EBV-genome-negative African Burkitt's lymphoma. Biomedicine 22: 276-284.

175. Meerbrey KL, Hu G, Kessler JD, Roarty K, Li MZ, et al. (2011) The pINDUCER lentiviral toolkit for inducible RNA interference in vitro and in vivo. Proc Natl Acad Sci U S A 108: 3665-3670.

176. Sarkar SN, Peters KL, Elco CP, Sakamoto S, Pal S, et al. (2004) Novel roles of TLR3 tyrosine phosphorylation and PI3 kinase in double-stranded RNA signaling. Nat Struct Mol Biol 11: 1060-1067.

177. Das SC, Nayak D, Zhou Y, Pattnaik AK (2006) Visualization of intracellular transport of vesicular stomatitis virus nucleocapsids in living cells. J Virol 80: 6368-6377.

178. Chin KC, Cresswell P (2001) Viperin (cig5), an IFN-inducible antiviral protein directly induced by human cytomegalovirus. Proc Natl Acad Sci U S A 98: 15125-15130.

179. Zhou X, Michal JJ, Zhang L, Ding B, Lunney JK, et al. (2013) Interferon induced IFIT family genes in host antiviral defense. Int J Biol Sci 9: 200-208.

180. Zhao F, Xuan Z, Liu L, Zhang MQ (2005) TRED: a Transcriptional Regulatory Element Database and a platform for in silico gene regulation studies. Nucleic Acids Res 33: D103-107.

181. Messeguer X, Escudero R, Farre D, Nunez O, Martinez J, et al. (2002) PROMO: detection of known transcription regulatory elements using species-tailored searches. Bioinformatics 18: 333-334.

182. Negishi H, Ohba Y, Yanai H, Takaoka A, Honma K, et al. (2005) Negative regulation of Toll-like-receptor signaling by IRF-4. Proc Natl Acad Sci U S A 102: 15989-15994.

183. Sjostrand M, Ambrosi A, Brauner S, Sullivan J, Malin S, et al. (2013) Expression of the immune regulator tripartite-motif 21 is controlled by IFN regulatory factors. J Immunol 191: 3753-3763.

184. Barton ES, Lutzke ML, Rochford R, Virgin HWt (2005) Alpha/beta interferons regulate murine gammaherpesvirus latent gene expression and reactivation from latency. J Virol 79: 14149-14160.

185. Mandal P, Krueger BE, Oldenburg D, Andry KA, Beard RS, et al. (2011) A gammaherpesvirus cooperates with interferon-alpha/beta-induced IRF2 to halt viral replication, control reactivation, and minimize host lethality. PLoS Pathog 7: e1002371.

186. Steed AL, Barton ES, Tibbetts SA, Popkin DL, Lutzke ML, et al. (2006) Gamma interferon blocks gammaherpesvirus reactivation from latency. J Virol 80: 192-200.

187. Gregory SM, Damania B (2009) KSHV and the toll of innate immune activation. Cell Cycle 8: 3246-3247.

188. Khodarev N, Ahmad R, Rajabi H, Pitroda S, Kufe T, et al. (2010) Cooperativity of the MUC1 oncoprotein and STAT1 pathway in poor prognosis human breast cancer. Oncogene 29: 920-929.

189. Duarte CW, Willey CD, Zhi D, Cui X, Harris JJ, et al. (2012) Expression signature of IFN/STAT1 signaling genes predicts poor survival outcome in glioblastoma multiforme in a subtype-specific manner. PLoS One 7: e29653.

190. Khodarev NN, Roizman B, Weichselbaum RR (2012) Molecular pathways: interferon/stat1 pathway: role in the tumor resistance to genotoxic stress and aggressive growth. Clin Cancer Res 18: 3015-3021.

191. Efimova EV, Liang H, Pitroda SP, Labay E, Darga TE, et al. (2009) Radioresistance of Stat1 over-expressing tumour cells is associated with suppressed apoptotic response to cytotoxic agents and increased IL6-IL8 signalling. Int J Radiat Biol 85: 421-431.

192. Khodarev NN, Beckett M, Labay E, Darga T, Roizman B, et al. (2004) STAT1 is overexpressed in tumors selected for radioresistance and confers protection from radiation in transduced sensitive cells. Proc Natl Acad Sci U S A 101: 1714-1719.

193. Khodarev NN, Roach P, Pitroda SP, Golden DW, Bhayani M, et al. (2009) STAT1 pathway mediates amplification of metastatic potential and resistance to therapy. PLoS One 4: e5821.

194. Pitroda SP, Wakim BT, Sood RF, Beveridge MG, Beckett MA, et al. (2009) STAT1-dependent expression of energy metabolic pathways links tumour growth and radioresistance to the Warburg effect. BMC Med 7: 68.

195. Andersen JB, Aaboe M, Borden EC, Goloubeva OG, Hassel BA, et al. (2006) Stage-associated overexpression of the ubiquitin-like protein, ISG15, in bladder cancer. Br J Cancer 94: 1465-1471.

196. Satake H, Tamura K, Furihata M, Anchi T, Sakoda H, et al. (2010) The ubiquitin-like molecule interferon-stimulated gene 15 is overexpressed in human prostate cancer. Oncol Rep 23: 11-16.

197. Reich NC (2013) A death-promoting role for ISG54/IFIT2. J Interferon Cytokine Res 33: 199-205.

198. Kent WJ, Sugnet CW, Furey TS, Roskin KM, Pringle TH, et al. (2002) The human genome browser at UCSC. Genome Res 12: 996-1006.

199. Zhong W, Wang H, Herndier B, Ganem D (1996) Restricted expression of Kaposi sarcoma-associated herpesvirus (human herpesvirus 8) genes in Kaposi sarcoma. Proc Natl Acad Sci U S A 93: 6641-6646.

200. Lee HR, Brulois K, Wong L, Jung JU (2012) Modulation of Immune System by Kaposi's Sarcoma-Associated Herpesvirus: Lessons from Viral Evasion Strategies. Front Microbiol 3: 44.

201. Kwun HJ, da Silva SR, Qin H, Ferris RL, Tan R, et al. (2011) The central repeat domain 1 of Kaposi's sarcoma-associated herpesvirus (KSHV) latency associated-nuclear antigen 1 (LANA1) prevents cis MHC class I peptide presentation. Virology 412: 357-365.

202. Kwun HJ, da Silva SR, Shah IM, Blake N, Moore PS, et al. (2007) Kaposi's sarcoma-associated herpesvirus latency-associated nuclear antigen 1 mimics Epstein-Barr virus EBNA1 immune evasion through central repeat domain effects on protein processing. J Virol 81: 8225-8235.

203. Schmidt K, Wies E, Neipel F (2011) Kaposi's sarcoma-associated herpesvirus viral interferon regulatory factor 3 inhibits gamma interferon and major histocompatibility complex class II expression. J Virol 85: 4530-4537.

204. Ballestas ME, Kaye KM (2011) The latency-associated nuclear antigen, a multifunctional protein central to Kaposi's sarcoma-associated herpesvirus latency. Future Microbiol 6: 1399-1413.

205. Shair KH, Schnegg CI, Raab-Traub N (2009) Epstein-Barr virus latent membrane protein-1 effects on junctional plakoglobin and induction of a cadherin switch. Cancer Res 69: 5734-5742.

206. Gao SJ, Boshoff C, Jayachandra S, Weiss RA, Chang Y, et al. (1997) KSHV ORF K9 (vIRF) is an oncogene which inhibits the interferon signaling pathway. Oncogene 15: 1979-1985.

207. Moore PS, Boshoff C, Weiss RA, Chang Y (1996) Molecular mimicry of human cytokine and cytokine response pathway genes by KSHV. Science 274: 1739-1744.

208. Lin R, Genin P, Mamane Y, Sgarbanti M, Battistini A, et al. (2001) HHV-8 encoded vIRF-1 represses the interferon antiviral response by blocking IRF-3 recruitment of the CBP/p300 coactivators. Oncogene 20: 800-811.

209. Lin YC, Brown K, Siebenlist U (1995) Activation of NF-kappa B requires proteolysis of the inhibitor I kappa B-alpha: signal-induced phosphorylation of I kappa B-alpha alone does not release active NF-kappa B. Proc Natl Acad Sci U S A 92: 552-556.

210. Brown K, Gerstberger S, Carlson L, Franzoso G, Siebenlist U (1995) Control of I kappa B-alpha proteolysis by site-specific, signal-induced phosphorylation. Science 267: 1485-1488.

211. Bagneris C, Ageichik AV, Cronin N, Wallace B, Collins M, et al. (2008) Crystal structure of a vFlip-IKKgamma complex: insights into viral activation of the IKK signalosome. Mol Cell 30: 620-631.

212. Thanos D, Maniatis T (1995) Virus induction of human IFN beta gene expression requires the assembly of an enhanceosome. Cell 83: 1091-1100.

213. Wei L, Fan M, Xu L, Heinrich K, Berry MW, et al. (2008) Bioinformatic analysis reveals cRel as a regulator of a subset of interferon-stimulated genes. J Interferon Cytokine Res 28: 541-551.

214. Pan Y, Nussinov R (2011) The role of response elements organization in transcription factor selectivity: the IFN-beta enhanceosome example. PLoS Comput Biol 7: e1002077.

215. Zhang T, Wang Y, Zhang L, Liu B, Xie J, et al. (2010) Lysine residues of interferon regulatory factor 7 affect the replication and transcription activator-mediated lytic replication of Kaposi's sarcoma-associated herpesvirus/human herpesvirus 8. J Gen Virol 92: 181-187.

216. Cosset FL, Takeuchi Y, Battini JL, Weiss RA, Collins MK (1995) High-titer packaging cells producing recombinant retroviruses resistant to human serum. J Virol 69: 7430-7436.

217. Seaman WT, Ye D, Wang RX, Hale EE, Weisse M, et al. (1999) Gene expression from the ORF50/K8 region of Kaposi's sarcoma-associated herpesvirus. Virology 263: 436-449.

218. Guito J, Lukac DM KSHV Rta Promoter Specification and Viral Reactivation. Front Microbiol 3: 30.

219. Bu W, Palmeri D, Krishnan R, Marin R, Aris VM, et al. (2008) Identification of direct transcriptional targets of the Kaposi's sarcoma-associated herpesvirus Rta lytic switch protein by conditional nuclear localization. J Virol 82: 10709-10723.

220. Dillon PJ, Gregory SM, Tamburro K, Sanders MK, Johnson GL, et al. (2013) Tousled-like kinases modulate reactivation of gammaherpesviruses from latency. Cell Host Microbe 13: 204-214.

221. De Regge N, Van Opdenbosch N, Nauwynck HJ, Efstathiou S, Favoreel HW (2010) Interferon Alpha Induces Establishment of Alphaherpesvirus Latency in Sensory Neurons <italic>In Vitro</italic>. PLoS ONE 5: e13076.

222. Zhu J, Ghosh A, Coyle EM, Lee J, Hahm ER, et al. (2013) Differential effects of phenethyl isothiocyanate and D,L-sulforaphane on TLR3 signaling. J Immunol 190: 4400-4407.

223. Pfeffer LM, Kim JG, Pfeffer SR, Carrigan DJ, Baker DP, et al. (2004) Role of nuclear factor-kappaB in the antiviral action of interferon and interferon-regulated gene expression. J Biol Chem 279: 31304-31311.

224. Konrad A, Wies E, Thurau M, Marquardt G, Naschberger E, et al. (2009) A systems biology approach to identify the combination effects of human herpesvirus 8 genes on NF-kappaB activation. J Virol 83: 2563-2574.

225. Cheng F, Weidner-Glunde M, Varjosalo M, Rainio EM, Lehtonen A, et al. (2009) KSHV reactivation from latency requires Pim-1 and Pim-3 kinases to inactivate the latency-associated nuclear antigen LANA. PLoS Pathog 5: e1000324.

226. Cohen A, Brodie C, Sarid R (2006) An essential role of ERK signalling in TPA-induced reactivation of Kaposi's sarcoma-associated herpesvirus. J Gen Virol 87: 795-802.

227. Deutsch E, Cohen A, Kazimirsky G, Dovrat S, Rubinfeld H, et al. (2004) Role of protein kinase C delta in reactivation of Kaposi's sarcoma-associated herpesvirus. J Virol 78: 10187-10192.

228. Ye J, Shedd D, Miller G (2005) An Sp1 response element in the Kaposi's sarcoma-associated herpesvirus open reading frame 50 promoter mediates lytic cycle induction by butyrate. J Virol 79: 1397-1408.

229. Wang SE, Wu FY, Yu Y, Hayward GS (2003) CCAAT/enhancer-binding protein-alpha is induced during the early stages of Kaposi's sarcoma-associated herpesvirus (KSHV) lytic cycle reactivation and together with the KSHV replication and transcription activator (RTA) cooperatively stimulates the viral RTA, MTA, and PAN promoters. J Virol 77: 9590-9612.

230. Scholz BA, Harth-Hertle ML, Malterer G, Haas J, Ellwart J, et al. (2013) Abortive lytic reactivation of KSHV in CBF1/CSL deficient human B cell lines. PLoS Pathog 9: e1003336.

231. Wang Y, Yuan Y (2007) Essential role of RBP-Jkappa in activation of the K8 delayed-early promoter of Kaposi's sarcoma-associated herpesvirus by ORF50/RTA. Virology 359: 19-27.

232. Carroll KD, Khadim F, Spadavecchia S, Palmeri D, Lukac DM (2007) Direct interactions of Kaposi's sarcoma-associated herpesvirus/human herpesvirus 8 ORF50/Rta protein with the cellular protein octamer-1 and DNA are critical for specifying transactivation of a delayed-early promoter and stimulating viral reactivation. J Virol 81: 8451-8467.

233. Harrison SM, Whitehouse A (2008) Kaposi's sarcoma-associated herpesvirus (KSHV) Rta and cellular HMGB1 proteins synergistically transactivate the KSHV ORF50 promoter. FEBS Lett 582: 3080-3084.

234. Lai IY, Farrell PJ, Kellam P (2011) X-box binding protein 1 induces the expression of the lytic cycle transactivator of Kaposi's sarcoma-associated herpesvirus but not Epstein-Barr virus in co-infected primary effusion lymphoma. J Gen Virol 92: 421-431.

235. Yang Z, Wood C (2007) The transcriptional repressor K-RBP modulates RTA-mediated transactivation and lytic replication of Kaposi's sarcoma-associated herpesvirus. J Virol 81: 6294-6306.

236. Gould F, Harrison SM, Hewitt EW, Whitehouse A (2009) Kaposi's sarcoma-associated herpesvirus RTA promotes degradation of the Hey1 repressor protein through the ubiquitin proteasome pathway. J Virol 83: 6727-6738.

237. Zurhein G, Chou SM (1965) Particles Resembling Papova Viruses in Human Cerebral Demyelinating Disease. Science 148: 1477-1479.

238. Padgett BL, Walker DL, ZuRhein GM, Eckroade RJ, Dessel BH (1971) Cultivation of papova-like virus from human brain with progressive multifocal leucoencephalopathy. Lancet 1: 1257-1260.

239. Bennett SM, Broekema NM, Imperiale MJ (2012) BK polyomavirus: emerging pathogen. Microbes Infect 14: 672-683.

240. Pipas JM (2009) SV40: Cell transformation and tumorigenesis. Virology 384: 294-303.

241. Bakkenist CJ, Kastan MB (2004) Initiating cellular stress responses. Cell 118: 9-17.

242. Dahl J, You J, Benjamin TL (2005) Induction and utilization of an ATM signaling pathway by polyomavirus. J Virol 79: 13007-13017.

243. Orba Y, Suzuki T, Makino Y, Kubota K, Tanaka S, et al. (2010) Large T antigen promotes JC virus replication in G2-arrested cells by inducing ATM- and ATR-mediated G2 checkpoint signaling. J Biol Chem 285: 1544-1554.

244. Jiang M, Zhao L, Gamez M, Imperiale MJ (2012) Roles of ATM and ATR-mediated DNA damage responses during lytic BK polyomavirus infection. PLoS Pathog 8: e1002898.

245. Boichuk S, Hu L, Hein J, Gjoerup OV (2010) Multiple DNA damage signaling and repair pathways deregulated by simian virus 40 large T antigen. J Virol 84: 8007-8020.

246. Shi Y, Dodson GE, Shaikh S, Rundell K, Tibbetts RS (2005) Ataxia-telangiectasia-mutated (ATM) is a T-antigen kinase that controls SV40 viral replication in vivo. J Biol Chem 280: 40195-40200.

247. Hein J, Boichuk S, Wu J, Cheng Y, Freire R, et al. (2009) Simian virus 40 large T antigen disrupts genome integrity and activates a DNA damage response via Bub1 binding. J Virol 83: 117-127.

248. Verma S, Ziegler K, Ananthula P, Co JK, Frisque RJ, et al. (2006) JC virus induces altered patterns of cellular gene expression: interferon-inducible genes as major transcriptional targets. Virology 345: 457-467.

249. Cantalupo PG, Saenz-Robles MT, Rathi AV, Beerman RW, Patterson WH, et al. (2009) Cell-type specific regulation of gene expression by simian virus 40 T antigens. Virology 386: 183-191.

250. Gamper AM, Rofougaran R, Watkins SC, Greenberger JS, Beumer JH, et al. (2013) ATR kinase activation in G1 phase facilitates the repair of ionizing radiation-induced DNA damage. Nucleic Acids Res.

251. Swift S, Lorens J, Achacoso P, Nolan GP (2001) Rapid production of retroviruses for efficient gene delivery to mammalian cells using 293T cell-based systems. Curr Protoc Immunol Chapter 10: Unit 10 17C.

252. Hahn WC, Counter CM, Lundberg AS, Beijersbergen RL, Brooks MW, et al. (1999) Creation of human tumour cells with defined genetic elements. Nature 400: 464-468.

253. Campbell KS, Mullane KP, Aksoy IA, Stubdal H, Zalvide J, et al. (1997) DnaJ/hsp40 chaperone domain of SV40 large T antigen promotes efficient viral DNA replication. Genes Dev 11: 1098-1110.

254. Poulin DL, Kung AL, DeCaprio JA (2004) p53 targets simian virus 40 large T antigen for acetylation by CBP. J Virol 78: 8245-8253.

255. Bluyssen HA, Levy DE (1997) Stat2 is a transcriptional activator that requires sequence-specific contacts provided by stat1 and p48 for stable interaction with DNA. J Biol Chem 272: 4600-4605.

256. Desai P, Person S (1998) Incorporation of the green fluorescent protein into the herpes simplex virus type 1 capsid. J Virol 72: 7563-7568.

257. Kato A, Cortese-Grogan C, Moyer SA, Sugahara F, Sakaguchi T, et al. (2004) Characterization of the amino acid residues of sendai virus C protein that are critically involved in its interferon antagonism and RNA synthesis down-regulation. J Virol 78: 7443-7454.

258. Rathi AV, Cantalupo PG, Sarkar SN, Pipas JM (2010) Induction of interferon-stimulated genes by Simian virus 40 T antigens. Virology 406: 202-211.

259. Pamment J, Ramsay E, Kelleher M, Dornan D, Ball KL (2002) Regulation of the IRF-1 tumour modifier during the response to genotoxic stress involves an ATM-dependent signalling pathway. Oncogene 21: 7776-7785.

260. Tanaka N, Ishihara M, Lamphier MS, Nozawa H, Matsuyama T, et al. (1996) Cooperation of the tumour suppressors IRF-1 and p53 in response to DNA damage. Nature 382: 816-818.

261. Tamura T, Ishihara M, Lamphier MS, Tanaka N, Oishi I, et al. (1997) DNA damage-induced apoptosis and Ice gene induction in mitogenically activated T lymphocytes require IRF-1. Leukemia 11 Suppl 3: 439-440.

262. Tamura T, Ishihara M, Lamphier MS, Tanaka N, Oishi I, et al. (1995) An IRF-1-dependent pathway of DNA damage-induced apoptosis in mitogen-activated T lymphocytes. Nature 376: 596-599.

263. Reis LF, Harada H, Wolchok JD, Taniguchi T, Vilcek J (1992) Critical role of a common transcription factor, IRF-1, in the regulation of IFN-beta and IFN-inducible genes. EMBO J 11: 185-193.

264. Fujita T, Kimura Y, Miyamoto M, Barsoumian EL, Taniguchi T (1989) Induction of endogenous IFN-alpha and IFN-beta genes by a regulatory transcription factor, IRF-1. Nature 337: 270-272.

265. Miyamoto M, Fujita T, Kimura Y, Maruyama M, Harada H, et al. (1988) Regulated expression of a gene encoding a nuclear factor, IRF-1, that specifically binds to IFN-beta gene regulatory elements. Cell 54: 903-913.

266. Brzostek-Racine S, Gordon C, Van Scoy S, Reich NC (2011) The DNA damage response induces IFN. J Immunol 187: 5336-5345.

267. Nikitin PA, Luftig MA (2012) The DNA damage response in viral-induced cellular transformation. Br J Cancer 106: 429-435.

268. McFadden K, Luftig MA (2013) Interplay between DNA tumor viruses and the host DNA damage response. Curr Top Microbiol Immunol 371: 229-257.

269. Mohni KN, Smith S, Dee AR, Schumacher AJ, Weller SK (2013) Herpes Simplex Virus Type 1 Single Strand DNA Binding Protein and Helicase/Primase Complex Disable Cellular ATR Signaling. PLoS Pathog 9: e1003652.

270. Wilkinson DE, Weller SK (2006) Herpes simplex virus type I disrupts the ATR-dependent DNA-damage response during lytic infection. J Cell Sci 119: 2695-2703.

271. Li J, Wang X, Diaz J, Tsang SH, Buck CB, et al. (2013) Merkel cell polyomavirus large T antigen disrupts host genomic integrity and inhibits cellular proliferation. J Virol 87: 9173-9188.

272. Moody CA, Laimins LA (2009) Human papillomaviruses activate the ATM DNA damage pathway for viral genome amplification upon differentiation. PLoS Pathog 5: e1000605.

273. Sinclair A, Yarranton S, Schelcher C (2006) DNA-damage response pathways triggered by viral replication. Expert Rev Mol Med 8: 1-11.

274. Xu LH, Huang M, Fang SG, Liu DX (2011) Coronavirus infection induces DNA replication stress partly through interaction of its nonstructural protein 13 with the p125 subunit of DNA polymerase delta. J Biol Chem 286: 39546-39559.

275. Wen C, He X, Ma H, Hou N, Wei C, et al. (2008) Hepatitis C virus infection downregulates the ligands of the activating receptor NKG2D. Cell Mol Immunol 5: 475-478.

276. Baer A, Austin D, Narayanan A, Popova T, Kainulainen M, et al. (2012) Induction of DNA damage signaling upon Rift Valley fever virus infection results in cell cycle arrest and increased viral replication. J Biol Chem 287: 7399-7410.

277. Lee J, Sayed N, Hunter A, Au KF, Wong WH, et al. (2012) Activation of innate immunity is required for efficient nuclear reprogramming. Cell 151: 547-558.

278. Kamangar F, Dores GM, Anderson WF (2006) Patterns of cancer incidence, mortality, and prevalence across five continents: defining priorities to reduce cancer disparities in different geographic regions of the world. J Clin Oncol 24: 2137-2150.

279. Heo DS, Snyderman C, Gollin SM, Pan S, Walker E, et al. (1989) Biology, cytogenetics, and sensitivity to immunological effector cells of new head and neck squamous cell carcinoma lines. Cancer Res 49: 5167-5175.

280. Umemura N, Zhu J, Mburu YK, Forero A, Hsieh PN, et al. (2012) Defective NF-kappaB signaling in metastatic head and neck cancer cells leads to enhanced apoptosis by double-stranded RNA. Cancer Res 72: 45-55.

281. Yoneyama N, Morimoto H, Ye CX, Ashihara H, Mizuno K, et al. (2006) Substrate specificity of N-methyltransferase involved in purine alkaloids synthesis is dependent upon one amino acid residue of the enzyme. Mol Genet Genomics 275: 125-135.

282. Yoneyama M, Kikuchi M, Natsukawa T, Shinobu N, Imaizumi T, et al. (2004) The RNA helicase RIG-I has an essential function in double-stranded RNA-induced innate antiviral responses. Nat Immunol 5: 730-737.

283. Meylan E, Curran J, Hofmann K, Moradpour D, Binder M, et al. (2005) Cardif is an adaptor protein in the RIG-I antiviral pathway and is targeted by hepatitis C virus. Nature 437: 1167-1172.

284. Seth RB, Sun L, Ea CK, Chen ZJ (2005) Identification and characterization of MAVS, a mitochondrial antiviral signaling protein that activates NF-kappaB and IRF 3. Cell 122: 669-682.

285. Xu LG, Wang YY, Han KJ, Li LY, Zhai Z, et al. (2005) VISA is an adapter protein required for virus-triggered IFN-beta signaling. Mol Cell 19: 727-740.

286. Kawai T, Takahashi K, Sato S, Coban C, Kumar H, et al. (2005) IPS-1, an adaptor triggering RIG-I- and Mda5-mediated type I interferon induction. Nat Immunol 6: 981-988.

287. Bruns AM, Horvath CM (2012) Activation of RIG-I-like receptor signal transduction. Crit Rev Biochem Mol Biol 47: 194-206.

288. Loo YM, Gale M, Jr. (2011) Immune signaling by RIG-I-like receptors. Immunity 34: 680-692.

289. Ablasser A, Bauernfeind F, Hartmann G, Latz E, Fitzgerald KA, et al. (2009) RIG-I-dependent sensing of poly(dA:dT) through the induction of an RNA polymerase III-transcribed RNA intermediate. Nat Immunol 10: 1065-1072.

290. Chiu YH, Macmillan JB, Chen ZJ (2009) RNA polymerase III detects cytosolic DNA and induces type I interferons through the RIG-I pathway. Cell 138: 576-591.

291. Oshiumi H, Matsumoto M, Seya T (2011) Ubiquitin-mediated modulation of the cytoplasmic viral RNA sensor RIG-I. J Biochem 151: 5-11.

292. Kristiansen H, Gad HH, Eskildsen-Larsen S, Despres P, Hartmann R (2011) The oligoadenylate synthetase family: an ancient protein family with multiple antiviral activities. J Interferon Cytokine Res 31: 41-47.

293. Rebouillat D, Marie I, Hovanessian AG (1998) Molecular cloning and characterization of two related and interferon-induced 56-kDa and 30-kDa proteins highly similar to 2'-5' oligoadenylate synthetase. Eur J Biochem 257: 319-330.

294. Hartmann R, Olsen HS, Widder S, Jorgensen R, Justesen J (1998) p59OASL, a 2'-5' oligoadenylate synthetase like protein: a novel human gene related to the 2'-5' oligoadenylate synthetase family. Nucleic Acids Res 26: 4121-4128.

295. Zeng W, Xu M, Liu S, Sun L, Chen ZJ (2009) Key role of Ubc5 and lysine-63 polyubiquitination in viral activation of IRF3. Mol Cell 36: 315-325.

296. Xu M, Skaug B, Zeng W, Chen ZJ (2009) A ubiquitin replacement strategy in human cells reveals distinct mechanisms of IKK activation by TNFalpha and IL-1beta. Mol Cell 36: 302-314.

297. Sharma S, DeOliveira RB, Kalantari P, Parroche P, Goutagny N, et al. (2011) Innate immune recognition of an AT-rich stem-loop DNA motif in the Plasmodium falciparum genome. Immunity 35: 194-207.

298. Hou F, Sun L, Zheng H, Skaug B, Jiang QX, et al. (2011) MAVS forms functional prion-like aggregates to activate and propagate antiviral innate immune response. Cell 146: 448-461.

299. Zeng W, Sun L, Jiang X, Chen X, Hou F, et al. (2010) Reconstitution of the RIG-I pathway reveals a signaling role of unanchored polyubiquitin chains in innate immunity. Cell 141: 315-330.

300. Jiang X, Chen Z (2012) The role of ubiquitylation in immune defence and pathogen evasion. Nature Reviews Immunology 12.

301. Hartmann R, Olsen HS, Widder S, Jorgensen R, Justesen J (1998) p59OASL, a 2'-5' oligoadenylate synthetase like protein: a novel human gene related to the 2'-5' oligoadenylate synthetase family. Nucleic acids research 26: 4121-4128.

302. Lin RJ, Yu HP, Chang BL, Tang WC, Liao CL, et al. (2009) Distinct antiviral roles for human 2',5'-oligoadenylate synthetase family members against dengue virus infection. J Immunol 183: 8035-8043.

303. Marques J, Anwar J, Eskildsen-Larsen S, Rebouillat D, Paludan SR, et al. (2008) The p59 oligoadenylate synthetase-like protein possesses antiviral activity that requires the C-terminal ubiquitin-like domain. J Gen Virol 89: 2767-2772.

304. Schoggins JW, Wilson SJ, Panis M, Murphy MY, Jones CT, et al. (2011) A diverse range of gene products are effectors of the type I interferon antiviral response. Nature 472: 481-485.